Division of Biomedical

And Life Sciences

Lancaster University

MSc in Biomedical Science (research)

The development of antibody loaded liposomes for the treatment of Alzheimer's Disease

Callum Ross

February 2019

Table of Contents

Declaration

This thesis is submitted to Lancaster University in accordance with the requirements of the degree of Master of Science in the department of Biomedical and Life Sciences. I confirm that this thesis has not been submitted for any other degree of any examining body.

Acknowledgements

I would like to thank Professor David Allsop for being my supervisor, giving me the opportunity to be part of his lab and his support throughout the project. I want to thank my second supervisor, Dr. Nigel Fullwood for his expertise and guidance, particularly with TEM techniques. I am grateful to Dr. Mark Taylor for his expertise with liposomes and peptide attachments and also to the rest of the Allsop lab including Jessica Hammond, Anthony Aggidis and Niklas Reich for their support throughout the project. I want to thank Professor Kamalinder Singh and Tamara Zwain at the University of Central Lancashire (UCLan) for allowing me to use the DLS system in the School of Pharmacy and Biomedical Science. I would also like to thank fellow Master's students Danny Ward and Amber Hayes for their support. Lastly, I want to thank my mother for her encouragement throughout my postgraduate studies.

List of Tables

List of Figures

Abbreviations

Abbreviation	Meaning
AB-NLs	Antibody-Nanoliposomes
ACE	Angiotensin Converting Enzyme
AD	Alzheimer's Disease
ADDLs	Amyloid β-derived diffusible ligands
Aβ	Amyloid-β
APOE	Apolipoprotein E (gene)
ApoE	Apolipoprotein E (protein)
APP	Amyloid Precursor Protein
BACE1	β-site APP-Cleaving Enzyme 1
BBB	Blood Brain Barrier
BCECs	Brain Capillary Endothelial Cells
CBSA	Cationized Bovine Serum Albumin
CH, Chl	Cholesterol
CJD	Creutzfeldt-Jacob Disease
CNS	Central Nervous System
CPP	Cell Penetrating Peptide
DLB	Dementia with Lewy bodies
DLS	Dynamic Light Scattering
ECE	Endothelin-Converting Enzyme
FTD	Frontotemporal Dementia
HD	Huntington's Disease
HIV	Human Immunodeficiency Virus
IDE	Insulin-Degrading Enzyme

LBs	**Lewy bodies**
LRP	**Low-density Lipoprotein Receptor-related Protein**
LTP	**Long Term Potentiation**
LUVs	**Large Unilamellar Vesicles**
MAP1,2	**Microtubule-Associated protein 1,2**
MAPT	**Microtubule-Associated protein Tau**
MCI	**Mild Cognitive Impairment**
Me	**Methanol**
MLVs	**Multilamellar Vesicles**
MND	**Motor Neuron Disease**
MPS	**Mononuclear Phagocytic System**
NFTs	**Neurofibrillary Tangles**
NMDA	**N-methyl-D-aspartate**
PBS	**Phosphate Buffered Saline**
PD	**Parkinson's Disease**
PDI	**Polydispersity Index**
PEG	**Polyethylene Glycol**
PEG-NLs	**PEG-Nanoliposomes**
PHF	**Paired Helical Filaments**
PINPs	**Peptide Inhibitor Nanoparticles**
PrP	**Prion Protein**
PS1,2	**Presenilin 1,2 (protein)**
PSEN1,2	**Presenilin 1,2 (gene)**
PTA	**Phosphotungstic Acid**
RAGE	**Receptor for Advanced Glycation End products**

RI-OR2-TAT-NLs	**RI-OR2-TAT-Nanoliposomes**
RI-OR2-TAT+AB-NLs	**RI-OR2-TAT+Antibody-Nanoliposomes**
ROS	**Reactive Oxygen Species**
RT	**Room Temperature**
SM	**Sphingomyelin**
SN	**Substantia Nigra**
SUVs	**Small Unilamellar Vesicles**
TAT	**HIV1-tat**
TEM	**Transmission Electron Microscopy**
TREM2	**Triggering Receptor Expressed on Myeloid Cells 2**
Tr X	**Triton X-100**
ULVs	**Unilamellar Vesicles**

Title: The development of antibody loaded liposomes for the treatment of Alzheimer's Disease.

Author: Callum Ross, February 2019.

Abstract

Purpose: To investigate the incorporation of antibodies into the hydrophilic core of liposomes. This includes studying the development of antibody incorporation techniques, the impact antibody incorporation has on the size and shape of liposomes, and the ability for antibody loaded liposomes (AB-NLs) to penetrate SH-SY5Y neuroblastoma cells, giving insight into whether these types of liposomes can be used to delivery antibodies into cells.

Methods: Antibodies were incorporated in the hydrophilic core during liposome preparation. Regular liposomes were then produced using a mini extruder, and then further processed for additional modifications. Analysis of liposome size and polydispersity index (PDI) was obtained by Dynamic Light Scattering (DLS), and then Transmission Electron Microscopy (TEM) was used to analyse the ultrastructure, size and lamellarity of formed vesicles. The Wako Assay measured the quantification of sphingomyelin in liposomes, which could then be used to produce liposomes with known lipid content. The ability for AB-NLs to penetrate SH-SY5Y cells was observed by a cell penetration assay.

Results: AB-NLs had a tendency to clump, but were otherwise stable. Antibody incorporation was successful, yet efficiency was poor. AB-NLs were delivered into SH-SY5Y cells, enhanced by TAT attachment and Antibody fluorescence was observed.

Conclusion: Development of current antibody incorporation techniques is essential for improved uptake. There is potential for AB-NLs as a therapeutic treatment with additional research.

CHAPTER ONE – Introduction

1.1 Ageing and brain diseases

Considerable neuronal death was once widely accepted to be an inevitable consequence of normal brain ageing, due to studies undertaken in the 1950s. However, it became clear that normal brain ageing is not associated with or explained by a large-scale decrease in neuronal or synaptic number (Reviewed by Morrison and Hof, 1997) and that synaptic loss and neuron death is instead a consequence of neuropathogenic changes associated with neurodegenerative disorders. This process is selective, where certain circuits are disrupted that reflect the symptoms and pathogenesis of specific disorders. Since these observations are in the most part not a consequence of normal ageing, they can be used for understanding, diagnosis and treatment of age-related disorders.

One way in which neuronal circuits can be disrupted is by the misfolding of proteins, which otherwise ensure normal cellular function. Protein disruption, as a result of altered 3D structure, can result in the formation of dysfunctional and misfolded proteins, capable of aggregation. There are a group of brain diseases that are associated with the accumulation of these proteins (Table 1.1) that involve neuronal degeneration in specific brain areas (Soto, 2003). These brain diseases are currently incurable, and are caused by an accumulation of multiple genetic and environmental factors (Martin, 1999). Alzheimer's Disease (AD) is the most common, and is therefore of particular interest for diagnostic and therapeutic research.

Disorder	Pathology
Alzheimer's Disease (AD)	Synaptic dysfunction and perikaryal degeneration in the limbic system and associated areas, resulting primarily from the formation and accumulation of amyloid plaques and neurofibrillary tangles (Selkoe, 2001).
Parkinson's Disease (PD)	Dopaminergic neuron cell loss in the substantia nigra (SN) and development of protein rich, intracytoplasmic Lewy bodies (LBs) (Shulman *et al.,* 2011).
Huntington's Disease (HD)	Neuronal loss in the striatum and cortex, as well as impact on nuclei in the thalamus, hypothalamus, subthalamic nucleus, SN and cerebellum. There is also reduction in tissue volume in the striatum and cortical white matter (Raymond *et al.,* 2011).
Dementia with Lewy bodies (DLB)	Fluctuating cognitive impairment and visual hallucinations caused by sharing symptoms of both Alzheimer's and Parkinson's Disease (McKeith, 2004).
Motor neuron disease (MND)	Selective cell death of lower motor neurons in the spinal cord and brain stem and upper motor neurons in the motor cortex. Pathogenic mechanisms are multifactorial, one of which involves the presence of proteinaceous inclusions in the cells and neurofilament accumulation in the axons (Shaw, 2005).
Frontotemporal dementia (FTD)	Degeneration of the frontal and temporal cerebral lobes, linked to abnormal accumulation of disease specific proteins (Mackenzie and Neumann, 2016).
Creutzfeldt-Jacob diseases (CJD)	Spongiform appearance and neuronal cell loss in the central nervous system (CNS), proliferation of astrocytes and accumulation of an abnormally folded form of the host prion protein (PrP). There is also occasional deposition of amyloid plaques (Trevitt and Singh, 2003), often the cerebellum.

Table 1.1: Age related brain diseases. *Table shows the pathology of brain diseases associated with protein accumulation and neuronal degeneration.*

1.2 Alzheimer's Disease - background

In 1901, Alois Alzheimer documented a detailed report of symptoms from a 51-year-old woman (Auguste D.) at Frankfurt Hospital, who was observed to have severe cognitive dysfunction, memory impairment, altered behaviour, disorientation, delusions and progressive decline in language function (Reviewed by Moller and Graeber, 1998). While originally this case was seemingly indistinguishable from common senile dementia, the pathological-anatomical examination showed atrophy of the brain and changes in internal cortical cell clusters. Alzheimer described some pathological changes: senile plaques and neurofibrillary tangles (NFTs), which are now known respectively to contain fibrils composed of amyloid β-protein (Aβ) and NFTs consisting of hyper-phosphorylated Tau protein (Hass and Selkoe, 2007) (Figure 1.1). As a result of Alzheimer's observations, Emil Kraepelin coined the term "Alzheimer's disease" (AD) for the illness in 1910 (Hoff and Hippus, 1989). Yet, it wasn't until the late 1960s when AD became accepted as the most common basis for senile dementia.

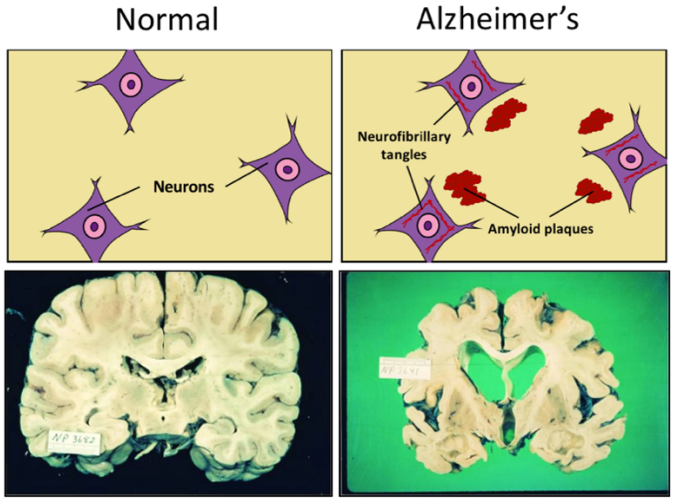

Figure 1.1: Comparison between normal and AD brain/neurons. *The left shows healthy brain and neuronal cells, with absence of amyloid plaques and neurofibrillary tangles. The right shows an Alzheimer's brain and neuronal cells, with senile amyloid plaques (red) and intracellular neurofibrillary tangles. The AD brain shows loss of cerebrocortical grey matter and enlarged fluid-filled ventricles (Bird, 2008).*

For many decades since the first case of AD was described by Alzheimer, many have tried to understand the underlying cause of this neurodegenerative disorder and determine how to cure it. In the 1970s, the first clue as to what might underlie AD came from the observation that neurons synthesizing and releasing acetylcholine usually underwent severe degeneration (Selkoe, 2001). As a result, three acetylcholinesterase inhibitors (donepezil, rivastigmine and galantamine) were developed and later approved to treat AD by enhancing acetylcholine levels in the synaptic cleft. However, these drugs do not target any causative underlying disease mechanisms, and do not slow the long-term progression of the disorder (Bullock and Dengiz, 2005). Instead, they provide only temporarily improved cognition by counterbalancing neurotransmitter disturbances, in addition to having many limitations and side effects (Yiannopoulou and Papageorgiou, 2013).

In recent years, a consensus has developed and a rough outline of the disease progression and pathogenesis has emerged. Certainly, the likelihood of developing this neurodegenerative disorder increases with age (affecting both genders mainly over the age of 65) (Blennow *et al.,* 2006). This is noteworthy as advancements in modern medicine and technology have meant that average life expectancy has increased, leading to an increased AD burden worldwide. Today, AD affects approximately 36 million people worldwide, and this number is set to rise to over 115 million by 2050, as populations age (World Alzheimer's Report, 2016).

1.3 Clinical and neuropathological features of AD

AD is characterized by the slow progressive impairment of episodic memory, and memory associated complications such as aphasia (difficulty speaking and understanding speech), agnosia (difficulty with object recognition) and apraxia (inability to make voluntary movements). This is combined with general symptoms of cognitive impairment such as impaired judgement, decision-making, mental uneasiness, disorientation and delusions (Blennow *et al.,* 2006). These clinical features are a result of underlying AD neuropathological changes. The most widely established, as in the original case described by Alois Alzheimer, are the accumulation Aβ plaques and NFTs. Other pathological changes include enlargement of brain ventricles, shrinkage of the hippocampus and cerebral cortex, general decrease in brain volume, gliosis, loss of grey matter and synaptic connections (including changes in acetylcholine transmission as a result of loss of cholinergic neurons), inflammation and extensive oxidative damage. Many of these pathological changes begin decades before clinical features can be observed (the preclinical phase) (Davies *et al.,* 1988).

During this preclinical phase, plaques and tangles accumulate until a threshold is met (that is different for each individual) when the first clinical symptoms start to appear. At this stage the term mild cognitive impairment (MCI) is given, which is based on close personal individuals verifying memory loss in a patient, supported by additional memory tests (Petersen, 2004). MCI is a heterogeneous entity as patients with MCI may go on to develop AD, or they may have a benign form of MCI or a different form of dementia (Gauthier *et al.,* 2006). The conversion rate from MCI to AD with clinical dementia is 10-15% per year (Visser *et al.,* 2005).

In the past there has been difficulty in separating AD from other types of dementia. The term Alzheimer's was originally used only for people with presenile onset of symptoms (before 65 years of age), whereas senile dementia was used when the onset was after 65. However,

further research showed that amyloid plaques and neurofibrillary tangles are present both in AD and in senile dementia, which made clinical diagnosis uncertain. It is now clear that the plaque and tangle burden is more severe in the early onset form of AD than senile dementia, which has made them clinically distinguishable (Roth, 1986; Blennow *et al.,* 1991).

1.4 The genetics of Alzheimer's Disease

It is noteworthy that the estimated proportion of genetically based AD cases is uncertain. Many consider the genetic influence is responsible for between 10% and 50% of cases, whilst many other investigators believe that over time, all cases have a genetic cause (Selkoe, 2011). There are 4 widely confirmed genes in which mutations or polymorphisms are known to result in familial AD: amyloid precursor protein (APP) gene, the apolipoprotein E (ApoE) gene, presenilin 1 (*PSEN1*) and presenilin 2 (*PSEN2*), as well as many others in the process of confirmation (e.g. complement receptor). Missense mutations in the APP gene result in a general increase in Aβ (specifically Aβ42) as a consequence of an increase in amyloidogenic cleavages of APP by β- or γ-secretases. Yet, since the missense mutations in the gene account to less than 0.01% of all Alzheimer's cases, research of APP variations are primarily useful for understand pathogenic mechanisms of AD in general. APP can also cause AD via an increased dosage of the gene, which occurs in Down's syndrome (trisomy 21) or in patients with APP microduplications on chromosome 21q and leads to overproduction of $A\beta_{40}$ and $A\beta_{42}$ (Rumble *et al., 1989*; Tokuda *et al.,* 1997). In these cases, the lifelong increase in APP expression leads to the appearance of Aβ plaques as early as 12 years old (Selkoe, 2001).

In the 1990's , two groups of scientists identified an association between Apolipoprotein E4 (*APOE4*) and AD that was later found to cause a 3-fold and 15-fold AD risk for heterozygotes and homozygotes respectively. ApoE is a glycoprotein, that is involved with the transport of cholesterol into cells (Pfrieger, 2003). The ApoE gene has three alleles (ε2, ε3, ε4) that result

in 3 ApoE isoforms (E2, E3, E4) that differ by amino acid substitutions at residue 112 or 158 (Mahley *et al.,* 2006). Inheritance of one or two of the ε4 alleles was found to be an importance risk factor for AD and are now known to account for more than 30% of AD cases, and are the most influential genetic factor predisposing the disease (Corder *et al.,* 1993; Saunders *et al.,* 1993). Yet, some individuals homozygous for the ApoE4 show no symptoms throughout their lifetime.

Dominantly inherited mutations in the genes encoding presenilin 1 (PS1) and presenilin 2 (PS2) lead to an aggressive form of AD with early onset (40 to 65 years old) (Rogaev *et al,* 1995; Levy-Lahad *et al.,* 1995). Accumulation of hyper phosphorylated neurofibrillary Tau tangles are prominent features in AD neuropathology. However, mutations in the Tau gene have not been found to be associated with familial AD and they instead influence a form of frontotemporal dementia linked to chromosome 17 (FTDP-17), historically termed Pick's disease (Hutton *et al.,* 1998). Amyloid deposits are not a pathological feature of this form of frontotemporal dementia, and it is instead characterised by widespread tangle formation as a result of altered microtubule-binding properties of mutant tau (Lee *et al.,* 2001). Transgenic mice and cell culture models have been used to analyse the effects that each of the four implicated genes in familial AD (Table 1.2). In all of these cases, the genetic variants were linked with an increase in the production or deposition of Aβ, providing strong evidence that AD is caused by accumulation of extracellular cerebral Aβ deposits.

Advances in whole-genome analysis technology have revealed a rare genetic variant linked to AD. Triggering receptor expressed on myeloid cells 2 (*TREM2*) is a gene that encodes a receptor on myeloid cells that is essential for inflammatory responses. It is thought to increase AD risk 3-fold, a similar risk to one copy of the *APOE* ε4 allele. 46 *TREM2* genetic variants have been associated with AD. One genetic variant known as p.Arg47His (rs75932628) increases the

risk of AD by 2 to 3 times in some European and North American populations. However, more studies are required to strongly link other variants and to understand the neuropathology of such rare conditions (Yaghmoor *et al.,* 2014; Carmona *et al.,* 2018).

Chromosome	Gene Defect	Inheritance	Phenotype
21	Missense βAPP mutations	Autosomal dominant	Increased production of all Aβ peptides (including $A\beta_{42}$)
19	ApoE4 polymorphism	Risk factor for late-onset AD	Increased density of $A\beta_{40}$ plaques
14	PS1 mutations	Autosomal dominant	Increased production of $A\beta_{42}$ peptides
1	PS2 mutations	Autosomal dominant	Increased production of $A\beta_{42}$ peptides
6	TREM2 mutations	Autosomal dominant	Reduced microglial clustering around plaques

Table 1.2: Genetic influence on familial AD. *The loci and genes involved in increasing Aβ levels linked to AD.*

1.5 Disease frequency

1.5.1 Incidence

This late-onset neurodegenerative disease typically affects individuals over 65 years of age. There is a 1% annual risk of developing the disease between the age of 65-70, which rises to ~8% for people over the age of 85. AD affects both genders, with a slightly higher incidence in women, and also African Americans. The median survival time for people with AD is ~4 years, yet the duration varies considerably between 2 and 20 years.

1.5.2 Prevalence

Prevalence, or the proportion of individuals surviving with AD dramatically varies with age. The disease is rare under age 65, yet by age 85 over ~10% of the population have AD, with individuals ranging from mild to severe forms. The population of the UK over age 65 in 2016 was 11.8 million, which means that the prevalence is almost 1.2 million people. This figure is set to increase as world populations age. Prevalence is higher and more sustained for African Americans, yet not amongst their respective native countries. These differences are likely to be due to a difference in lifestyle. For example: African Americans are more susceptible to vascular disease, which is linked with AD risk. Nevertheless, the lifetime risk remains 2 fold higher (Prince *et al.,* 2016).

1.6 Risk factors

Epidemiology is a form of analytical research that in AD, typically involves the identification and analysis of risk factors in order to reduce disease burden. Advances that have occurred in genetic understanding have proven useful for the analysis of other risk factors. For example, identification of novel genetic susceptibilities give insight into particular behavioural and environmental risk factors involved.

1.6.1 Ageing

It has been historically difficult to differentiate between normal age-related brain changes and pathological changes such as those observed in AD. Brain cognition and function should remain separate when trying to understand these differences. It is obvious, however, that ageing has at least a secondary role in the development of AD since incidence is rare under age 65.

1.6.2 Education, early life and brain activity

AD prevalence is significantly higher in individuals with poor education compared to those who have been well-educated (Stern *et al.,* 1994). This sparked the theory that we have two independent 'reserves' (cognitive and brain) (Stern, 2012). This concept suggests that where brain reserve may be identical for two individuals (e.g. they have the same intensity of pathological changes or brain damage), differences in cognitive reserve may allow one person to cope more effectively than the other. It is considered that years of formal education acquire a cognitive reserve which protects individuals from AD later in life.

1.6.3 Alcohol

Excessive alcohol consumption has been known to cause dementia through acute toxicity and associated nutritional deficiencies. A French study found that individuals that drank red wine in moderate amounts were less likely to develop AD than heavy drinkers or abstainers, and another study reported that any alcohol in moderation is associated with reduced AD risk, due to antioxidant properties and its effect on lipid metabolism (Orgogozo *et al.,* 1997; Ruitenberg *et al.,* 2002).

1.6.4 Smoking

Studies have shown that smokers have a two- to fourfold increase in AD risk, particularly in those without an APO-ε4 allele. Smoking is thought to increase dementia risk through an interaction with cerebral vessels. Although nicotine is thought to have beneficial effects, administration through smoking is still likely to be disadvantageous (Merchant *et al.,* 1999; Nordberg *et al.,* 2002).

1.6.5 Down Syndrome

Adults with Down's syndrome develop the neuropathological changes associated with AD by the age of 40, but only some become demented. AD risk is increased two- to threefold within a family with a history of Down's syndrome and individuals who have a child with Down's syndrome are at higher risk of developing AD than those that have children with other types of mental retardation. It is thought that this might be due to a form of accelerated ageing that develops in these mothers that predisposes them to AD (Schupf *et al.,* 2001).

1.7 Amyloidosis and Alzheimer's Disease

Amyloid disease (amyloidosis) refers to a disease caused in parts of the body and some brain regions, as a result of amyloid fibril deposition. The deposited fibrils are 6-8 nm wide, and are composed of a key 39-43 amino acid peptide, termed Aβ (amyloid β-peptide) (Glenner and Wong, 1984). Formed fibrils are resistant to proteolytic degradation, which leads to cell damage, organ dysfunction and ultimately death. All types of amyloid proteins share common properties: insolubility, fibrillar appearance with electron microscopy (Figure 1.2), β-pleated sheet conformation, and green birefringence under polarised light after Congo red staining. Although 26 proteins and 80 genetic variants have been linked with amyloid deposition, the pathogenic mechanisms for fibril formation are still under intensive investigation.

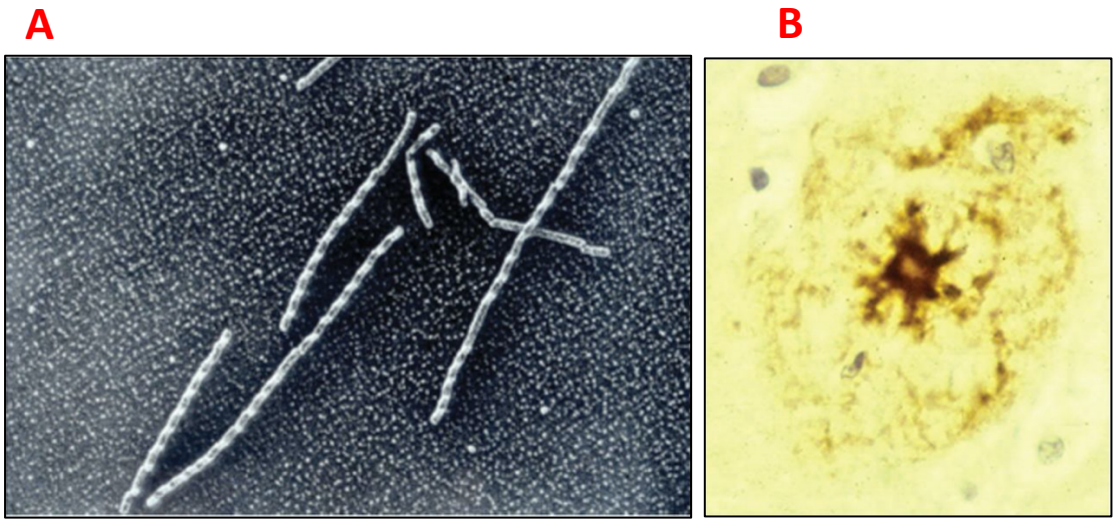

Figure 1.2: Aβ in amyloid and senile plaque formation. A) *Fibrillar appearance of Aβ fibrils, detected by electron microscopy with rotary metal shadowing.* ***B)*** *Aβ peptide can be detected in the centre of senile plaques by immunostaining (Taken from: Allsop and Mayes, 2014).*

AD is the most common form of amyloidosis in humans. Amyloid deposits in AD are found at the centre of extracellular senile plaques, surrounded by abnormal nerve processes and microglia, located in the brain parenchyma of AD patients. Aβ is the major component of AD parenchymal plaques, and can be detected *in vivo* using antibodies against Aβ (Figure 1.2). This peptide is also the main constituent of cerebral amyloid deposits in Down's syndrome, familial AD, sporadic cases of cerebral amyloid angiopathy and in normal ageing.

1.8 Aβ precursor protein (APP)

The 39-42 amino acid Aβ peptide is a product of a larger type I transmembrane precursor glycoprotein, known as amyloid-β precursor protein (APP). It is coded by a single multiexonic gene located on chromosome 21. This gene is more than 190 kb in length, and generates more than 10 isoforms of APP mRNA by alternative splicing. Only 4 isoforms of mRNA encode proteins that contain the Aβ peptide (APP695, APP714, APP751 and APP770). The largest

isoform, APP770, is distinguished by its KPI (kunitz-type protease inhibitor) domain and an OX-2 antigen domain. There is evidence to suggest that Aβ is preferentially formed from APP695, the predominant isoform in the human brain, which lacks both domains described in APP770. 12-14 amino acids of the Aβ domain of APP reside in the transmembrane domain and the remaining residues lie outside (Barnham *et al.,* 2003). APP is cleaved by proteolysis at three major sites. The α-secretase site (between residues 16-17 of the Aβ region) prevents the formation of Aβ, whereas the sequential cleavage at β- and γ-secretase sites produces the full length Aβ peptide (Figure 1.3) (Selkoe, 2001; Blennow *et al.,* 2006).

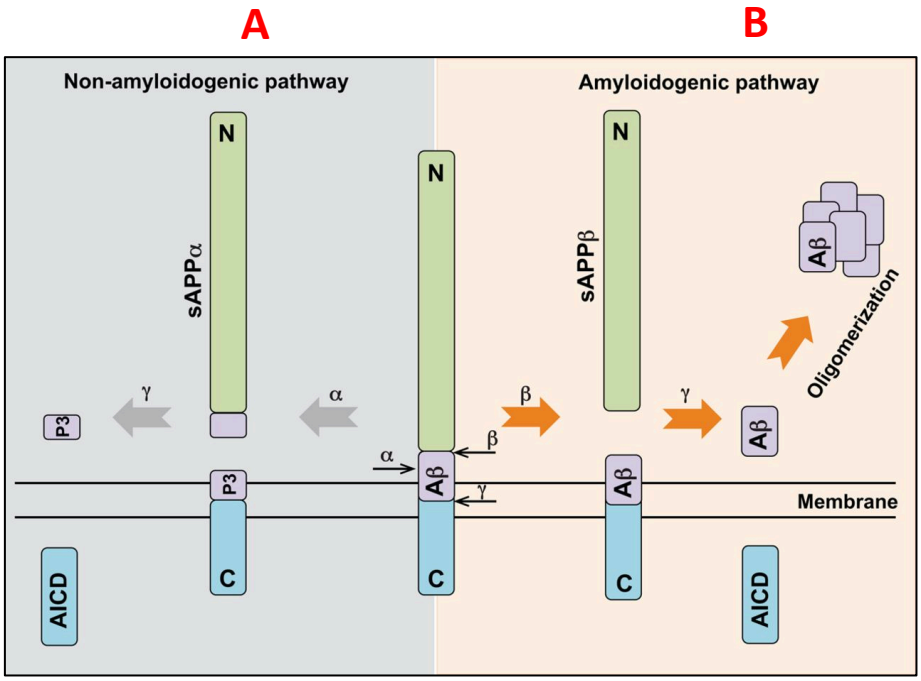

Figure 1.3: APP proteolytic processing pathway. A) *Involves cleavage of APP by α-secretase at peptide bond 16-17, which prevents formation of the Aβ fragment.* ***B)*** *involves cleavage of APP by β-secretase followed by γ-secretase, to form the full Aβ fragment, potentially leading to oligomerisation. Abbreviations: Amyloid precursor protein intracellular domain (AICD), Amyloid beta (Aβ), soluble amyloid precursor protein α (sAPPα), soluble amyloid precursor protein β (sAPPβ). (Taken from: Nicolas and Hassan, 2014).*

The ADAM (a disinterin and metalloproteinase) family have been identified as α-secretase, capable of cleaving APP at the α-site, with ADAM10 being the strongest candidate relevant to AD pathogenesis. The major β-secretase has been identified as BACE1 (β-site APP-cleaving enzyme 1) and the γ-secretase is an intramembrane complex composed of nicastrin, PEN-2, APH-1 and presenilin. This enzyme has aspects of heterogeneity, which is responsible for the varied length of Aβ between individuals, such as the two major isoforms (Aβ42 and Aβ40), both of which spontaneously aggregate *in vitro* into fibrils, but Aβ42 does this more rapidly. After formation, Aβ can be degraded by proteolysis or cleared into the peripheral blood stream via the blood brain barrier (BBB). Many enzymes are capable of degrading Aβ: IDE (insulin-degrading enzyme), ECE (endothelin-converting enzyme), ACE (angiotensin-converting enzyme) and Neprilysin, and the clearance across the BBB is mediated by LRP (low-density lipoprotein receptor-related protein). RAGE (receptor for advanced glycation end products) controls it's influx back to the brain (Hardy and Selkoe, 2002). Sporadic AD is due to an imbalance in these proteolytic events, or imbalance of Aβ between the brain and the periphery. Whereas for Inherited cases, mutations in APP, PS1 and PS2 genes result in the overproduction of Aβ (Allsop and Mayes, 2014).

1.9 The amyloid cascade hypothesis

Disruption of control mechanisms related to Aβ production and clearance is thought to be linked directly to the pathogenesis of AD. This is known as the "amyloid cascade" hypothesis, whereby an imbalance in Aβ production and clearance results in accumulation and aggregation of Aβ through a cascade of events, leading to tangle formation and eventual neuronal cell death (Verdile *et al.,* 2004), and is the most widely accepted mechanism for the formation of amyloid fibrils, which are thought to be toxic to nerve cells (Figure 1.4). Soluble oligomers, ADDLs (amyloid β-derived diffusible ligands) and protofibrils are thought to be the

predominant toxic forms of Aβ (Walsh and Selkoe, 2007). They have also been shown to block long-term potentiation (LTP) and synaptic capacity, resulting in the loss of neuronal firing and deficits in memory processing (Tabner *et al.,* 2005). Subsequently, oligomers (dimers and trimers) are considered a key drug target for the treatment of AD. Aβ is also likely to act as a trigger to set off other damaging processes such as neurofibrillary tau formation, reactive oxygen species (ROS) formation and synaptic damage, all of which contribute to neurodegeneration (Allsop and Mayes, 2014).

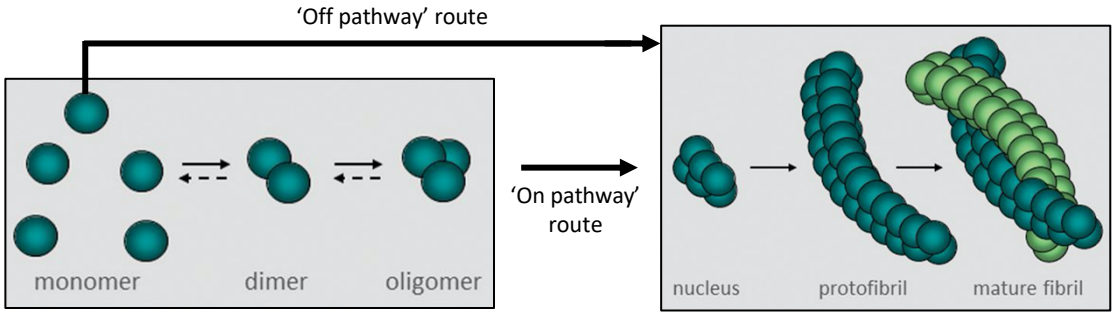

Figure 1.4: Aggregation of Aβ into oligomers and amyloid fibrils. *Oligomers are either 'on pathway' or 'off pathway' towards amyloid fibril formation. On pathway involves early intermediates leading to fibre formation. Off pathway involves monomer assembly directly into the nucleus required to initiate fibril formation.* (Adapted from Allsop and Mayes, 2014).

1.10 Neurofibrillary tangles (Tau)

In AD, Tau pathology exists as abnormally folded Tau protein that forms hyperphosphorylated and aggregated bundles of paired helical filaments (PHF). In the AD brain these are seen as intraneuronal neurofibrillary tangles and are thought to be a downstream impact of Aβ accumulation and aggregation (Braak *et al.,* 1986). In humans, Tau proteins are encoded by a single microtubule-associated protein Tau (*MAPT*) gene mapped to chromosome 17q21 (Himmler *et al.,* 1989). Microtubules are tubular polymers that form part of the cytoskeleton. They provide structure and shape to the cytoplasm of eukaryotes and some bacteria and are

involved in multiple cellular processes including intracellular transport of secretory vesicles and organelles as well as being major constituents of mitotic spindles in cell division. Healthy neurons contain microtubules, which contribute towards these cellular processes (Grundke-Iqbal *et al.,* 1986). Yet, abnormal folding leads to AD. In humans, alternative splicing of Tau pre-mRNA produces six isoforms of the protein that differ in containing three or four microtubule binding repeats (Goedert *et al.,* 1989). Tau interacts with tubulin and promotes its assembly into microtubules and stabilises their structure. In a normal mature healthy neuron, the amount of tubulin is tenfold greater than Tau (~2 μM) and nearly all Tau is continuously bound to microtubules in cells. Overexpression of Tau can cause microtubule bundling *in vitro*, but this has not been seen in AD or other tauopathies (Butner and Kirschner, 1991).

Degeneration of abnormally hyperphosphorylated Tau does occur in AD, which has been observed in all six Tau isoforms. Additional pathologies include conformational changes and truncation of Tau following hyperphosphorylation (Jicha *et al.,* 1997; Novak *et al.,* 1991). Total Tau is four to eight fold higher in AD brains than normal aged brains which is solely caused by the hyperphosphorylated version of Tau protein (Khatoon *et al.,* 1992). This toxic form of Tau self-assembles into PHFs, forming neurofibrillary tangles. It also sequesters normal Tau as well as two other major neuronal microtubule associated proteins (MAP1 and MAP2), and this is likely to be the cause and/or contributor to the neurodegeneration observed in AD (Alonso *et al.,* 1997; Alonso *et al.,* 1996). It is evident however that 40% of this toxic Tau is not polymerised into neurofibrillary tangles and instead resides in the cytosol and this cytosolic tau does not bind tubulin or promote microtubule assembly, and instead inhibits assembly (Kopke *et al.,* 1993). It remains clear that inhibiting abnormal hyperphosphorylated of Tau is a promising therapeutic target for AD treatment.

1.11 Current treatment of AD

1.11.1 Aβ drug therapy

Cholinergic neurons that protrude from regions deep inside the brain, that are involved in memory, are selectively lost early in the course of AD. This led to the development of three acetylcholinesterase inhibitors, Galantamine, Donepezil and Rivastigmine, that have the ability to block the breakdown of acetylcholine at the synapse, in order to boost cholinergic transmission (Blennow *et al.,* 2006). However, these drugs currently available for the treatment of AD only address symptoms of the disease and do not target any of the underlying disease mechanisms, or slow down the long term progression of the disorder. They also have many other side effects such as nausea, vomiting and liver toxicity in some cases (Yiannopoulou and Papageorgiou, 2013). An N-methyl-D-aspartate (NMDA) antagonist, memantine, is another drug used for the treatment of AD. The formation of learning and memory involves the NMDA receptor and its interaction with glutamate, and memantine is the only approved drug for advanced AD, yet still only has a temporary therapeutic impact (Areosa *et al.,* 2004).

Intermediates in the proteolysis of APP has been considered for AD therapy, targeting β- and γ- secretases responsible for the production of Aβ. BACE1, an integral membrane aspartyl protease required for β secretase activity, has been a target for inhibition without much success. γ- secretase is involved in notch processing as well as APP proteolysis and so inhibition would lead to notch dysregulation, which is involved in essential development processes and dysfunction linked with cancer. α-secretase prevents the formation of Aβ and has been considered as a therapeutic target, yet it is easier to produce therapies that inhibit rather than stimulate enzyme activity (Gandy, 2005; Petit *et al.,* 2001).

1.11.2 Immunotherapy

An active immunotherapeutic agent was developed in the form of an AD vaccine, termed AN1792, which involves triggering an immune response to aggregated Aβ42. However, clinical trials were halted in phase three as patients developed encephalitis and brain inflammation Gilman *et al.,* 2005). Following on from AN1792 therapy, anti Aβ antibodies are in development, which can which can clear amyloid plaques from the brain. Passive immunotherapies have also been developed such as solanezumab, bapineuzumab and gantenerumab. Solanezumab, for example, is a humanized monoclonal anti-Aβ antibody that targets and reduces plaque burden. However, in the case of solanezumab and other passive immunotherapeutics, there is so far no or little impact on the clinical outcomes of AD (Fu *et al.,* 2010).

1.11.3 Tau drug therapy

The Inhibition of neurofibrillary tangles produced by aggregated Tau protein is another potential therapeutic approach for AD treatment. Inside neurons, tau tangles are likely to cause damage by inhibiting axonal transport (Mangialasche *et al.,* 2010). Inhibition of Tau aggregation is therefore an attractive therapeutic strategy. Yet, attempts to produce an effective drug have been somewhat unsuccessful. Methylioninium chloride has been one of the most successful drugs, which showed promising results in phase 2 clinical trials (Wischik *et al.,* 2008). A major drawback was that methylioninium chloride has multiple effects, such as on mitochondrial function by enhancing key biochemical pathways, which can lead to worsening AD pathology (Atamna *et al.,* 2008).

1.12 Peptide inhibitors against Aβ

Small peptide molecules that have the potential to bind to Aβ and prevent early formation of amyloid-β oligomers, provide a promising strategy which could halt or delay the progression of AD. Many of these peptides developed are not suitable for clinical trials, with only a few even progressing to animal testing (Taylor *et al.,* 2010; Parthsarathy *et al.,* 2013). Most of the peptide inhibitors are designed based on the findings that the internal sequence KLVFF (amino acids 16-20) is essential for binding interactions between Aβ molecules (Tjernberg *et al.,* 1996). Several approaches were made, such as adding proline residues into the binding region of the amyloid peptide in order to induce destabilization or linking an oligolysine disrupting element to the Aβ peptide binding sequence, all of which did not completely inhibit aggregation, but typically altered the aggregation kinetics (Ghanta *et al.,* 1996).

Austen *et al.* (2008) designed two peptide aggregation inhibitors that both contain the key region (KLVFF) required for Aβ interactions between molecules. The peptides, known as OR1 and OR2, also contained arginine (R) and glycine (G) residues on both ends to enhance solubility. OR1 has an amide group at the N-terminal and a carboxyl at the C terminal, whereas OR2 has an amide group at both terminals. Both inhibitors were shown to inhibit the formation of Aβ fibrils, yet OR2 was proven more effective at inhibiting oligomers (Taylor *et al.,* 2010).

OR2 (RGKLVFFGR-NH_2) inhibits the aggregation of Aβ into oligomers and fibrils, and blocks the toxic effects of Aβ on cultured cells. However, this peptide is sensitive to proteolysis, and was not designed to cross the BBB (Austen *et al*., 2008). To improve its stability, a retro-inverso version (RI-OR2) was made (Taylor *et al*., 2010), and this was enhanced further by the addition of a retro-inverted version of HIV-1 tat (TAT) to RI-OR2, producing RI-OR2-TAT (Parthsarathy *et al*., 2013). Following its peripheral injection, a fluorescein-labelled version of RI-OR2-TAT was found to cross the BBB and bind to the amyloid plaques present in the cerebral cortex of APPswe/PS1ΔE9 transgenic mice. Daily intraperitoneal (i.p.) injection of RI-OR2-TAT, for 3

weeks, into these mice resulted in substantial (25-45%) reductions in brain Aβ oligomer levels, amyloid plaque counts, oxidative damage, and inflammatory processes. However, RI-OR2-TAT inhibits Aβ aggregation only at relatively high concentrations (i.e. at a molar ratio of RI-OR2-TAT:Aβ of 1:5 at best) and so its therapeutic potential is likely to be limited.

1.13 The Blood Brain Barrier (BBB)

An effective treatment for AD would most likely require the therapeutic agent concerned to be transported across the BBB, a metabolic and transport barrier that protects the brain from harmful stimuli. The BBB is comprised of brain capillary endothelial cells (BCECs) that are attached to each other through tight junctions, resulting in restricted paracellular transport (Bhowmik and Khan, 2015; Sanchez-Navarro *et al*., 2017). Degrading enzymes are also present at the BBB, which can destroy molecules during their attempted passage into the brain (Abbott *et al*., 2010). As a consequence, the BBB is permeable only to certain molecules, ions and macromolecules such as nutrients, that are either essential for brain function or a waste products. Only 2% of molecules with molecular weight of <500 Da can cross the BBB, and molecules greater than 1 kDa are unable to cross at all (Pardridge, 2007). There are specific mechanisms in place to mediate the transportation of these essential molecules, and these can be exploited for therapeutic drug delivery. Still, the BBB prevents access to the brain of around 98% of neurotherapeutics, thus therapeutic potential remains limited.

1.13.1 Early strategies for BBB transportation

Passive diffusion permits the passage of some small lipophilic compounds across the BBB, such as certain amino acids, nucleosides, and small peptides. An early strategy utilised this simple mechanism by developing small lipophilic drugs that might pass through the endothelial cells. However, this excluded the vast majority of potential therapeutic molecules. A second approach was to develop small water-soluble drugs, in order to facilitate BBB transport *via* the

paracellular hydrophilic diffusion pathway. However, most of these potential molecules could not penetrate past the tight endothelial cell junctions (Hersh *et al.,* 2016).

1.13.2 Alternatives

Intracerebral or intracerebroventricular injection of drugs provides a strategy that avoids the BBB, but these procedures are highly invasive, and so are not widely used. Drugs administered by any peripheral route (e.g. orally or by intravenous injection) will encounter the BBB (Agrawal *et al*., 2017). Alternative methods, such as bypassing the BBB by delivery through the olfactory region (e.g. as a nasal spray) have some potential (Li et al., 2012; Zheng et al., 2015; Illum, 2012). Another strategy looks to utilize existing active BBB transport mechanisms, namely carrier-mediated transcytosis (also known as transporter-mediated transcytosis), receptor-mediated transcytosis, cell-mediated endocytosis, and adsorptive transcytosis (Table 1.3) (Gao, 2016; Sanchez-Navarro *et al*., 2017).

Transport mechanism	Explanation	Examples
Carrier-mediated transcytosis	Some essential materials required in the brain have specific transporters for active uptake across the BBB. Drugs can exploit these transporters for brain delivery.	**Glutathione** (Gaillard *et al*., 2014). **Choline** (Li *et al*., 2011). **Glucose** (Xie *et al.,* 2012).
Receptor-mediated transcytosis	Receptors on the BBB endothelium can bind specifically bind with corresponding ligands and trigger internalization. Drugs can incorporate these ligands, or their modified forms, for enhanced brain penetration.	**Transferrin receptor** (Qian *et al*., 2002). **Insulin receptor** (Guo *et al*., 2012). **Lactoferrin receptor** (Fillebeen *et al*., 1999).
Cell-mediated endocytosis	Endocytosis into endothelial cells can deliver drugs across the BBB. This mechanism is almost exclusive to the action of CPPs which exhibit various features to trigger transportation, and they are often highly positively charged.	**TAT (**Lindgren *et al*., 2000). **Penetratin** (Derossi *et al*., 1994) **Polyarginines** (Futaki et al., 2001)
Adsorptive transcytosis	Adsorptive-mediated targeting utilizes a modified, positively charged biological macromolecule for interaction	**Cationized bovine serum albumin (CBSA)** (Lu *et al*., 2005).

	with the negatively charged BBB, based on electrostatic attraction.	**Cationized immunoglobulins/ monoclonal antibodies** (Guo *et al*., 2012)

Table 1.3: Transport mechanisms for BBB transit and brain delivery.

1.14 Cell penetrating peptides (CPPs)

In the last 20 years, cell penetrating peptides (CPPs) have been identified, which are able to translocate across biological membranes including the BBB (Lindgren *et al*., 2000). They cross in a non-toxic manner, independent of membrane receptors and energy, which could reduce limitations of receptor saturation that have been observed with other methods. Most CPPs rely on positively charged amino acids interacting with the negatively charged membrane. Arginine, and to a lesser extent lysine, are particularly effective, as they form hydrogen bonds with the negatively charged phosphates, which may lead to internalization. CPPs with different properties vary in their internalization mechanisms (Table 1.4), but remain similar in their effective direct penetration of cell membranes.

Among all CPPs, TAT protein is best described, and has been used successfully for delivery of liposome nanoparticles into the brain (Gregori *et al*., 2017). TAT triggers steps for non-specific endocytotic delivery due to ionic interactions between positive charges of the peptide and negative charges of the BBB (Vivès *et al*., 2003). Recent studies have utilised a retro-inverted version of TAT, where L-amino acids are replaced with D-amino acids, and the sequence is reversed. This reduces potential problems with TAT, such as protease degradation and poor bioavailability *in vivo*, but still maintains the ability for transport across the BBB (Parthsarathy *et al*., 2013). Alternative CPPs, such as polyarginines (e.g. octaarginine) and penetratin have also shown potential for the delivery of therapeutics directly to the brain in SAMP8 mice (Kamei *et al.,* 2017).

CPP	Mechanism	Origin	References
TAT	Non-specific endocytosis	HIV-1	Pathsarathy *et al*., 2013; Vivès *et al*., 2003
Penetratin	Endocytosis	Antennapedia *Drosophila melanogaster*	Derossi *et al*., 1994; Tseng *et al*., 2002.
Pep-1	Pore formation	Chimeric	Henriques and Castanho, 2008.
Pep-7	Pore formation	CHL8 peptide phage clone	Gao *et al.*, 2002
pVEC	Transporter mediated	Murine endothelial cadherin	Koren and Torchilin, 2012.
Transportan	Endocytosis	Galanin-mastoparan	Pooga *et al*., 1998.
Polyarginines	Multiple mechanisms	Chemically synthesised	Futaki et al., 2001; Wender et al., 2000
DPV1047	Energy dependent mechanisms, independent of GAGs (charge interactions, HSPH binding)	Chemically synthesised	De Coupade et al., 2005
MPG	Pore formation	HIV glycoprotein 41/SV40 T antigen NLS	Morris et al., 2008
ARF	Endocytosis	p14 ARF protein	Johansson et al., 2008
p28	Caveolar-mediated/nonclathrin-caveolar-mediated	Azurin	Taylor et al., 2009
BPrPr	Macropinocytosis (fluid-phase endocytosis)	N terminus of unprocessed bovine prion protein	Magzoub et al., 2006
VT5	Non-specific endocytosis	Chemically synthesised	Oehlke et al., 1997
Bac 7	Likely non-specific endocytosis	Bactenecin family of antimicrobial peptides	Sadler et al., 2002
C105Y	Energy-independent process via caveolin- and clathrin-independent lipid rafts	α1-Antitrypsin	Rhee and Davies, 2006
PFVYLI	Energy-independent process via caveolin- and clathrin-independent lipid rafts	Derived from synthetic C105Y	Rhee and Davies, 2006

Table 1.4: Cell-penetrating peptides (CPPs) and their mechanism of internalization.

1.15 Liposomes

1.15.1 Introduction

The therapeutic potential of liposomes was recognised shortly after their development by Alex Bangham in 1961, but have only more recently been considered as a suitable vehicle for delivery of drugs that act on the central nervous system (CNS) (Lai *et al.,* 2013; Vieira and Gamara, 2016). Generally, liposomes are defined as auto-assembled spherical vesicles varying in diameter from a few nanometres (20 nm) to several micrometres (5 μm). They are made primarily from non-toxic lipids and phospholipids consisting of one or more bilayers that enclose a hydrophilic space (Vemuri and Rhodes, 1995) (Figure 1.5). They have been recognised as an attractive delivery system due to their chemical composition allowing easy modification of size, structure and composition. They are biocompatible and highly flexible, with the potential for carrying many different types of bioactive molecules, which typically are functionalised in the liposome core. Surface functionalisation can enhance diagnostic potential and drug delivery, giving liposomes unique advantages over alternative nanocarriers that have many limitations including poor delivery and limited therapeutics potential (Akbarzadeh *et al.,* 2013*;* Malam *et al.,* 2009).

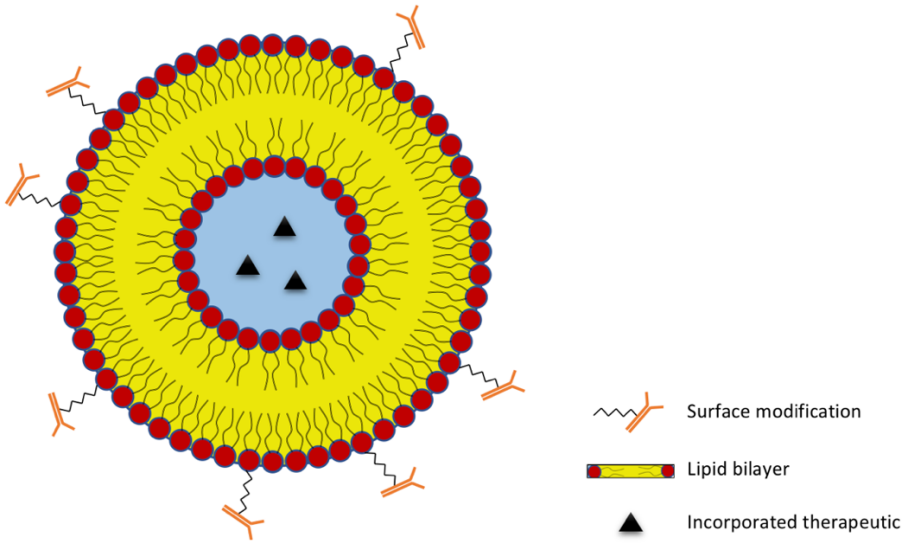

Figure 1.5: Simple schematic of a functionalised liposome. *Liposome shows drug incorporated in the hydrophilic core, with PEG-Antibody surface functionalization.*

1.15.2 Composition and assembly

The liposome size, as well as the lipid composition, affects their circulation in the bloodstream and uptake into the brain (Abra and Hunt, 1981; Harashima and Kiwada, 1996). Brain delivery requires liposomes to be roughly nano- or microsized and consist of one or more lipid bilayers surrounding an aqueous core. Only certain sizes will allow passage across the BBB for neuro-therapy (such as in AD) and so small vesicles (<100 nm in diameter) are often preferred. There are studies, however, that have shown that liposomes from 100-140 nm have certain advantages, such as a longer half-life in blood circulation and avoidance of plasma proteins. Large nano-liposomes (250 nm in diameter) are cleared twice as fast as 100 nm liposomes (Fanciullino and Ciccolini, 2009). Yet, liposomes 100 nm and smaller have more limited storage capacity, leading to poor encapsulation efficiency (Allen, 1997). A consideration of size should be made based on factors such as their therapeutic application, encapsulation efficiency and stability.

Common materials used for liposome creation are a combination (one or more) of biodegradable and biocompatible lipids such as sphingomyelin, phosphatidylcholine and phosphoglycerates. These phospholipids are amphipathic in aqueous media, having two hydrophobic tails made from hydrocarbon chains and a hydrophilic phosphate head, and support the self-assembly of liposomes into spherical bilayers. Other properties can differ greatly with lipid composition, impacting the liposome rigidity or fluidity and charge of the bilayer. For instance, naturally sourced unsaturated phosphatidylcholine gives much more permeable and less stable bilayers, whereas the saturated phospholipid with long acyl chains forms an impermeable rigid bilayer (Gabizon *et al.,* 1998; Allen *et al.,* 1997).

For the preparation of liposome self-assembled vesicles, the lipid composites are often dissolved in a solvent (e.g. chloroform) and evaporated to form a lipid film (Bangham method). Upon hydrating the lipid film, lipid bilayers are spontaneously produced, forming vesicles with a distinct inner space separated from surrounding space (Akbarzadeh *et al.,* 2013). The hydrophobic and hydrophilic properties of the lipids incorporated impacts the shape of the vesicles and nature of the hydrophilic core. Therefore the lipid composition has an important impact on the function of the liposome vesicle product. As well as phospholipids, cholesterol is often an appropriate inclusion in liposomes. Cholesterol not only maintains the stability of membranes *in vivo* and *in vitro*, but also reduces membrane permeability, which overall alters the structure and function of the vesicle products (Masserini, 2013). The four hydrocarbon ring molecular structure of cholesterol makes it hydrophobic in nature, which results in its interaction with unsaturated lipids in the core of the membrane. This causes a kink to form in the chain and allows phospholipids to take up more space in the bilayer, producing a less flexible membrane and substantially more rigid and stable structure (Figure 1.6) (Bozzuto and Molinari, 2015).

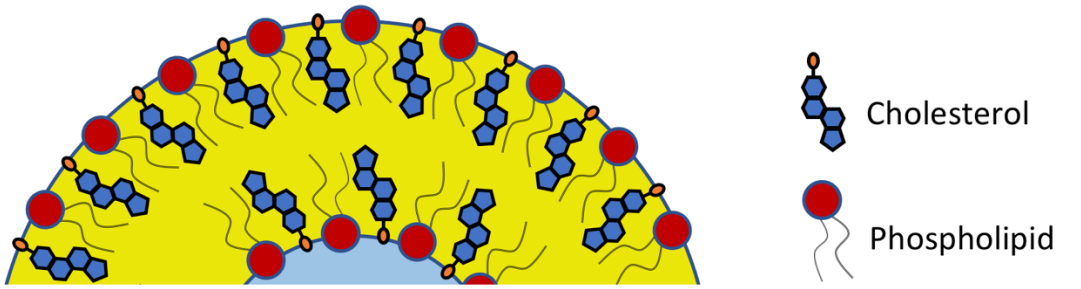

Figure 1.6: Interaction of cholesterol with unsaturated lipids. *Cholesterol integrates in the core of the lipid bilayers, causing a kink to form in the phospholipid (e.g. sphingomyelin) hydrocarbon tails. The cholesterol situates parallel to the phospholipids, and the hydroxyl group (orange) interacts with the phospholipid heads (red).*

There are multiple preparation methods for producing nanoliposomes. The appropriate method is dependent on several factors. These include the physiochemical characteristics of the liposome or the drug to be loaded (e.g. the hydrophilicity/hydrophobicity or the concentration of the loaded substance), the medium in which liposomes are dispersed (e.g. phosphate buffered saline (PBS)), the application and delivery of the liposomes and additional factors for liposome production for large scale clinical practice (Gómez-Hens and Fernández-Romero, 2006; Wagner and Vorauer-Uhl, 2011). The most commonly used technique is likely to be the Bangham or thin-film hydration method, which involves the dissolution of lipid in an organic solvent, evaporation to form a film and hydration in aqueous solution. A drug can be trapped in the hydrophilic core or in the lipophilic bilayers, depending on the properties of the therapeutic molecule. The disadvantage, however, is a poor encapsulation efficiency of water-soluble drugs (~10%) (Bangham *et al.,* 1965; Bozzuto and Molinari, 2015).

Alternative methods such as reverse-phase evaporation and solvent-injection provide higher encapsulation efficiency than the Bangham method, yet after having dissolved the lipids in the solvent, it is more challenging separating the solvent from the liposome product. The detergent-depletion method involves hydration of a lipid film with a detergent, but is rarely

used as it has both poor encapsulation efficiency and a long preparation period (Deamer and Bangham, 1976; Szoka and Papahadjopoulous, 1978; Lasch *et al.,* 2003). However, the Bangham method remains one of the most widely used techniques. The Bangham method requires additional processes after hydration in aqueous media, as the standard method producing large, non-homogenous vesicles that require a freeze and thaw, sonication and extrusion processes in order to produce homogenous liposomes of controlled sizes.

1.15.3 Classification

Liposomes are classified on their size and lamellarity as well as their preparation method and composition. Liposome size is tailored for its therapeutic application and is important for the success of the nanocarrier. For example, only certain sizes will allow passage across the BBB for neuro-therapy (such as in AD) and so small vesicles (less than 100 nm) are often preferred.

Liposomal size is linked to the specific preparation method used (described above) and the subsequent lamellarity of the liposome. Lamellarity refers to the number of lipid bilayers in liposomes, and is an important method of classification. Liposomes can either form unilamellar vesicles (ULVs) or multilamellar vesicles (MLVs) (Figure 1.7) depending on the preparation method and any other additional processes conducted. ULVs only have one bilayer with diameter ranging from a few nm to 400 nm. They enclose a large hydrophilic core and so their application is to encapsulate hydrophilic drugs. ULVs are subcategorised into large unilamellar vesicles (LUVs) with a diameter of 100 nm and more, and small unilamellar vesicles (SUVs) with a diameter of 20-100 nm (Masserini, 2013). MLVs are much larger (1-5 μm) and have two or more concentric lipid bilayers. They preferentially entrap lipophilic drugs, due to their large area of lipophilic bilayer (Immordino *et al.,* 2006;). The Bangham preparation method produces large non-homogenous MLVs, and it is the additional sonication and extrusion that produces variously sized ULVs.

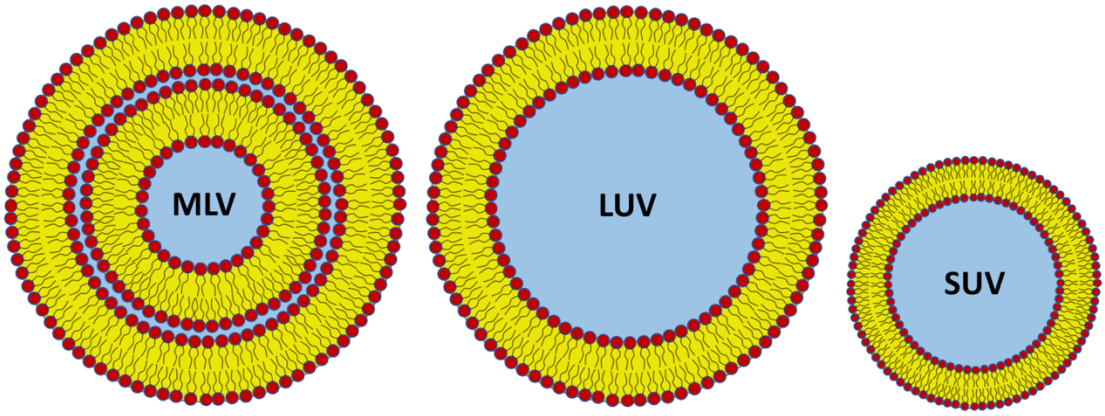

Figure 1.7: Schematic illustration of MLVs and ULVs. *MLV shows two lipid bilayers with a small aqueous hydrophilic core, suited for lipophilic drug entrapment. ULVs are subcategorised into LUVs and SUVs. LUVs (100 nm diameter and more) have a large enclosed aqueous core, suitable for hydrophilic drug incorporation. SUVs (20-100 nm) are similar LUVs, but suited to applications requiring small nano-carriers.*

1.15.4 Stability and modification

One essential function of the lipid bilayer of the liposome product is that their physiological composition facilitates numerous modifications, in comparison to other nano-carriers. These modifications can improve stability, facilitate transport into cells, or across the BBB, and allow specific molecular targeting for therapeutic benefit.

1.15.4.1 Stealth liposomes

Although liposomes are considered harmless to the human body, they are detected by the mononuclear phagocytic system (MPS). Liposomes are covered in plasma proteins (e.g. fibrinogen, immunoglobulins and complement proteins) during blood circulation, so that a 'protein corona' is formed around them. This leads to the activation of phagocytic systems and removal of liposomes from the bloodstream (Palchetti *et al.,* 2016), creating problems with their *in vivo* stability.

In order to improve stability, methods have been developed to improve the pharmacokinetic profile of liposomes to allow longer time-periods in circulation. Polyethylene glycol (PEG) or other polysaccharides are coated on the liposomes or incorporated into the lipid components of the bilayer, producing these so-called 'stealth' liposomes. PEG has high hydration capacity and this increases hydrodynamic volume and allows the formation of a water cloud around the polymer. Any hydrophilic molecule bound covalently to PEG also exhibits these properties, providing increased solubility, and resistance to interaction with plasma proteins. Subsequently, PEGylated liposomes in circulation are less prone to formation of a protein corona, allowing dramatically improved circulation times (Veronese and Mero, 2008).

1.15.4.2 BBB delivery

Possible mechanisms for the transport of liposomes across the BBB have been highly debated (Agrawal et al., 2017). An initial theory was that the phospholipid bilayer of the liposomes on its own might facilitate transportation across various biological membranes, including the BBB, but this simple mechanism proved to be ineffective. A strategy with increasing interest involves the use of CPPs to directly penetrate the BBB endothelium increase liposome transport to the brain. Classical methods to enhance transport instead utilize existing BBB active transport mechanisms (Figure 1.8).

In order to enhance BBB transportation, liposome surface modification can use two different techniques: (a) ligands are attached onto liposomes during preparation, or (b) ligands are covalently conjugated to the liposome surface post-preparation. The attachment during preparation involves incorporating the ligand into lipid mixture before lipid extrusion, and will produce varied ligand binding efficiency. Covalent conjugation is often carried out with ligands that contain thiol groups to react with maleimide or bromoacetyl anchors, forming thioether

or disulphide bonds (Schuber *et al.,* 2007). A second common conjugation attaches ligands to the end of PEG chains already attached or integrated at the liposome surface (Sudimack and Lee, 2000).

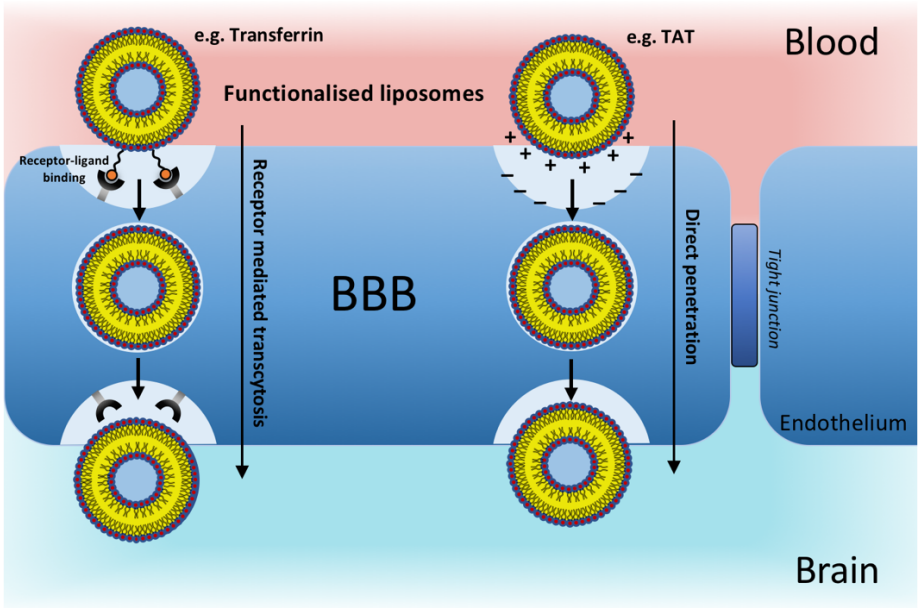

Figure 1.8: Promising liposomal BBB transport mechanisms. *Receptor-mediated transcytosis exploits receptors highly expressed at the BBB (e.g. transferrin receptor). Receptor ligand binding triggers internalization and brain delivery. A relatively new mechanism, direct penetration, involves internalization primarily exhibited by CPPs (e.g. TAT). Positively charged amino acids (+++) permit endocytosis by interacting with the negatively charged endothelial cell membrane (- - -).*

1.15.4.3 AD targeting

It is likely that the accumulation and aggregation of Aβ in the brain has an important role, directly or indirectly, in the induction of synaptic damage and memory deficits in AD (Hardy and Allsop, 1991; Hardy and Selkoe, 2002). The accumulation of Aβ oligomers or fibrils may be caused by overproduction, inefficient clearance from the brain, or by a combination of both of these. Effective therapeutic molecules can have an impact on one of these mechanisms to reduce Aβ burden. Many of these molecules on their own have low uptake across the BBB, but their incorporation into a multi-functionalised liposomal system, with molecules that enhance BBB transport, can help to resolve this problem and allow effective targeting to Aβ (Figure 1.9).

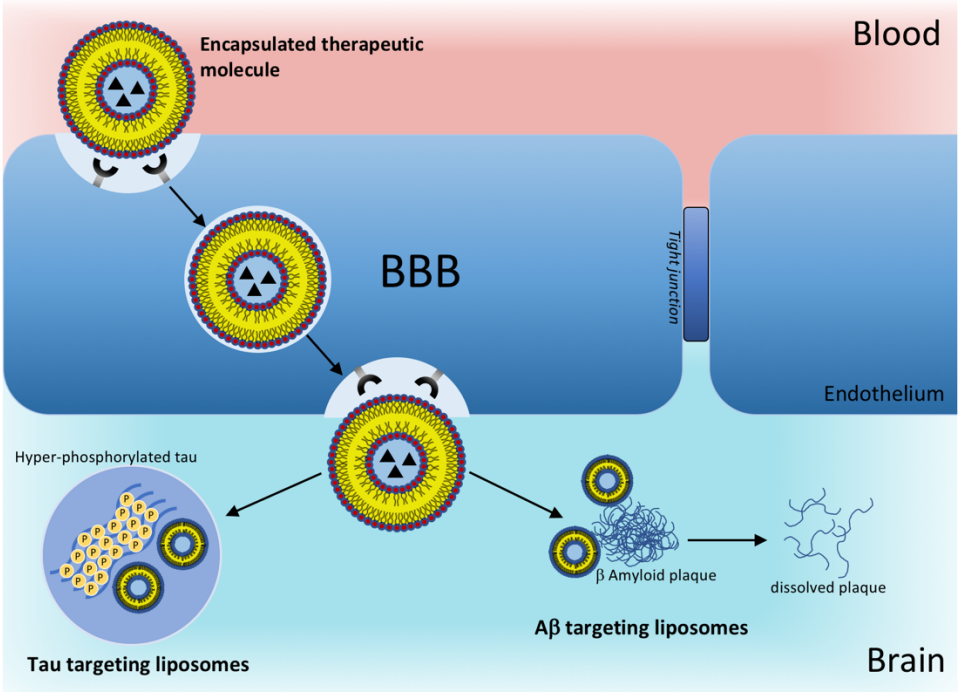

Figure 1.9: Functionalised Liposome AD targets. *Post BBB transport, functionalised liposomes specific for Aβ or Tau will respectively accumulate at Aβ plaques and neurofibrillary Tau tangles. Encapsulated drugs can be released for therapeutic treatment.*

Various types of therapeutic agents can be attached to the surface of the liposomes. These various configurations can be combined to give a targeted multi-drug delivery system, which is particularly relevant for treatment of AD since it is a multifactorial disease (Noble *et al*., 2014). Theoretically, anti-Aβ and anti-Tau molecules can be integrated into one liposome delivery system in order to produce a treatment more potent than current therapies.

1.15.5 Peptide Inhibitor Nanoparticles (PINPs)

A small peptide, named OR2 (RGKLVFFGR-NH_2), inhibits the aggregation of Aβ into oligomers and fibrils, and blocks the toxic effects of Aβ on cultured cells (Austen *et al*., 2008). To improve its stability, a retro-inverso version (RI-OR2) was made (Taylor *et al*., 2010), and this was enhanced further by the addition of a retro-inverted version of TAT to RI-OR2, producing RI-OR2-TAT (Ac-rGffvlkGrrrrqrrkkrGy-NH_2) (Parthsarathy *et al*., 2013). However, RI-OR2-TAT inhibits Aβ aggregation only at relatively high concentrations, (i.e. at a molar ratio of RI-OR2-TAT:Aβ of 1:5 at best) limiting its therapeutic potential.

In order to improve RI-OR2-TAT further, it was attached to the surface of stealth liposomes by covalent linkage to the PEGylated lipid, *via* an additional cysteine residue on the peptide, to produce 'peptide inhibitor nanoparticles' (PINPs) (Gregori *et al*., 2017) (Figure 1.10). The presence of the liposome carrier greatly improves the potency of RI-OR2-TAT, so that a molar ratio of 1:2000 of liposome-linked inhibitory peptide to Aβ now gives ~50% inhibition of Aβ aggregation. This great increase in potency could be due to a multivalent effect. Many copies of the RI-OR2-TAT decorate each liposome, which should allow the simultaneous interaction of multiple inhibitory peptides with any multimeric form of Aβ, so increasing efficiency as an aggregation inhibitor. EM studies (Sherer *et al*., 2015) have shown that PINPs can attach themselves to the free ends of amyloid fibrils, apparently terminating fibril growth, and

preventing the formation of Aβ oligomers (the free ends of fibrils act as 'factories' for generation of oligomeric Aβ) (Eisenberg and Jucker, 2012).

Studies in transgenic mice have shown that peripheral injection of PINPs protects against memory loss in TG2576 mice (Gregori *et al*., 2017). The TAT region of the inhibitory peptide facilitates brain penetration, with a brain:blood ratio of around 50% being achieved shortly after intravenous (i.v.) injection. However, most of the dose accumulates in peripheral tissues, such as lungs, liver, and spleen, most likely due to clearance of liposomes *via* the reticuloendothelial system, and so it is possible that the 'sink' effect could explain some of the *in vivo* properties of PINPs. The effectiveness of these PINPs could be improved in the future by incorporation of alternative or additional modifications.

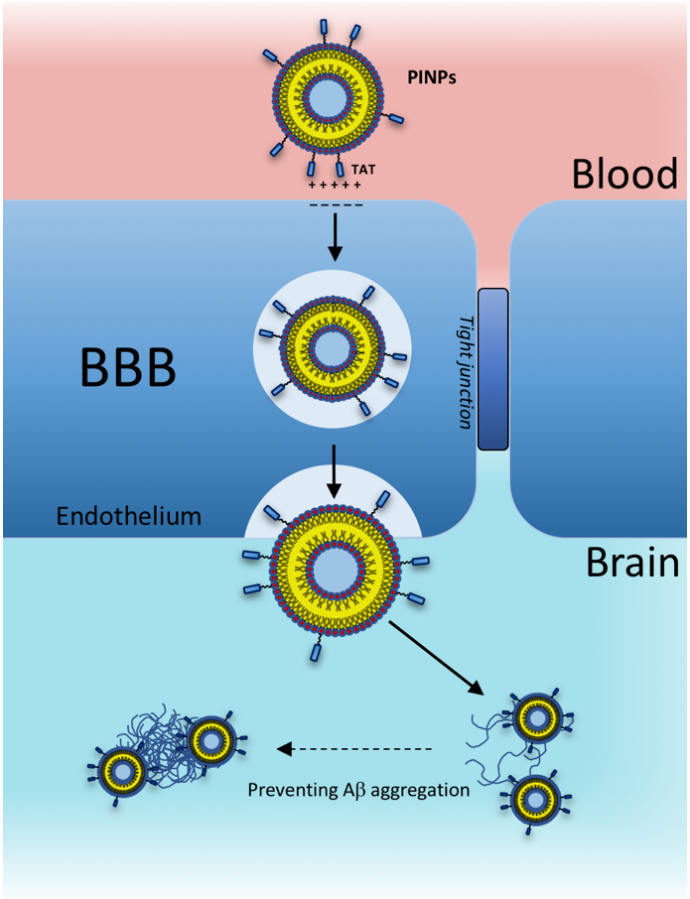

Figure 1.10: Targeting strategy with PINPs. *PINPs transport across the BBB by non-specific endocytosis, triggered by positively charged TAT interaction with the negatively charged membrane. RI-OR2-TAT inhibitor acts to prevent the aggregation of Aβ into oligomers and fibrils.*

1.15.6 Antibody loaded liposomes with RI-OR2-TAT surface modification

In the current study, RI-OR2-TAT has been attached onto liposomes, loaded with monoclonal antibodies. Anti-Aβ (van Dyck, 2018) and anti-Tau (Yanamandra *et al.,* 2017) antibodies have been developed with the therapeutic potential to treat AD. To improve plain and RI-OR2-TAT liposomes for AD therapy, a good strategy looks to load them with anti-Aβ and anti-Tau antibodies, which can then be analysed to determine their therapeutic potential for future use. Liposomes have widely been used for antibody delivery, but studies are limited for AD treatment and even fewer have looked to incorporate antibodies into the hydrophilic core, and instead have involved surface attachment. Rotman *et al* (2015) utilised G-Technology for

the delivery of an anti-amyloid antibody fragment into APP_{swe}/PS1dE9 double transgenic mice, which successfully passed the BBB (Rotman *et al.,* 2015). The current study will utilise the Bangham method to observe the uptake into neuronal cells rather than transport across the BBB. The principles of the study remain the same, to evaluate the potential for the use of antibody incorporated liposomes for AD therapy, by analyzing the ultrastructure, stability and cell penetration efficacy.

1.16 Scope of the Thesis

The aim of this project is to investigate the incorporation of antibodies into the hydrophilic core of liposomes. This involves:

1. Development and refinement of antibody encapsulation in liposomes, and to determine which size liposome is appropriate (50, 100 or 200 nm).
2. Characterise the impact of antibody incorporation on size and shape of the liposomes.
3. Evaluate their ability to penetrate SH-SY5Y neuroblastoma cells, using RI-OR2-TAT for cell penetration, giving an insight into whether these types of liposomes can be used to deliver antibodies into cells.

CHAPTER TWO - Materials and Methods

Table 2.1 Chemicals

Chemical	Producer
Phosphotungstic acid PBS tablets	Sigma – Aldrich (Poole, UK)
Gold nanoparticles	BBI solutions (Cardiff, UK)
Chloroform Methanol Ethanol	VWR Chemicals (Leighton Buzzard, UK)
Ethanol 70%	Fisher Scientific (Loughborough, UK)
LabAssay^{TM} Phospholipid	Wako chemicals (Richmond, USA)

Table 2.2 Lipids

Name	Abbreviation	Producer
Cholesterol (plant derived)	CH	Avanti Polar Lipids Inc., U.S.
Sphingomyelin (Bovine brain)	SM	Avanti Polar Lipids Inc., U.S.
1,2-Distearoyl-*sn*-Glycero-3-Phosphoethanolamine-N-[Maleimide(Polyethylene Glycol)2000] (Ammonium Salt) (mal-PEG-PE)	DSPE-PEG-MAL	Avanti Polar Lipids Inc., U.S.
23-(dipyrromethene boron difluoride)-24-norcholesterol	BDP-Chol (Bodipy)	Avanti Polar Lipids Inc., U.S.

Table 2.3 Antibodies

Antibody	Producer
Immunogold conjugate EM goat anti-fluorescein: 10nm	BBI solutions (Cardiff, UK)
Goat Anti-Fluorescein antibody (Biotin)	Abcam (Cambridge, UK)
Anti-Rabbit IgG F(ab')$_2$-Peroxidase antibody produced in goat	Sigma – Aldrich (Poole, UK)
β-Actin Rabbit mAb (Alexa Fluor 594 Conjugate)	Cell Signalling Technology (Hertfordshire, UK)

Table 2.4 Peptide Inhibitor

RI-OR2-TAT-Cysteine ((Ac-rGffvlkGrrrrqrrkkrGyc-NH$_2$)	Cambridge peptides (Birmingham, UK)

2.1 Buffered solutions

Phosphate buffered saline (PBS) was made with 5 PBS tablets (Sigma – Aldrich) dissolved in 500 mL distilled deionized water to produce 500 mL stock PBS with pH ~7.3 at 25**°**C (10mM phosphate Buffer and 150mM NaCl). Stock was autoclaved to sterilise for further use.

2.2 Development of RI-OR2-TAT antibody loaded liposomes

2.2.1 Preparation of lipids

Sphingomyelin and Cholesterol were weighed at 47.5 molar % and mixed in a glass vial. 5 molar % DSPE – PEG – MAL was then added to the two lipids and the lipid mixture was dissolved in chloroform. The liposome suspension contains a 1:1 molar ratio of sphingomyelin to Cholesterol, with 5% molar DSPE – PEG – MAL. Using 5% DSPE – PEG – MAL in theory allowed ~2.5% entrapped in the liposome and ~2.5% attached to the surface.

2.2.2 Hydration of lipid film

Lipid mixture was dissolved in chloroform, and evaporated under nitrogen stream (~200 bar pressure) in a round bottom tube, rotated manually every few minutes until chloroform was evaporated and a thin lipid film was created (~30 minutes). At this point, antibody (~10 μL per 1 mL sample) was directly added to the lipid film (for liposomes with antibodies incorporated) and incubated at room temperature (RT) for 3 mins. All liposome samples were then resuspended in filtered PBS, pH 7.3 at 5mM lipid. The hydrated lipid film was vortexed to detach the lipid from the glass vial and stored overnight at 4°C. Lipids were alternatively sonicated by bath sonication at RT until the lipid film was not visible and then vortexed to mix.

2.2.3 Antibody incorporation

Antibodies were added after rehydration of the lipid film. The methodology for antibody incorporation was later refined, and antibodies were applied directly to the lipid film before resuspension (as described above).

2.2.4 Freeze and thaw process

Rapid freezing and thawing is necessary to produce nano-liposomes smaller than 200 nm in diameter. It also produces unilamellar vesicles from multilamellar vesicles. (Akbarzadeh *et al.,* 2013). The 4 mL solution with lipid film was shaken, vortexed and then split into 1 mL aliquots in Eppendorfs. Each tube containing the lipid suspension was frozen for 15 secs in liquid nitrogen and thawed using a heating block at 42°C for 3 mins. This process was repeated for 5 cycles per 1 mL sample.

2.2.5 Sonication

The lipid suspensions were then sonicated for 5 minutes at 45°C in an ultrawave bath sonicator.

2.2.6 Liposome extrusion

The Avanti Lipids mini-extruder was used for the extrusion of unilamellar nano-liposomes. After assembly, the system was checked for leaks by pumping one passage of filtered PBS through the membrane. This also moistened the membrane for enhanced liposome passage. For this process, one Hamilton syringe was filled and rinsed with distilled water and then filtered PBS and then pumped through the membrane to the other syringe and discarded. After the system has been checked for leaks, 1 mL liposome suspension was added to a Hamilton syringe which was positioned in the extruder, and passaged slowly through the

system. 11 passages were conducted for each sample. This was repeated for polycarbonate membranes with pore sizes of 50 nm, 100 nm and 200 nm to make different sized liposomes.

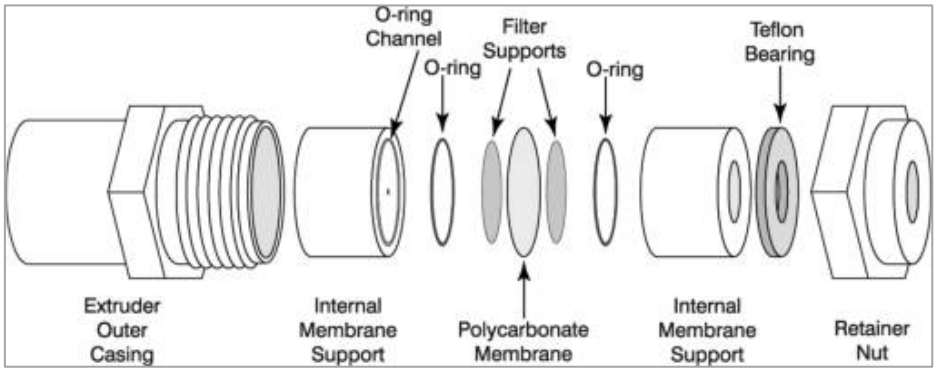

Figure 2.1: Construct of the Avanti lipids mini extruder. *The schematic shows labelled parts and assembly (Avantilipids.com).*

2.2.7 The attachment of RI-OR2-TAT

The peptide inhibitor RI-OR2-TAT was covalently bound to the surface of liposomes by 'click chemistry'. This requires the addition of a cysteine residue, forming RI-OR2-TAT-Cys (Ac-rGffvlkGrrrrqrrkkrGyc-NH_2). This peptide inhibitor was added to the extruded liposomes at 2.5 molar % of the total liposome suspension and incubated at 37°C for 2 hours. The inhibitor covalently bound to the DSPE – PEG – MAL, which is statistically at 2.5 molar % on the liposome surface (5% total, 2.5% internalised and 2.5% on the surface). Washing steps were taken to remove any unbound peptide or antibody that was not incorporated inside the vesicles. The mixture was centrifuged at 50k RPM for 1 hour at 4°C (70.1 Ti rotor). The supernatant was discarded and the pellet was resuspended in 1 mL filtered PBS and vortexed to mix the solution. Liposomes produced were stored at 4°C.

The above procedure can also be conducted to produce antibody loaded PEGylated liposomes. For this, the above protocol was followed without the inclusion of the RI-OR2-TAT attachment. Similarly, plain PEGylated liposomes were made without antibody incorporation steps.

Fluorescent liposomes were also produced following the same procedure, using a different composition of lipids. Fluorescent cholesterol is included at 1% of the total cholesterol (0.475 molar % of the total liposome solution). During the preparation of fluorescent liposomes the whole procedure was carried out in a darkened room because fluorescent cholesterol is sensitive to light.

2.3 Dynamic Light Scattering (DLS)

Analysis of liposome size, polydispersity index (PDI) and zeta potential was obtained by DLS using a Zetasizer Nano ZS instrument (Malvern Instruments Ltd., U.K.) at 25°C. Small samples (~40 µL) were added to disposable micro cuvettes, and larger samples (~1 mL) were added to disposable cells, both of which were suited for the instrument. Photon Correlation Spectroscopy determined the particle size and PDI by measuring Brownian motion of the particles in the samples. This worked on the theory that movement speed of liquid is dependent on the size of the particle. Backscatter was measured at 175°. Data was obtained in triplets and presented as a mean of these repeats. Specialised disposable cuvettes were used to measure zeta potential (Malvern Instruments Ltd., U.K.).

2.4 Phospholipid WAKO assay (Choline oxidase-DAOS method)

The concentration of liposomes was performed using the Phospholipid B WAKO assay kit. It worked on the basis that the quantification of sphingomyelin can be measured by an enzymatic reaction using N-ethyl-N-(2-hydroxy-3-sulfopropyl)-3,5- dimethoxyaniline (DAOS) as a blue pigment. Measurements gained were analysed to obtain the overall liposome concentration.

2.4.1 Preparation of solutions

The assay used three standard phospholipid concentrations, which was extended to five by further dilutions with deionized water (Table 2.5). 50 mL Chromogenic substrate were dissolved into 50 mL assay buffer (1:1) and mixed. All solutions were stored at 4°C.

Phospholipid concentration (mg/mL)	Standard Dilution	Sample volume
0.375	1/8	2μL
0.75	1/4	2μL
1.5	1/2	2μL
3	Undiluted	2μL
5.961	Undiluted	4μL

Table 2.5: Preparation of phospholipid standards for the WAKO assay.

2.4.2 Chromogenic assay

Assay was completed using a clear 96 well plate (ThermoFisher) and all samples were performed in triplicates. Standard samples volumes were added to wells according to Table. 2 μL of each lipid or liposomes suspension was added to each well. Chromogenic substrate was added to each well to produce a final volume of 300 μL. The plate was shaken well and then incubated at 37°C for 5 mins. Absorbance was measured at 600 nm on a plate reader. 700 nm absorbance was also taken, to account for background.

2.5 Transmission Electron Microscopy (TEM)

PEGylated liposomes of three sizes (50 nm 100 nm and 200 nm), antibody loaded liposomes and liposomes with attached RI-OR2-TAT inhibitor were prepared and examined by TEM.

2.5.1 Preparation of liposomes on TEM grids

The heavy metal phosphotungstic acid (2%) (PTA) was used for liposome staining. For preparation, 0.1 g PTA stock was dissolved in 4 mL distilled H_2O (dH_2O). The solution was vortexed for 1 min and mixed with a magnetic stirrer for 5 mins, then filled to 5 mL with dH_2O. Liposomes were pipetted onto Formvar copper grids (G2004, 400Thin, copper 3.05 mm – ATHENE). ~20 µL of liposome solution (1 mM) was added to the shiny copper side of the grid for 2 mins so that the liposomes were adsorbed. The surplus was removed with filter paper. ~5 µL of 2% PTA was added and left for 2 mins. Filter paper was again used to remove the surplus and the samples were left to dry at RT. Grids were stored in a glass petri dish until they were ready for further use. Samples that incorporated gold conjugates did not require PTA staining, and so the procedure was conducted in absence of PTA incubation.

2.5.2 TEM and image processing

The film plates (Kodak Electron Microscopy Film 4489, Agar scientific, UK) used for image capture and underwent dehydration using a vacuum desiccator before capture. The TEM (JEOL JEM 1010) was then used for the capture of images, and the exposed film plates were stored in complete darkness until further use. Developer was prepared at approximately 20°C and consisted of 1 part developer to 4 parts distilled water. In a dark room, the films were transferred to a black developing rack, then immersed in developer (Ilford phenisol developer) contained in a black vessel and left for 4 mins. The rack was washed, and then moved into a container with fixation solution (Ilford hypam fixer) for 4 mins. At each stage, the developing rack was agitated every 1 min to allow effective development of films. The rack was then

transported out of the dark room, and placed in a water bath for 2 hours with a fresh water flow. ~5 drops of wetting agent (Kodak foto – flo) was added 5 mins prior to the end of the 2 hour water bath incubation. Afterwards, racks were air-dried overnight. Images were scanned, then processed using TEM Analysis software and edited using Image J and Microsoft Office. Some images were alternatively captured with a TEM digital camera (AMT Nano sprint 500 sCMOS) and analysed with Advanced Microscope Techniques (AMT) software (AMT Capture Engine).

2.6 Cell penetration assay

In order test the ability of prepared liposomes to penetrate cells, a cell penetration assay was designed using various liposome modifications and a neuroblastoma (SH-SY5Y) cell line. Cells were grown in Dulbecco's Modified Eagle Medium and F12 (DMEM/F12 – 1:1 ratio), containing 10% Fetal Calf Serum and 1% antibiotics (Streptomycin and Penicillin – 1:1 ratio) and grown at 37°C and 5% CO_2.

2.6.1 Cell maintenance

Cells were grown as above and the medium was changed every 3-7 days and cells were split at ~80% confluency. For splitting, cells are detached with trypsin by incubation at 37°C and 5% CO_2, centrifuged at 1000 RPM for 7 mins at 25°C and the pellet was resuspended in growth medium as described, and transferred into a new flask.

2.6.2 Immunostaining of SH-SY5Y cells

Liposome cell penetration was studied by immunostaining SH-SY5Y cells. Fluorescent (BODIPY) cholesterol and β-Actin Rabbit mAb (Alexa Fluor) were used for fluorescence observation. Cells were grown in 6 well plates with DMEM growth medium. Cover slips were incubated in the cell culture for 24 h at 37°C and 5% CO_2, where cells grew on the surface of the cover slips.

Liposomes of varying concentrations (50 µM, 100 µM and 200 µM) and properties were added to each well and incubated for 2 h at 37°C and 5% CO_2. A spiking solution of 2% PFA in PBS was prepared into each well and incubated at RT for 2 minutes. The cover slips were then washed and incubated with 4% PFA at RT for a further 20 minutes. 3 µL antifade mountant with DAPI (Invitrogen – Gibco®) was added to glass slides. Coverslips were removed from the wells and placed cell slide down onto the Fluoroshield and allowed to dry at RT for 24 h. Samples were examined under confocal microscope (LSM 510 – Laser Module – Zeiss).

2.7 Ethics and data analysis

2.7.1 Ethical consideration

All experimentation was submitted to the University of Lancaster research and ethical body. Research undertaken was considered to be acceptable and was therefore approved.

2.7.2 Statistical analysis

Microsoft excel and SPSS statistical software was used for data analysis, evaluation and the production of figures and tables. A variety of analytical tests were used for analysis, including Paired and un-paired T-tests and one way ANOVA. Each were used appropriately for different types of data.

CHAPTER THREE – Dynamic Light Scattering Results

3.1 Characterisation of liposomes by size

Dynamic light scattering (DLS) was used to assess the diameter, polydispersity and stability of each liposome size (50 nm, 100 nm and 200 nm) and type (Table 3.1) produced according to protocol (Zetasizer Nano ZS, Malvern Instruments Ltd., U.K.). Standard gold nanoparticles of distinct sizes were also examined to calibrate the system for liposome measurements. Table 3.1 shows the abbreviations used for each type of liposomes, which are consistent throughout each section of the thesis.

Abbreviation	Liposome modification
PEG-NLs	Plain liposomes of sphingomyelin (SM) and cholesterol (CH), with the addition of DSPE-MAL-PEG.
AB-NLs	PEGylated liposomes with antibodies incorporated in the hydrophilic core.
RI-OR2-TAT-NL	PEGylated liposomes with attached RI-OR2-TAT peptide inhibitor.
RI-OR2-TAT+AB-NL	PEGylated liposomes with attached RI-OR2-TAT and incorporated antibodies.

Table 3.1: The different types of liposomes produced for experimentation. *All of the liposomes above were used in various experiments.*

3.2 Standard gold nanoparticles

Four distinct sizes (20 nm, 40 nm, 60 nm and 80 nm) of nanogold were used for calibration. Each size of gold particle was examined at the most suitable dilution. Each dilution was prepared using filtered Phosphate Buffered Saline (PBS). The optimal 80 nm nanogold dilution of 1:250 gave mean size and standard deviation (±SD) of 79.09 ± 28.68 nm. The 60 nm nanogold dilution of 1:250 gave mean size of 57.20 ± 20.29 nm. The 40 nm nanogold dilution of 1:500 gave mean size of 40.39 ± 14.48 nm. The 20 nm nanogold dilution of 1:500 gave mean size of 23.59 ± 8.996 (Figure 3.1).

PDI is a measurement of the polydispersity, performed by DLS, that was observed to determine the size distribution of the gold standards. High PDI can be a result of a wide distribution of sizes or multiple peaks in one population. Gold nanoparticles of 80 nm, 60 nm, 40 nm and 20 nm all had one peak with PDI of 0.115, 0.137, 0.148 and 0.167, respectively (Figure 3.2).

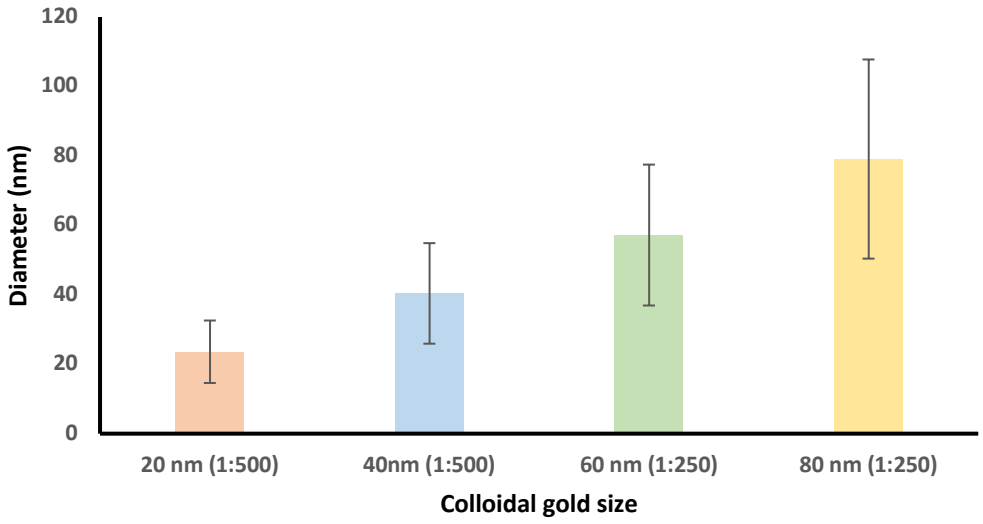

Figure 3.1: Average diameter of gold nanoparticles at optimal dilutions. *Bars show mean diameter ± SD at optimal dilutions of different gold nanoparticles. The larger gold nanoparticles diluted at 1:250 showed unexpectedly high SD.*

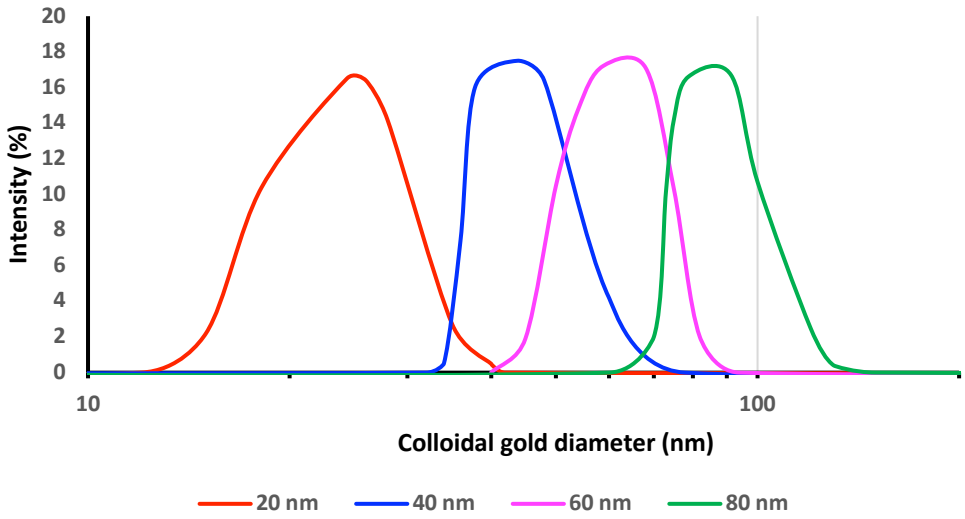

Figure 3.2: Size distribution of gold nanoparticle standards at optimal dilutions*. The red, blue, pink and green lines represent 20 nm, 40 nm, 60 nm and 80 nm gold nanoparticles at optimal dilutions. The PDI of the particles is higher than expected, with many overlapping size distributions.*

3.3 PEGylated liposomes

PEG-NLs are composed of sphingomyelin (SM), cholesterol (CH) and DSPE-MAL-PEG in a molar ratio of 47.5% SM, 47.5% CH and 5% PEG. PEG allows the formation of a lipid molecule with increased stability in blood circulation in order to maximise brain delivery of incorporated therapeutics (Wang *et al.,* 2012). Optimum dilutions of PEGylated liposomes were determined by analysis of the gold nanoparticle results. Three sizes (200 nm, 100 nm and 50 nm) of liposomes were produced and examined by DLS. In the case of 200 nm PEGylated liposomes, a 1:125 dilution gave mean size of 213.50 $\pm$ 9.30 nm. The dilution of 100 nm liposomes gave mean size 180.30 $\pm$ 5.16 nm. The dilution of 50 nm liposomes gave mean size of 49.51 $\pm$ 0.49 nm (Figure 3.3).

The 200 nm PEG-NLs had a PDI of 0.373. They were widely distributed with a broad peak observed at 220.20 nm and a tighter peak at 5560 nm (Figure 3.4). The 100 nm PEG-NLs had a

PDI of 0.44, with a fairly broad peak at 164.2 nm and a tighter peak at 4460 nm. The 50 nm PEG-NLs had a PDI of 0.282, with distinct peaks of 220.70 nm and 50.75 nm.

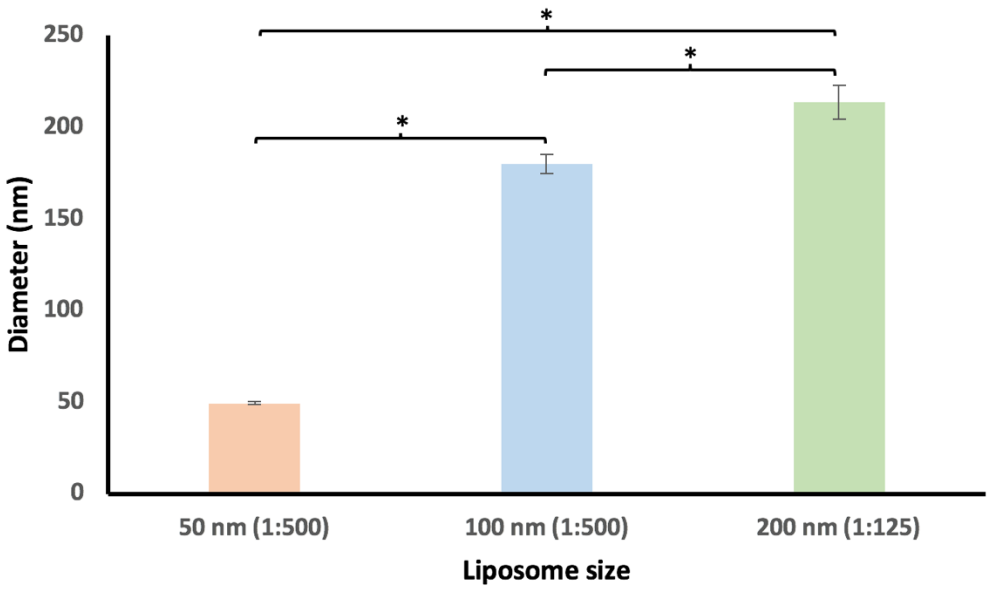

Figure 3.3: PEG-NLs at optimal dilutions. *Bars show mean diameter ±SD (n=3) at optimal dilutions of different sized PEG-NLs . Results were significant at a 5% confidence level (P=0.0034).*

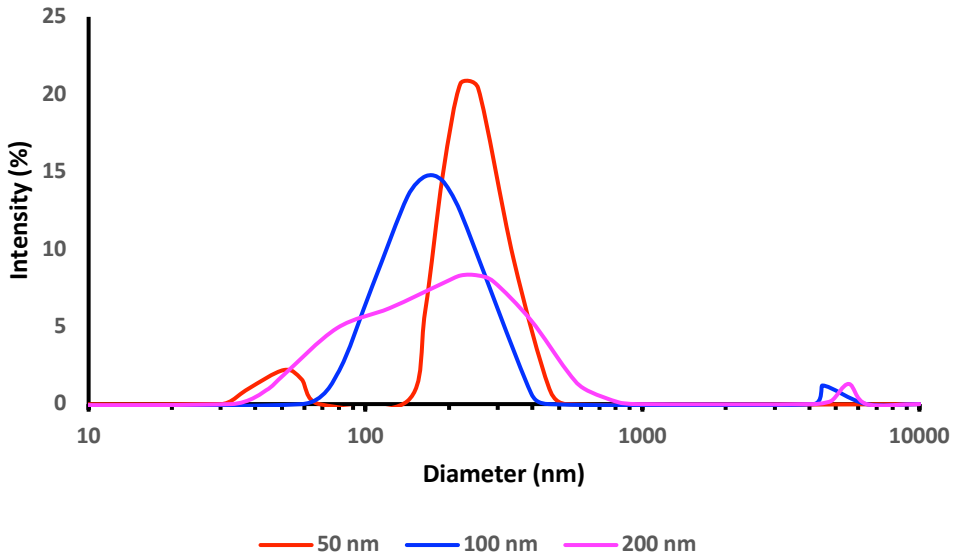

Figure 3.4: Size distribution of PEG-NLs. *The red, blue and pink lines represent 50 nm, 100 nm and 200 nm liposomes at optimal dilutions. 200 nm is widely distributed and highly polydisperse. 50 nm are larger than expected, with the strongest peak at 220.20 nm. 100 nm are the most monodisperse.*

3.4 Antibody loaded liposomes

AB-NLs are composed of SM, CH and DSPE-MAL-PEG in a molar ratio of 47.5%, 47.5% and 5%. During liposome preparation, β-Actin Rabbit mAb Alexa Fluor 594 Conjugate (Alexa Fluor) was added to the lipid film before rehydration and incubated at RT for 3 mins. Optimal dilutions for loaded liposomes were determined from the PEGylated liposomes results. 200 nm and 100 nm antibody loaded liposomes were prepared and compared to plain PEGylated liposomes.

The 200 nm antibody loaded liposomes 1:125 dilution gave a mean diameter of 213.5 ± 9.68 nm. They had a PDI of 0.362 and were distributed as one distinct peak (Figure 3.5 and 3.6). The 100 nm antibody loaded liposomes 1:500 dilution gave a mean size of 196.7 ± 9.51 nm. They had a PDI of 0.362 and were distributed as one distinct peak (Figure 3.7 and 3.8).

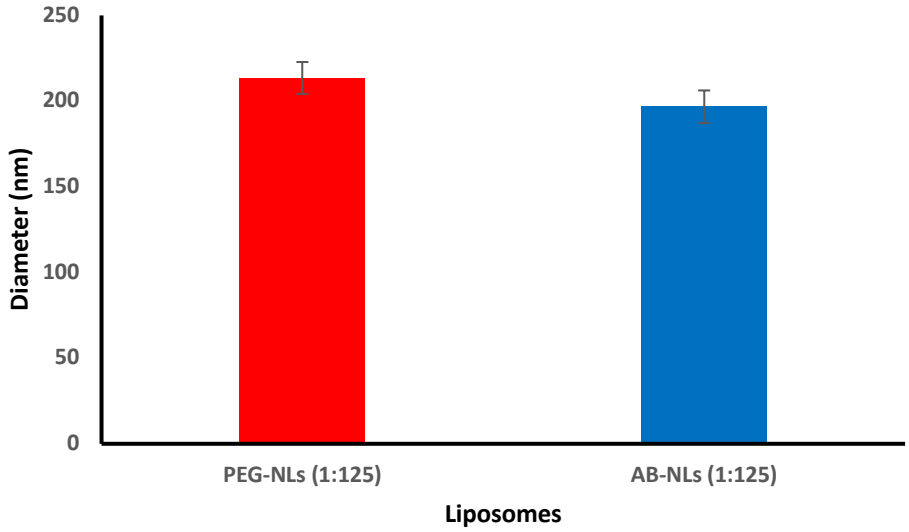

Figure 3.5: PEG-NLs and AB-NLs (200 nm). *Bars show mean diameter ± SD (n=3) at optimal dilutions of 200 nm PEG-NLs and AB-NLs. Results were insignificant, as expected.*

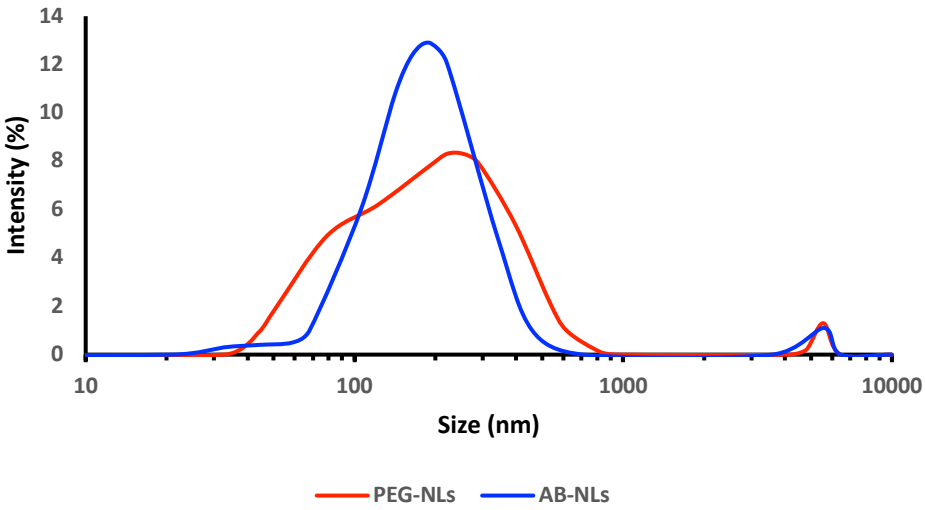

Figure 3.6: Size distribution of PEG-NLs and AB-NLs (200 nm). *The red and blue line represent PEG-NLs and AB-NLs respectively. AB-NLs were unexpectedly more monodisperse than the PEG-NLs.*

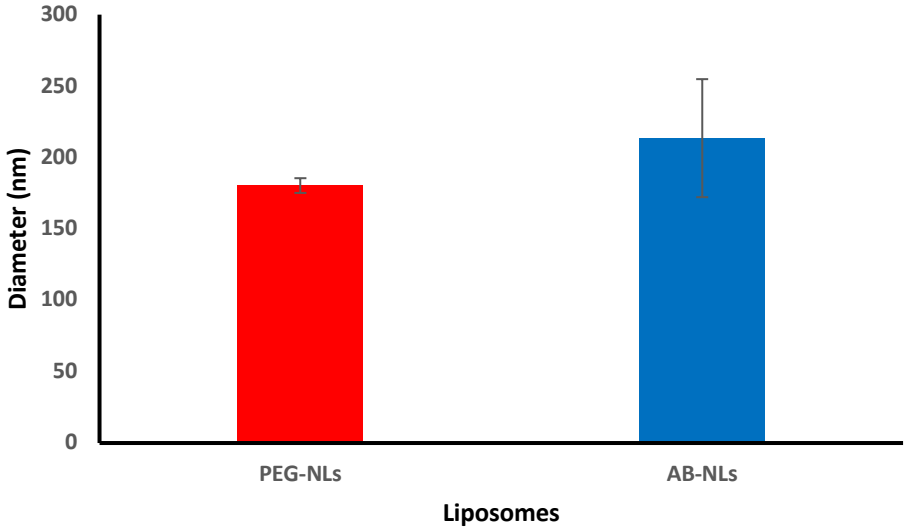

Figure 3.7: PEG-NLs and AB-NLs (100 nm). *Bars show mean diameter ± SD (n=3) at optimal dilutions of 100 nm PEG-NLs and AB-NLs. Results were insignificant, as expected.*

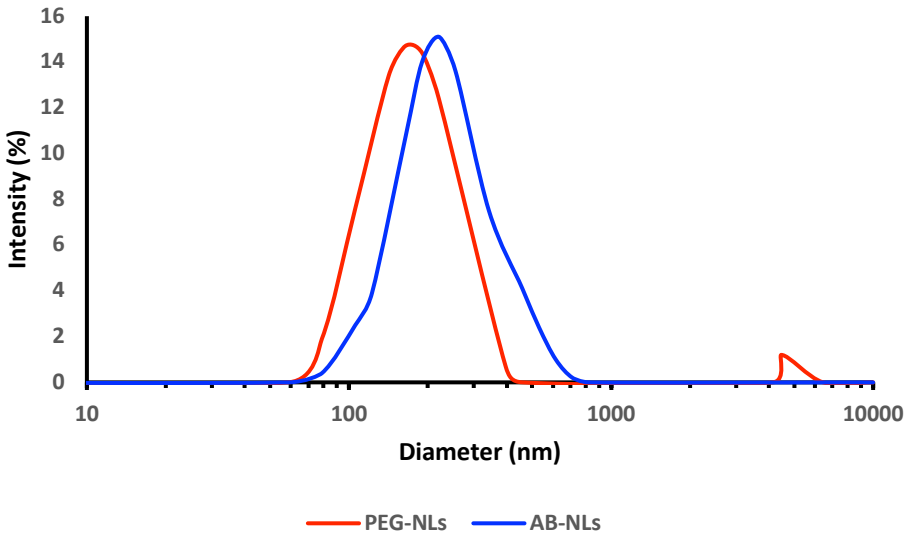

Figure 3.8: Size distribution of PEG-NLs and AB-NLs (100 nm). *The red and blue line represent PEG-NLs and AB-NLs respectively. There was no significant difference between distribution.*

3.5 RI-OR2-TAT and RI-OR2-TAT+AB modified liposomes

Antibody loaded liposomes were prepared as before, with additional attachment of RI-OR2-TAT-Cysteine ((Ac- rGffvlkGrrrrqrrkkrGyc-NH_2) peptide inhibitor. The RI-OR2-TAT attaches to liposomes via click chemistry, and has a TAT CPP sequence capable of enhancing cell internalization. Liposomes (100 nm in diameter) were produced with RI-OR2-TAT and antibody (Alexa Fluor) loaded RI-OR2-TAT modification. A diameter of 100 nm (1:500 dilution) was used based on previous antibody loaded liposome results and the fact that 100 nm liposomes are stable in blood circulation, suitable for BBB transportation and for neuronal cell uptake. These RI-OR2-TAT-NLs and RI-OR2-TAT+AB-NLs were compared with PEG-NLs and AB-NLs.

Figure 3.9 and 3.10 show the DLS results of these modifications. The RI-OR2-TAT+AB-NLs dilution gave a mean diameter of 363.4 $\pm$ 60.72 nm. They had a PDI of 0.469 and were distributed with two distinct peaks. RI-OR2-TAT-NLs gave a mean diameter of 279.2 $\pm$ 46.62 nm. They had a PDI of 0.559 and were distributed with two distinct peaks.

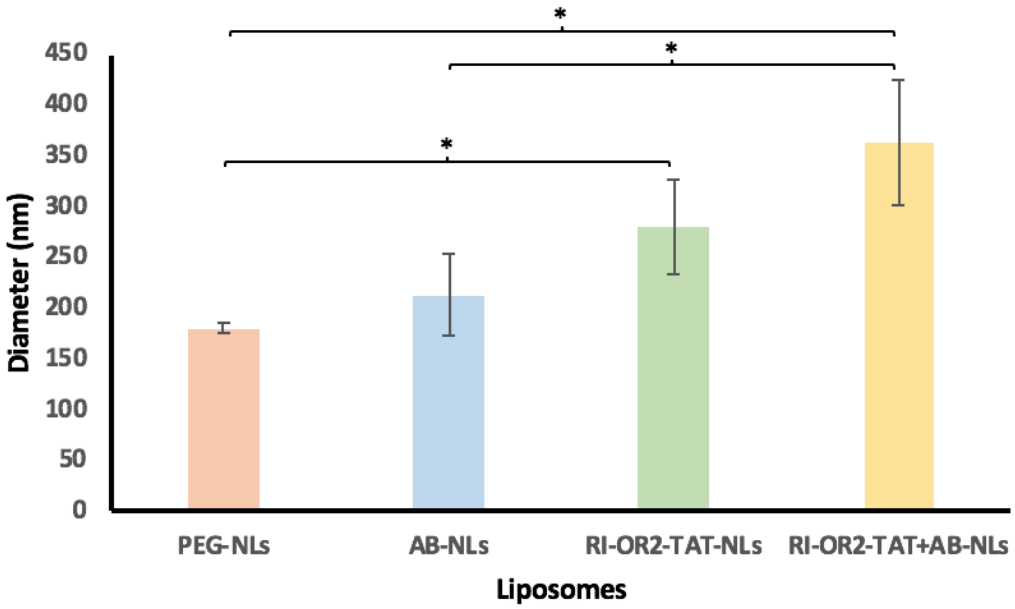

Figure 3.9: Diameter of various liposome modifications (100 nm). *Bars show mean diameter ± SD (n=3) at a 1:500 dilution of RI-OR2-TAT+AB-NLs, RI-OR2-TAT-NLs, AB-NLs and PEG-NLs. The RI-OR2-TAT- and RI-OR2-TAT+AB-NLs had significantly increased diameter than expected.*

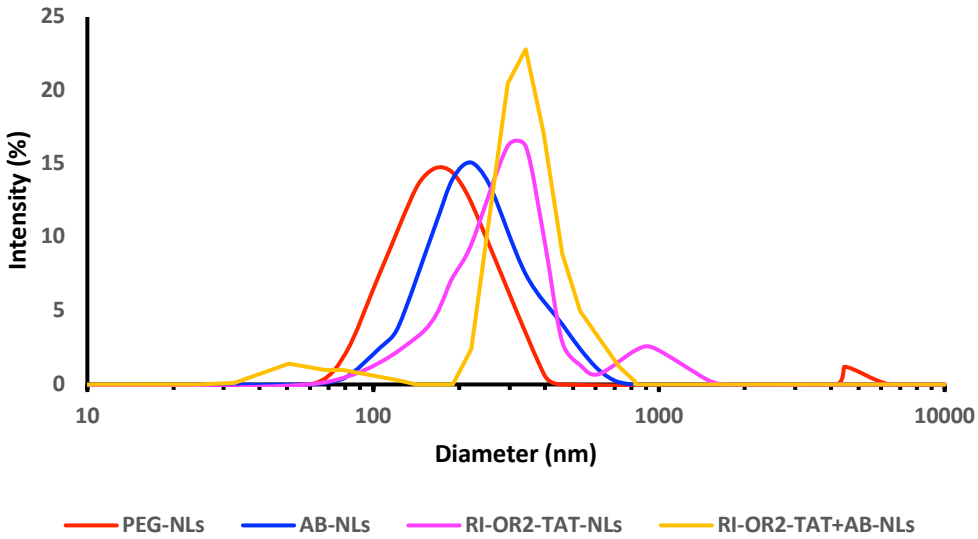

Figure 3.10: Size distribution of various liposome modifications (100 nm). *The red, blue, pink and yellow line represent PEG-NLs, AB-NLs, RI-OR2-TAT-NLs and RI-OR2-TAT+AB-NLs respectively at a 1:500 dilution. Both RI-OR2-TAT- and RI-OR2-TAT+AB-NLs unexpectedly had increase diameter and distribution.*

CHAPTER FOUR – Transmission Electron Microscopy Results

4.1 The characterisation of liposomes by Transmission electron microscopy (TEM)

The morphology and ultrastructure of four types of nanoliposomes was investigated using TEM. This powerful imaging tool cannot determine behavioural or chemical differences between NL, AB-NL, RI-OR2-TAT-NL, RI-OR2-TAT+AB-NL but will highlight differences between their size and shape. TEM is additionally able to identify an antibody that is conjugated with a heavy metal, e.g. gold. A key structural property TEM can reveal is the lamellarity of liposomes. Freeze thaw and sonication steps in the preparation method aid the formation of unilamellar rather than multilamellar vesicles, which are desirable for therapeutic application. However, additional modifications (such as RI-OR2-TAT attachment) may also impact on vesicle lamellarity. TEM samples were prepared using 3 mM liposomes diluted with filtered PBS. Overall, this was an appropriate concentration, yet occasionally samples were too dilute with few vesicles present. Regardless of this, all samples had a tendency to clump.

4.2 The characterisation of PEG-NLs

PEG-NLs were prepared and negatively stained with phosphotungstic acid (PTA) for visualisation. Micrographs of 50 nm, 100 nm and 200 nm NLs were prepared for TEM analysis.

4.2.1 PEG-NLs - 50 nm

The following negative staining micrographs include liposomes of 50 nm in diameter. Liposomes were subjected to freeze and thaw and bath sonication during their preparation in expectation to produce unilamellar vesicles. As shown, vesicles were all regular in size and unilamellar (Figure 4.1).

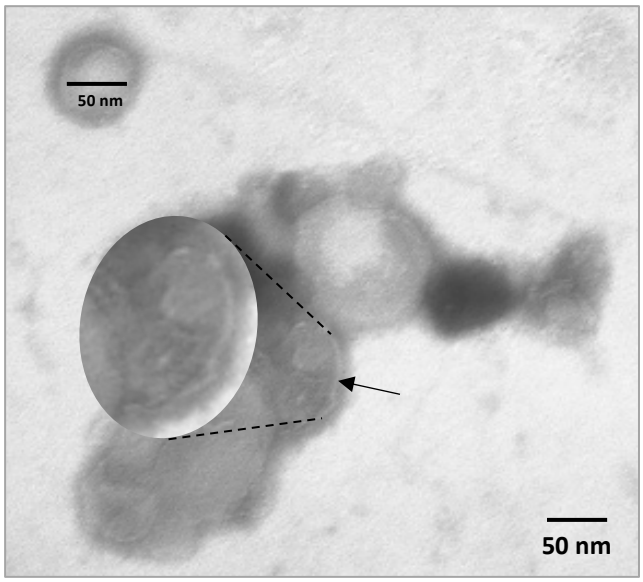

Figure 4.1: 50 nm PEG-NLs in filtered PBS. *The liposomes are seen as round in shape with diameter close to 50 nm. Arrow shows unilamellar structure and dashed line shows the single layer at higher magnification. Scale bar = 50 nm.*

4.2.2 PEG-NLs - 100 nm

The following negative staining micrographs show liposomes of 100 nm in diameter. Liposomes were subjected to freeze and thaw and bath sonication during their preparation in expectation to produce unilamellar vesicles. Liposomes were fairly irregular in shape and varied in size (Figure 4.2).

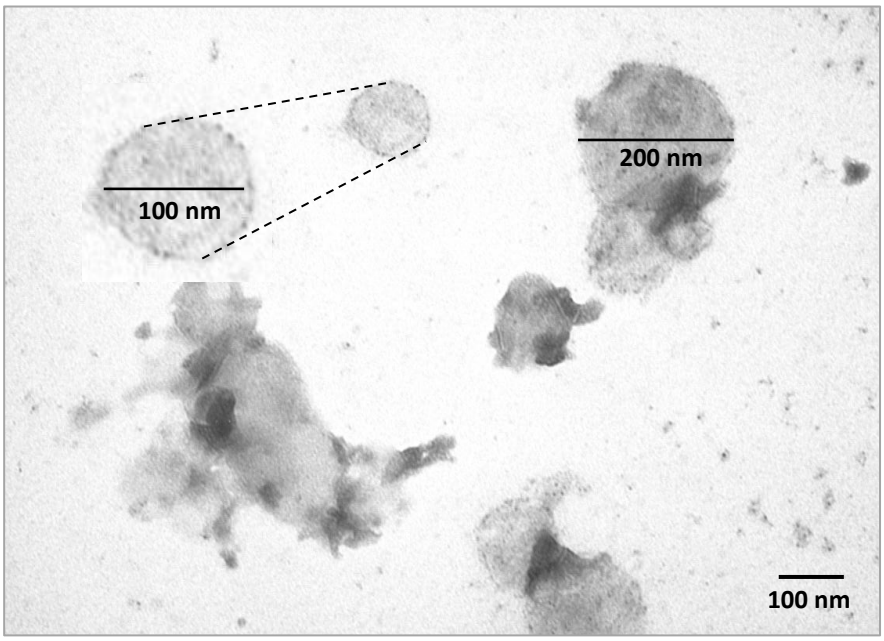

Figure 4.2: 100 nm PEG-NLs in filtered PBS. *The liposomes are seen as round in shape and vary in diameter with some close to 100 nm. Dashed line shows a liposome 100 nm in diameter at a higher magnification. Note that some liposomes have greater diameters (200 nm). Scale bar = 100 nm.*

4.2.3 PEG-NLs - 200 nm

The following negative staining micrographs include liposomes of 200 nm in diameter. 200 nm liposomes were not subjected to freeze and thaw and bath sonication during their preparation, as it decreases the diameter of produced vesicles.

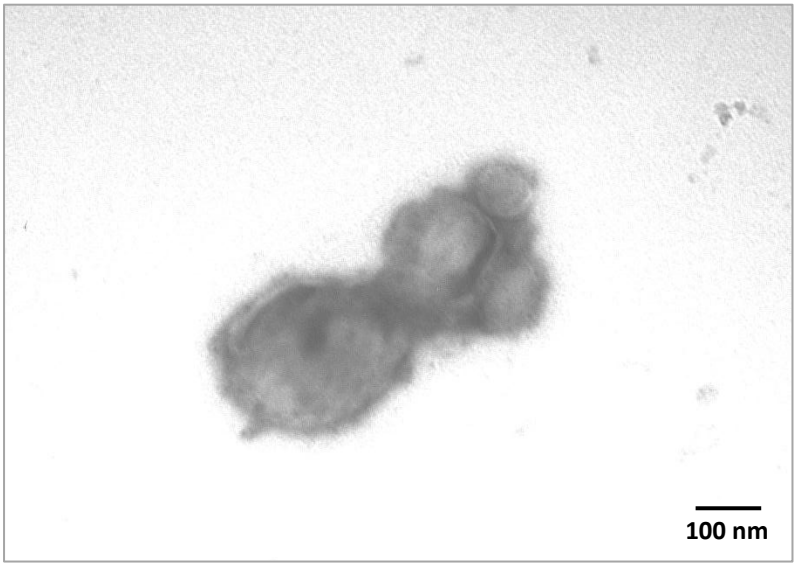

Figure 4.3: 200 nm PEG-NLs in filtered PBS. *The liposomes are seen as round in shape and vary in diameter with some close to 200 nm. Scale bar = 100 nm.*

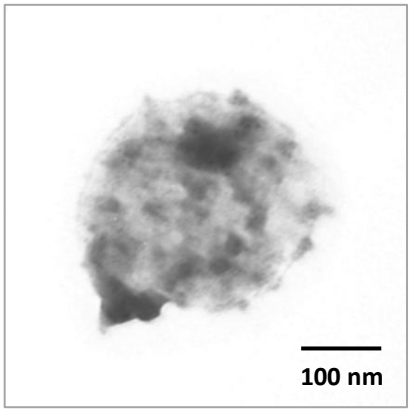

Figure 4.4: Increased magnification of 200 nm PEG-NLs in filtered PBS. *The liposome is round in shape and approximately 200 nm in diameter.*

4.3 The characterisation of immunogold conjugated AB-NLs

PEGylated liposomes were produced with the incorporation of gold-conjugated antibodies (AB-NLs) to produce loaded liposome samples for TEM analysis. Immunogold (10 nm) conjugated goat anti-fluorescein antibody was used for liposome incorporation. This antibody is a gold conjugate and can be visualised by TEM despite its small diameter. The vesicles therefore did not require negative PTA staining for visualisation. Consideration was given to the incorporation step for antibody loading. Liposomes of 200 nm in diameter were loaded with antibody at two different stages of production. Liposomes were additionally washed to remove non-bound excess antibody. Liposomes of 200 nm diameter were thought to be the best candidate to obtain the highest antibody encapsulation efficiency.

4.3.1 AB-NLs (after lipid film rehydration) - 200 nm

At first, the antibody was added to the preparation after rehydrating the lipids in filtered PBS. Immunogold conjugate (10 μL) was added to the 200 nm liposome sample (3 mM). As shown, the vesicles were regular in shape, but varied in size (Figure 4.5 and 4.6). The antibody appeared to be randomly distributed, with no evidence for selective incorporation into any particular liposomal compartment, i.e incorporation over random distribution.

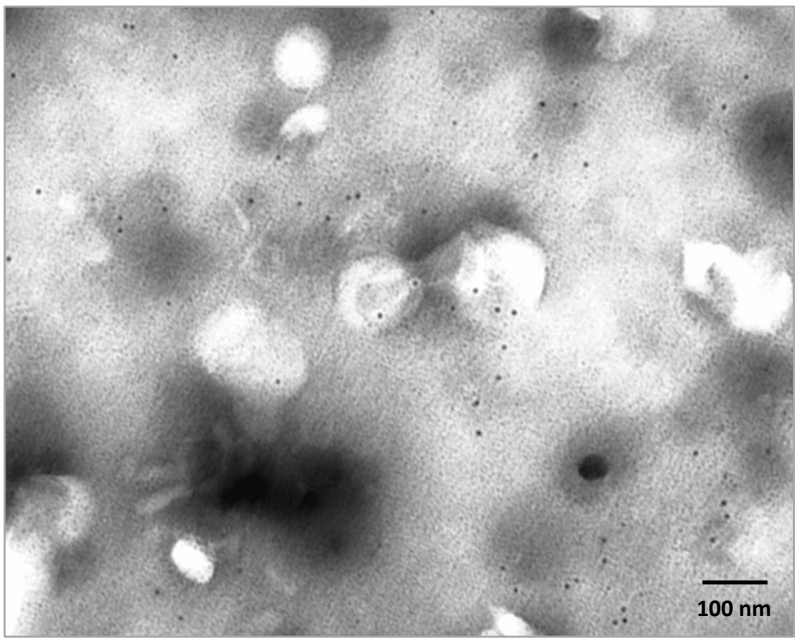

Figure 4.5: First attempt at AB-NLs (200 nm) in filtered PBS *The negative staining micrograph shows liposomes with gold-conjugated antibody added after lipid film rehydration in filtered PBS. The liposomes are round in shape and smaller than 200 nm in diameter. The antibody appears to be randomly distributed.*

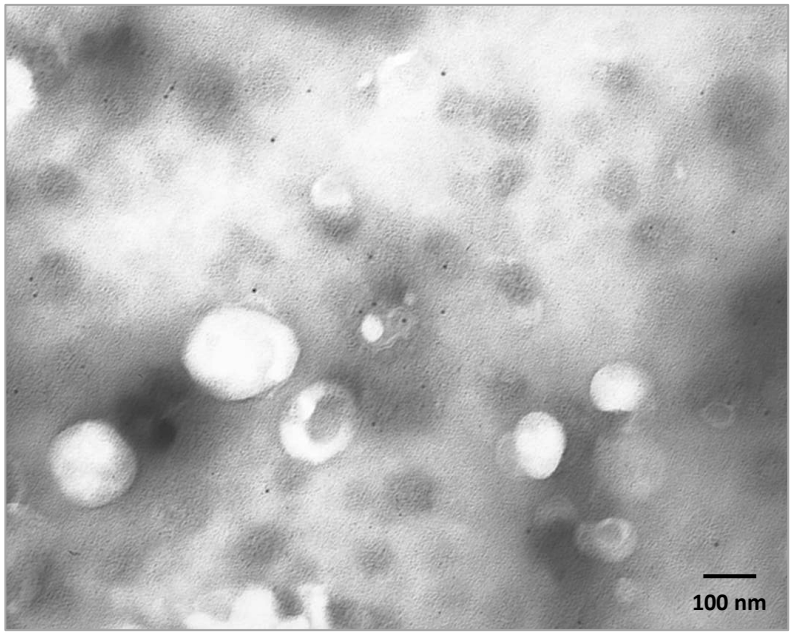

Figure 4.6: First attempt at AB-NLs (200 nm) in filtered PBS. *The negative staining micrograph shows liposomes with gold-conjugated antibody added after lipid film rehydration in filtered PBS. The liposome is round in shape and smaller than 200 nm in diameter. Antibodies appear randomly distributed, not many are contained within liposomes.*

Figure 4.7 gives a graphical comparison between the number of antibody-conjugated gold particles found to be residing inside liposomes (40.05 ± 13.81 per µm^2) and those in surrounding non-liposomal areas (11.74 ± 3.92 per µm^2). There was no significant difference between the number of gold particles found associated with liposomes and those in the surrounding area.

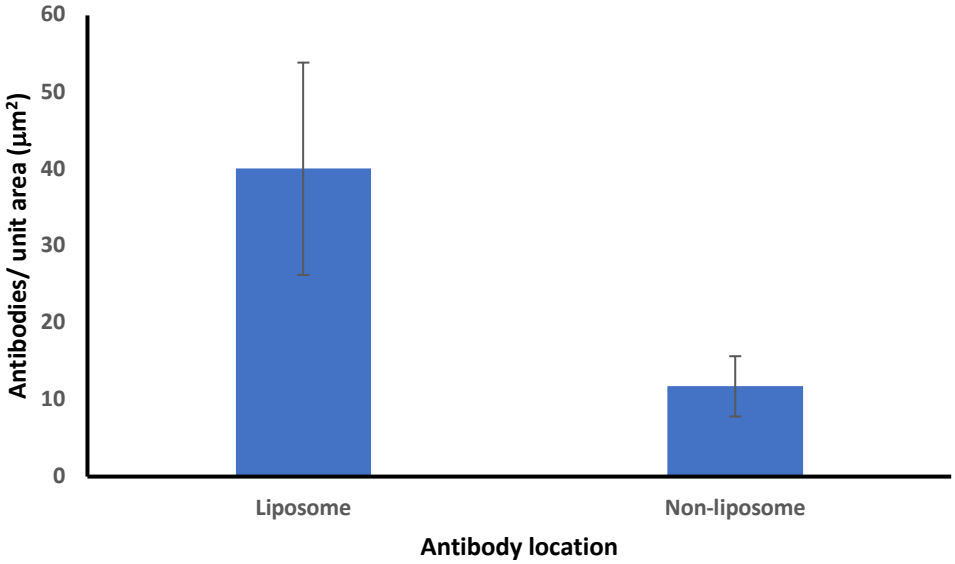

Figure 4.7: Gold-conjugated antibody found in liposome and non-liposomal areas, when added after rehydration. *The graph shows gold particles/unit area (µm^2) on the y-axis and antibody location (liposomal or non-liposomal area) on the x-axis. Bars show average ±SD (n=9) at a 3 mM concentration of antibody loaded liposomes. There was no significant difference between them (p=0.067).*

4.3.2 AB-NLs (before hydration, no wash) - 200 nm

Due to the results obtained when antibody was added after the lipid rehydration step, an alternative method was conducted in order to increase the encapsulation efficiency of antibody into liposomes so that there is clear selective incorporation into the liposomes in comparison with the surrounding area. This involved the addition of antibodies to the lipid mixture before rehydration in filtered PBS. The theory is that incubation of the dry lipid film with antibody would allow more effective encapsulation when vesicles are subsequently formed upon rehydration (Figure 4.8). Therefore, 10 µL of immunogold conjugate was added to the lipid film, incubated for 3 mins, and vortexed extensively. Filtered PBS (1 mL) was added and the liposomes were otherwise produced as normal.

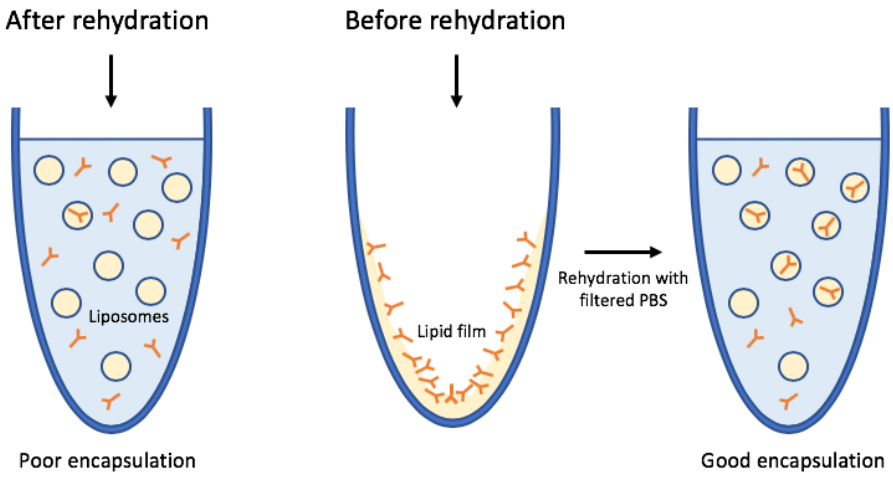

Figure 4.8: Schematic showing the two methods of antibody encapsulation in liposomes. *Antibodies were first added after the rehydration of the lipid film with filtered PBS (a). A second strategy applied the antibodies to the lipid film before rehydration, which was likely to improve the encapsulation efficiency (b).*

The 200 nm antibody loaded liposomes (before rehydration) were regular in shape but were often considerably larger than expected (Figure 4.9 and 4.10). Lipids appear as droplets rather than liposomes. The gold particles showed much better association with the lipid vesicles.

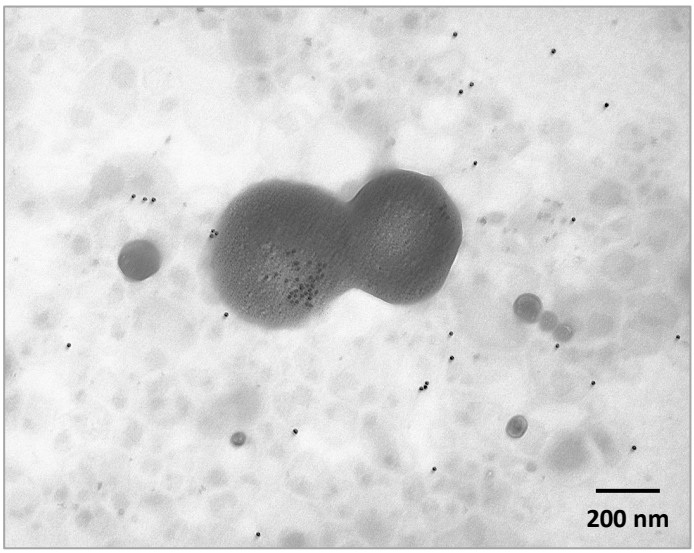

Figure 4.9: Alternative method for antibody loaded liposomes (200 nm) in filtered PBS. *The negative staining micrograph shows antibodies added before the lipid film rehydration in filtered PBS. The liposomes are irregular in shape and structure with increased diameter than expected. Antibodies appear to be clustered at vesicles.*

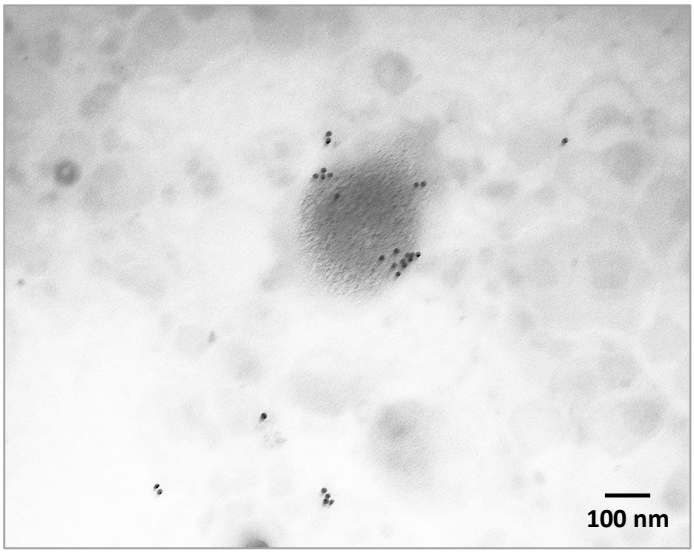

Figure 4.10: Alternative method for antibody loaded liposomes (200 nm) in filtered PBS. *The negative staining micrograph shows antibodies added after lipid film rehydration in filtered PBS. The liposomes are irregular in shape and structure with diameter close to 200 nm. Antibodies appear to be clustered at vesicles.*

Figure 4.11 shows a graphical comparison between the numbers of gold-conjugated antibodies associated with liposomes and those in surrounding non-liposomal areas. The liposomal area gave a mean count of 103.84 ± 17.29 gold particles/μm^2, whereas the non-liposomal area gave a mean count of 2.07 ± 0.66/μm^2, with this difference being statistically significant ($p<0.0001$).

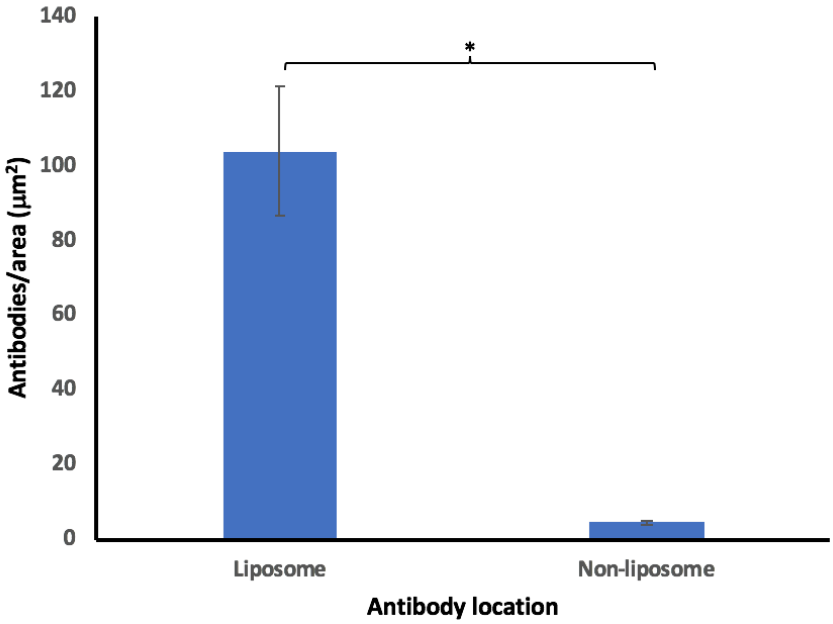

Figure 4.11: Antibody in liposome and non-liposomal areas (before rehydration, no wash). *The graph shows gold particle location (liposomal or non-liposomal area) on the x-axis and antibody particles/unit area (μm^2) on the y-axis. Bars show average ± SD (n=10) at a 3 mM (total lipid) liposome concentration. Results were statistically significant ($p<0.0001$).*

4.3.3 AB-NLs (before hydration, with wash) - 200 nm

A washing step was developed in order to remove any excess antibody not incorporated into the lipid vesicles. Antibody loaded liposomes were prepared, by adding the antibody to the lipid film before rehydration. They were then centrifuged at 50K rpm [~ 257 xg max (RCFmax)] for 1 h at 4°C (70.1 Ti rotor) and resuspended in filtered PBS. The 200 nm liposomes loaded with antibody were irregular in shape and closer to 100 nm in diameter (Figure 4.12 and 4.13). The lipids appeared to be more like 'solid' droplets than liposomes. The gold

particles were mainly associated with the lipid vesicles, with almost no gold-conjugated antibody present outside of them.

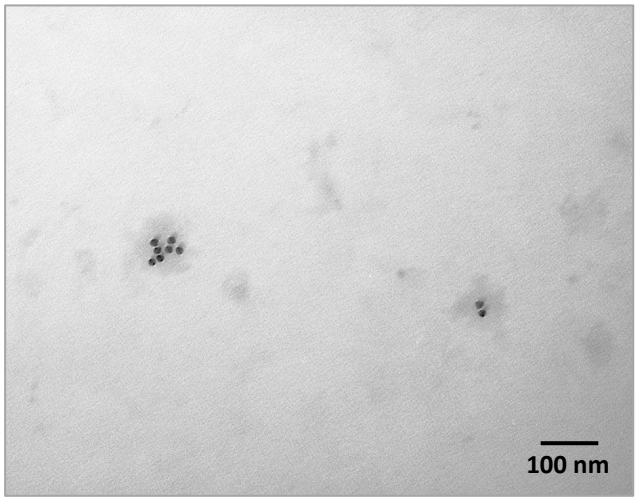

Figure 4.12: AB-NLs (200 nm) in filtered PBS (added before hydration, with wash). *The liposomes are irregular in shape with a diameter close to 100 nm. Lipids appear as droplets instead of liposomes. Antibodies are entirely clustered at the site of the lipid vesicles.*

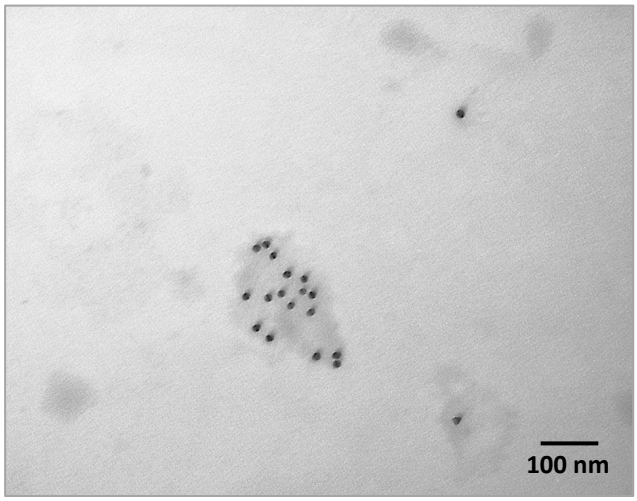

Figure 4.13 AB-NLs (200 nm) in filtered PBS (added before hydration, with wash). *The liposomes are irregular in shape, some of which have diameter close to 100 nm. Antibodies are entirely clustered at vesicles.*

Figure 4.14 is a graphical comparison between antibodies residing in liposomes and those in surrounding non-liposomal areas. Liposomal area showed a mean count of 263.22 ± 66.14 gold particles/μm^2, whereas the non-liposomal area gave a mean count of 0 gold particles/μm^2.

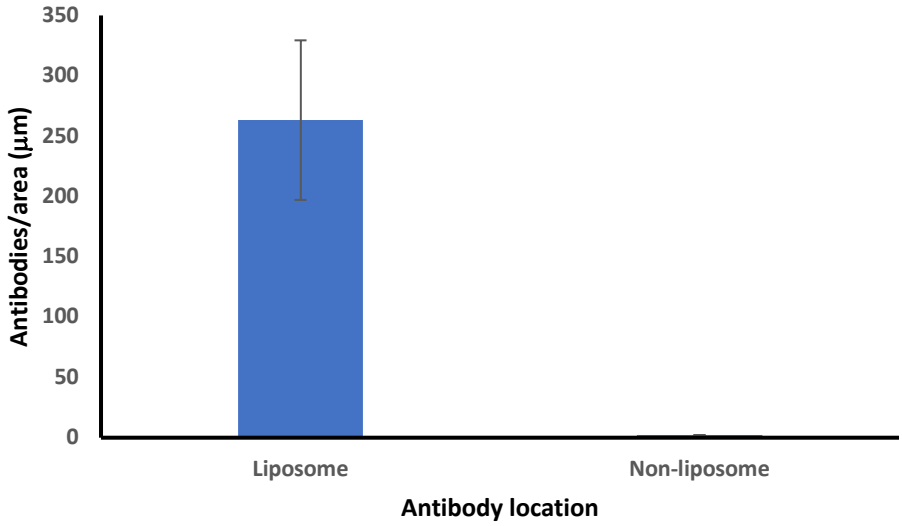

Figure 4.14: Antibody in liposome and non-liposomal areas (before rehydration, with wash). *The graph shows gold particles location (liposomal or non-liposomal area) on the x-axis and antibodies particles/unit area (μm^2) on the y-axis. Bars show average $\pm$ SD (n=8) at a 3mM liposome concentration.*

4.4 The characterisation of RI-OR2-TAT and Alexa Fluor loaded liposomes

Antibody loaded liposomes were produced with the incorporation of β-Actin Rabbit mAb (Alexa Fluor 594 Conjugate) for TEM analysis. Alexa Fluor cannot be detected on TEM, but the size and ultrastructure of the loaded liposomes can still be observed. Antibody incorporation was conducted by means of the most efficient protocol (before rehydration, with wash). Additional modification with amyloid-β peptide inhibitor RI-OR2-TAT-Cysteine ((Ac-rGffvlkGrrrrqrrkkrGyc-NH_2) was also performed. The size and ultrastructure of NL, AB-NL, RI-OR2-TAT-NL and RI-OR2-TAT+AB-NL modified liposomes (3 mM total lipids) was examined by TEM. Produced vesicles required negative PTA staining for visualisation. It was clear that 200 nm AB-NLs allowed incorporation of sufficient antibody, therefore liposomes of 100 nm in diameter were used for RI-OR2-TAT and Alexa Fluor loaded antibodies. This is because 100 nm liposomes are large enough to allow substantial antibody incorporation and small enough to allow passage across the BBB and uptake into cells.

4.4.1 AB-NLs (Alexa Fluor)

Alexa Fluor loaded liposomes were prepared for TEM, at 3 mM total lipid concentration. This followed the same protocol as refined by the immunogold conjugate experimentation, adding the antibody before the rehydration of the lipid film and then washing away excess antibody. Alexa Fluor would be undetectable by TEM, but the ultrastructure and size of the liposomes can be observed.

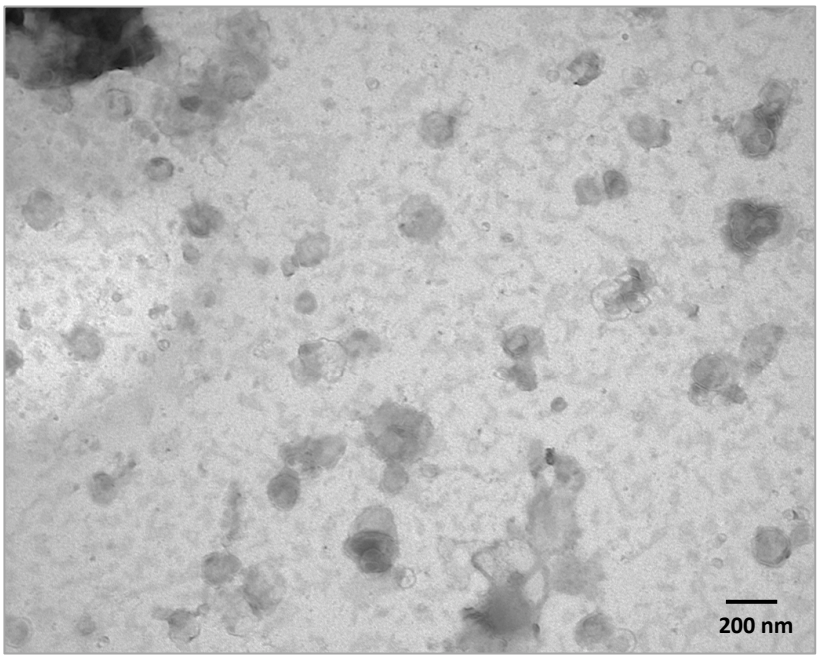

Figure 4.15: AB-NLs (100 nm) in filtered PBS (added before hydration, with wash). *The liposomes are regular in shape and have diameter close to 100 nm. Ultrastructure and size is appropriate and few are clumped.*

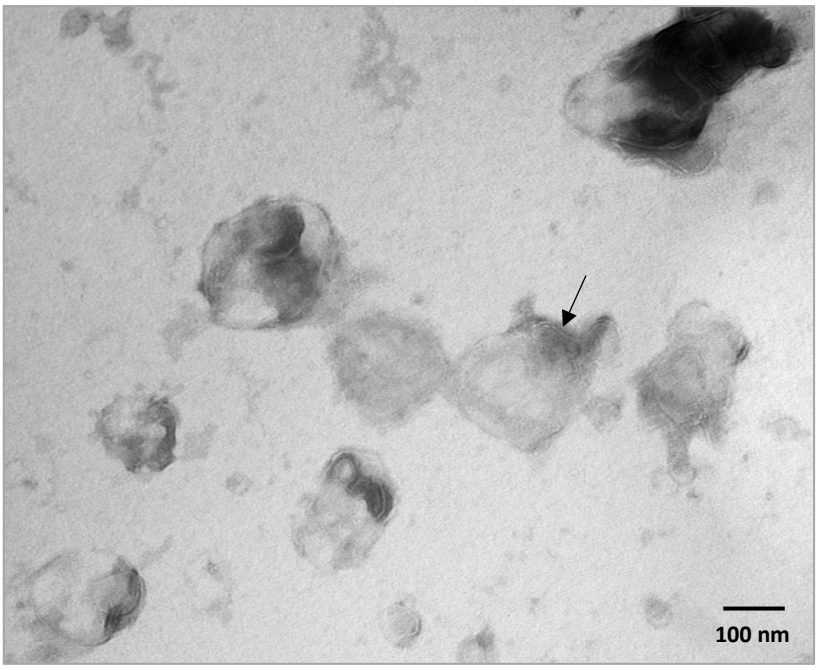

Figure 4.16: AB-NLs (100 nm) in filtered PBS (added before hydration, with wash). *The liposomes are regular in shape and have diameter close to 100 nm. Ultrastructure and size is appropriate and few are clumped. Arrow shows unilamellar vesicle formation*.

4.4.2 RI-OR2-TAT-NLs

RI-OR2-TAT-NLs were prepared for TEM at 3mM (total lipid). RI-OR2-TAT is undetectable by TEM, but the ultrastructure and size of the liposomes can be observed.

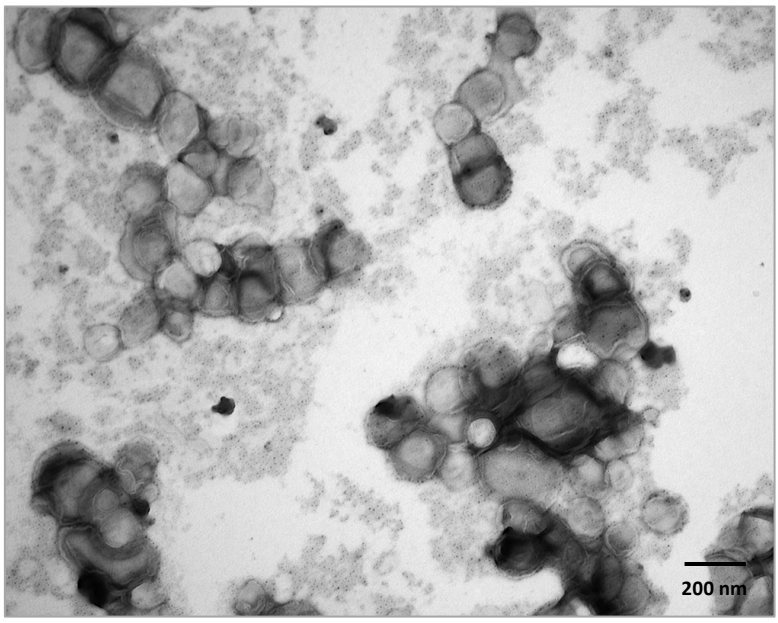

Figure 4.17: RI-OR2-TAT-NLs (100 nm) in filtered PBS. *The negative staining micrograph shows 100 nm RI-OR2-TAT peptide inhibitor attached to liposomes. The liposomes are regular in shape and many have diameter close to 100 nm. Ultrastructure and size is appropriate, although many are clumped.*

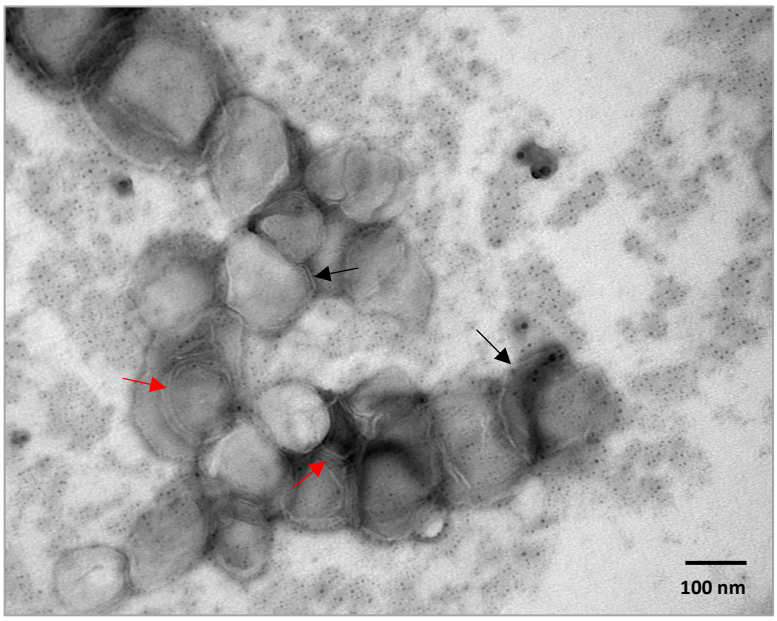

Figure 4.18: RI-OR2-TAT-NLs (100 nm) in filtered PBS - high magnification. *The negative staining micrograph shows a higher magnification of Figure 4.43 micrograph, with 100 nm RI-OR2-TAT peptide inhibitor modified liposomes. Black arrows show unilamellar liposomes, red arrows show some are multilamellar.*

4.4.3 RI-OR2-TAT+AB-NLs

RI-OR2-TAT modified liposomes loaded with Alexa Fluor were prepared for TEM at 3mM (total lipid). This followed the same protocol as refined by the immunogold conjugate experimentation, adding the antibody before the rehydration of the lipid film and then washing away excess antibody. RI-OR2-TAT was then attached after liposome extrusion. Both RI-OR2-TAT and Alexa Fluor would be undetectable by TEM, but the ultrastructure and size of the liposomes can be observed.

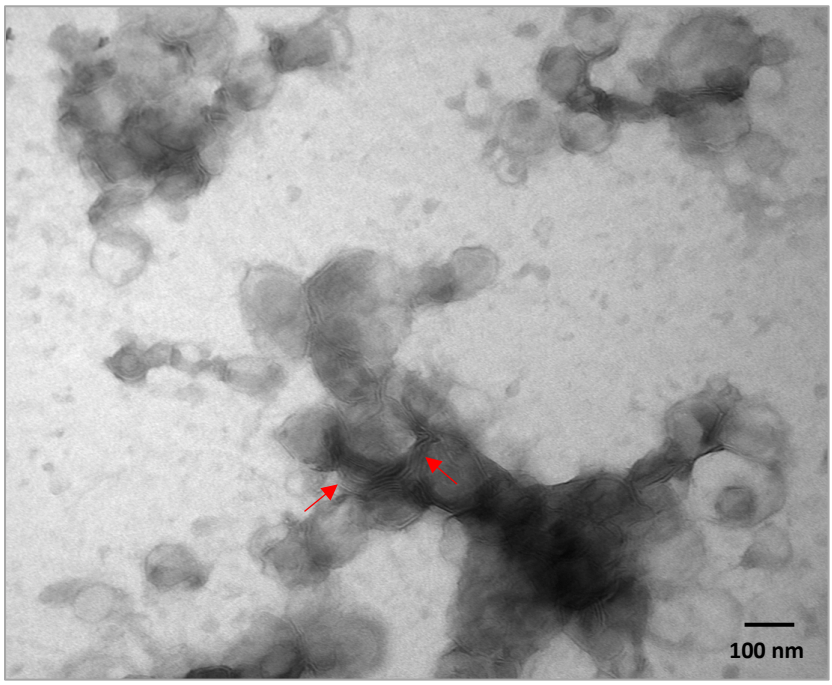

Figure 4.19: RI-OR2-TAT+AB-NLs (100 nm) in filtered PBS. *The liposomes are regular in shape and many have diameter close to 100 nm. Red arrows show that some liposomes are multilamellar, many are clumped together.*

CHAPTER FIVE – Wako Assay Results

5.1 Wako assay (FUJIFILM Phospholipids C assay) refinement to determine liposome concentration

The calculation of exact total lipid concentration (μg/mL) in liposomes can be problematic. The lipid concentration can be estimated based on the quantity of lipid or DSPE-PEG-MAL weighed out for production, but once the liposomes are extruded, some of that lipid will not be incorporated into liposomes, therefore reducing the total lipid concentration. Also, the lipid components will have combined together to form vesicles which are now difficult to assay. The FUJIFILM Phospholipids C assay (Wako assay) is an enzymatic method utilising choline oxidase in a reaction that is measured photometrically. The assay can measure SM concentration in solution, and was therefore used to determine the SM concentration in the liposomes made for this project. SM is present at 47.5 molar % in PEGylated liposomes, and so the concentration obtained from the Wako assay must be multiplied by ~2.1 to reach the actual total lipid concentration of the liposomes (100 molar %). It is apparent that in order for this assay to work effectively, the SM must be dissolved in a solvent. The liposomes must also be lysed in order for the sphingomyelin to be exposed to the enzymatic reaction. This section considers different solvents and preparation methods for the Wako assay in order to effectively measure the concentration of SM in these liposomes.

5.2 Standard curve for phospholipid solutions

A standard lipid solution (3 mM) was provided as part of the LabAssay™ Phospholipid (Choline Oxidase-DAOS method) kit. The chromogenic substrate and enzyme exist as a powder that after reconstitution in substrate buffer (1:1), produce a photometric product. Absorbance was measured at 600 nm to produce a standard curve (Figure 5.1). Each test sample was analysed alongside a standard curve in order to obtain the corresponding phospholipid concentration. A standard curve was repeated for each experiment.

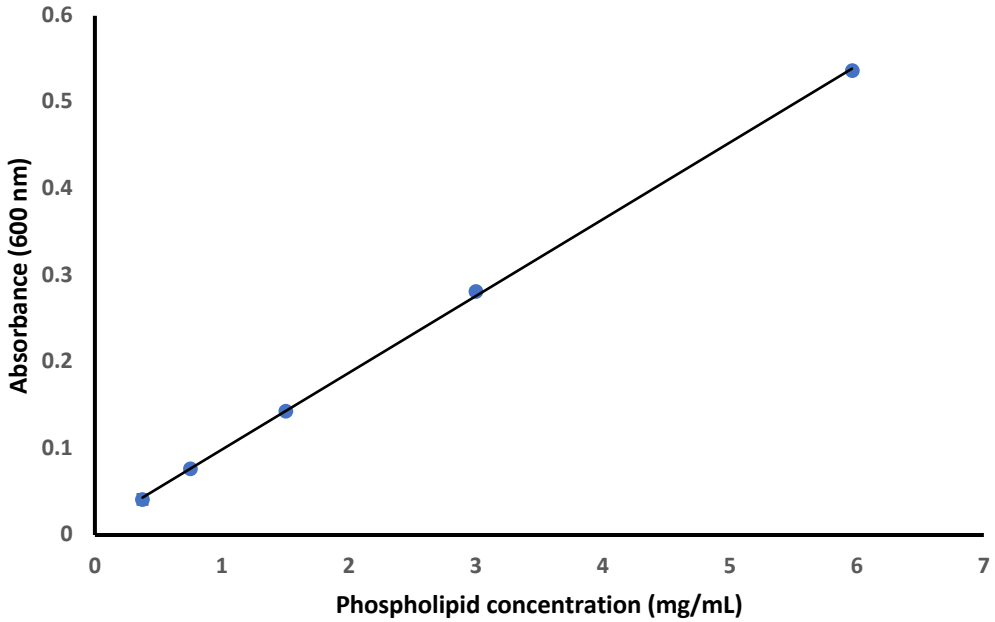

Figure 5.1: Wako assay standard curve. *The standard dilutions absorbance was measured to produce a standard curve. Curve has equation y=0.0887x + 0.01.* R^2 = 0.9998. This suggests the assay kit is reliable.

5.3 Sphingomyelin in various solvents and conditions

Before lysing and measuring the SM concentration in liposomes, free SM was dissolved in different solvents, under different conditions in order to evaluate which of these methods would allow SM concentration to be most accurately calculated. Conditions included 5 mins of heat block (50°C), sonication (50°C) or no incubation, followed by 10 mins incubation at 37°C. SM was dissolved in each of the following solutions: PBS, Chloroform (Chl), Chl + Methanol (Chl/Me) (2:1), PBS + 0.1% Triton X-100 (Tr X), PBS + 2% Tr X and PBS + 2% Tr X in Me. SM has been shown to dissolve effectively in Chl, Me and in a mixture of both. Tr X is a detergent that can be used to lyse liposomes. Chl. and PBS as solvents alone showed significantly decreased lipid concentration, compared to other solvents. All other samples produced similar lipid concentrations, with any differences for the various solvent conditions being insignificant.

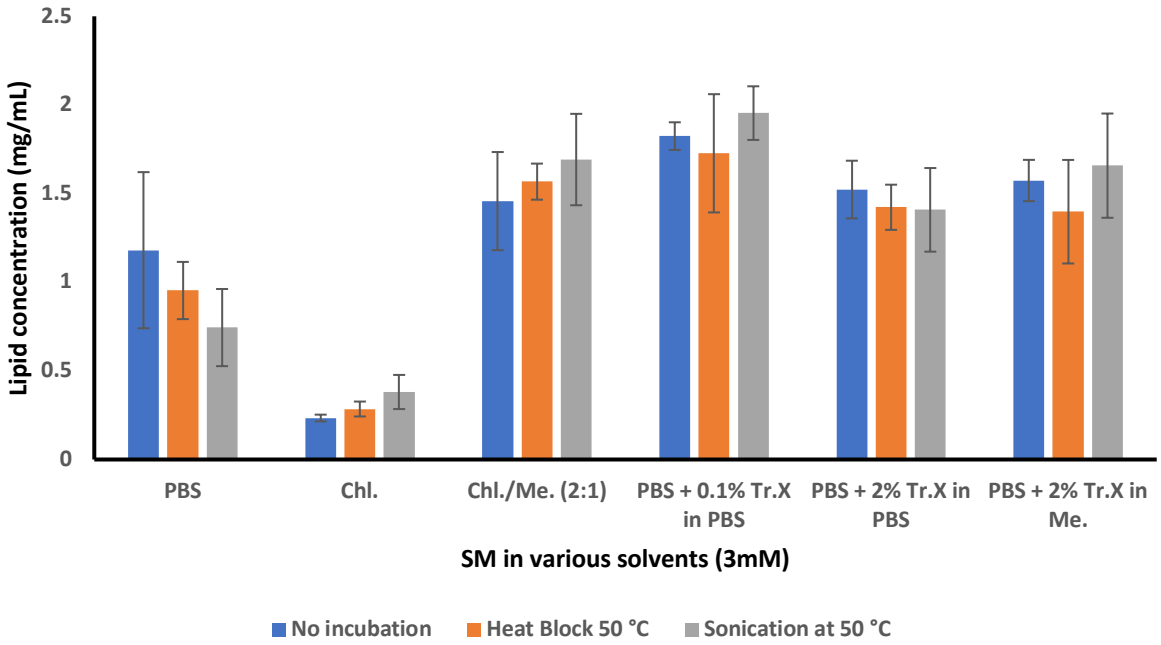

Figure 5.2: Wako assay lipid concentration of SM in various solvents. *The graph shows lipid concentration (mg/mL) on the y-axis and SM in various solvents and preparation methods on the x-axis. Bars show average ± SD (n=3) at a SM concentration of 3 mg/mL. Significance shown in Table 5.1.*

No incubation	ANOVA (P VALUES)
PBS/Chl.	0.0205
PBS/Chl.+Me (2:1)	0.4089
PBS/PBS+0.1% Tr.X in PBS	0.0674
PBS/PBS+2% Tr.X in PBS	0.2756
PBS/PBS+2% Tr.X in Me	0.2100
Chl./Chl.+Me (2:1)	0.0016
Chl./PBS+0.1% Tr.X in PBS	<0.0001
Chl./PBS+2% Tr.X in PBS	0.0002
Chl./PBS+2% Tr.X in Me	<0.0001
Chl.+Me (2:1)/PBS+0.1% Tr.X in PBS	0.0918
Chl.+Me (2:1)/PBS+2% Tr.X in PBS	0.7427
Chl.+Me (2:1)/PBS+2% Tr.X in Me	0.5404
PBS+0.1% Tr.X in PBS/PBS+2% Tr.X in PBS	0.0444
PBS+0.1% Tr.X in PBS/PBS+2% Tr.X in Me	0.0363
PBS+2% Tr.X in PBS/PBS+2% Tr.X in Me	0.6833

Heat block (50°C)	ANOVA (P VALUES)
PBS/Chl.	0.0052
PBS/Chl.+Me (2:1)	0.0125
PBS/PBS+0.1% Tr.X in PBS	0.0981
PBS/PBS+2% Tr.X in PBS	0.0347
PBS/PBS+2% Tr.X in Me	0.2002
Chl./Chl.+Me (2:1)	<0.0001
Chl./PBS+0.1% Tr.X in PBS	0.0040
Chl./PBS+2% Tr.X in PBS	0.0001
Chl./PBS+2% Tr.X in Me	0.0058
Chl.+Me (2:1)/PBS+0.1% Tr.X in PBS	0.4652
Chl.+Me (2:1)/PBS+2% Tr.X in PBS	0.1995
Chl.+Me (2:1)/PBS+2% Tr.X in Me	0.3959
PBS+0.1% Tr.X in PBS/PBS+2% Tr.X in PBS	0.2251
PBS+0.1% Tr.X in PBS/PBS+2% Tr.X in Me	0.4037
PBS+2% Tr.X in PBS/PBS+2% Tr.X in Me	0.8988

Sonication (50°C)	ANOVA (P VALUES)
PBS/Chl.	0.0573
PBS/Chl.+Me (2:1)	0.0082
PBS/PBS+0.1% Tr.X in PBS	0.0014
PBS/PBS+2% Tr.X in PBS	0.0231
PBS/PBS+2% Tr.X in Me	0.0124
Chl./Chl.+Me (2:1)	0.0012
Chl./PBS+0.1% Tr.X in PBS	0.0001
Chl./PBS+2% Tr.X in PBS	0.0022
Chl./PBS+2% Tr.X in Me	0.0020
Chl.+Me (2:1)/PBS+0.1% Tr.X in PBS	0.2037
Chl.+Me (2:1)/PBS+2% Tr.X in PBS	0.2324
Chl.+Me (2:1)/PBS+2% Tr.X in Me	0.8862
PBS+0.1% Tr.X in PBS/PBS+2% Tr.X in PBS	0.0280
PBS+0.1% Tr.X in PBS/PBS+2% Tr.X in Me	0.1955
PBS+2% Tr.X in PBS/PBS+2% Tr.X in Me	0.3159

Table 5.1: One way ANOVA for Wako assay comparing SM in various solvents. *Table shows the significance between no incubation, heat block (50° C) and sonication (50° C) groups comparing SM in various solvents in a Wako assay (Figure 5.2). Significance determined at a 5% confidence level.*

5.4 Sphingomyelin in various solvent volumes with Triton-X

Results from SM in various solvents and conditions highlighted that the solvent itself, rather than the preparation method, was the most influential factor on the success of the assay. As a consequence, SM was then dissolved in different volumes of solvents for observation. Samples were produced in a ratio of solvent to Tr X in PBS, which included 50:50, 40:60, 30:70, 20:80 and 10:90. This was conducted to determine whether the volume of solvent or Triton-X was influential on achieving the expected lipid concentration. Chloroform did not perform well as a solvent in the SM previously. Therefore, only PBS and methanol were used as solvents in a solution with 0.1% Tr X and 2% Tr X (Figure 5.3). This would determine which solvent is more effective and if an increased Tr X concentration is beneficial. It was shown that the ratio of solvent to Tr X did not have a significant impact on the total lipid concentration yielded.

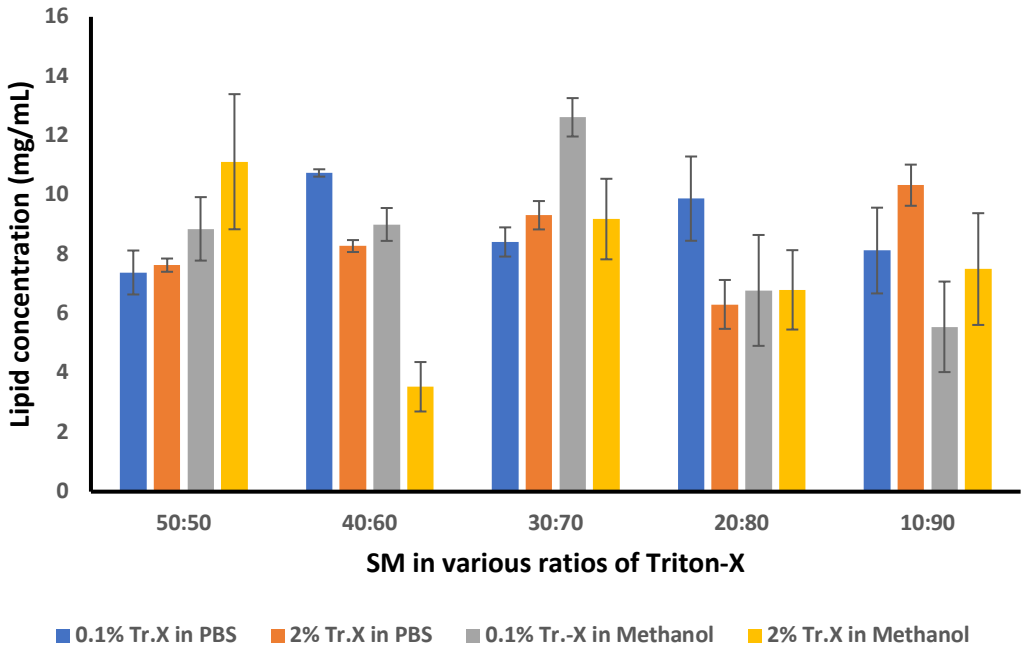

Figure 5.3: Wako assay lipid concentration of SM in various solvent volumes with Tr X. *The graph shows lipid concentration (mg/mL) on the y-axis and SM in various volume ratios of solvents and Tr X on the x-axis. Bars show average ± SD (n=3) at a SM concentration of 12 mg/mL. Significance shown in Table 5.2.*

0.1% Tr. -X in PBS	ANOVA (P VALUES)	2% Tr. -X in PBS	ANOVA (P VALUES)
50:50/40:60	.123	50:50/40:60	1.000
50:50/30:70	1.000	50:50/30:70	.987
50:50/20:80	.554	50:50/20:80	.999
50:50/10:90	1.000	50:50/10:90	.608
40:60/30:70	.815	40:60/30:70	1.000
40:60/20:80	1.000	40:60/20:80	.944
40:60/10:90	.470	40:60/10:90	.922
30:70/20:80	.997	30:70/20:80	.249
30:70/10:80	1.000	30:70/10:80	1.000
20:80/10:90	.947	20:80/10:90	.026
0.1% Tr. -X in PBS+Me	**ANOVA (P VALUES)**	**2% Tr. -X in PBS+Me**	**ANOVA (P VALUES)**
50:50/40:60	1.000	50:50/40:60	.000
50:50/30:70	.766	50:50/30:70	.979
50:50/20:80	.818	50:50/20:80	.038
50:50/10:90	.138	50:50/10:90	.159
40:60/30:70	.396	40:60/30:70	.005
40:60/20:80	1.000	40:60/20:80	.290
40:60/10:90	.790	40:60/10:90	.080
30:70/20:80	.025	30:70/20:80	.785
30:70/10:80	.001	30:70/10:80	.987
20:80/10:90	.999	20:80/10:90	1.000

Table 5.2: One way ANOVA for Wako assay comparing SM in various solvent volumes with Tr X.

Table shows the significance between various ratios of solvent solutions with Tr X (Figure 5.3). Groups include 0.1% Tr X in PBS, 2% Tr X in PBS, 0.1% Tr X in PBS+Me and 2% Tr X in PBS+Me Significance determined at a 5% confidence interval.

5.5 Liposomes and SM in different solvents in 0.1% Triton-X

Having characterised the Wako assay for SM, liposomes were now subjected to these same conditions to observe if the SM in liposomes can also dissolve and be measured effectively. Results shown in Figure 5.2 and 5.3 suggested that 0.1% Tr X was sufficient for SM to dissolve, and therefore was the only concentration of Tr X used. SM and liposomes in PBS and PBS + Me were prepared in 0.1% Tr X (3 mg/mL). SM showed lipid conc. for PBS and PBS + Me samples to be 2.85 and 2.60 (mg/mL) respectively, as expected. Liposome results showed lipid conc. for PBS and PBS+Me to be 0.40 and 1.98 (mg/mL) respectively. Lipid concentration was significantly increased in PBS+Me over PBS alone.

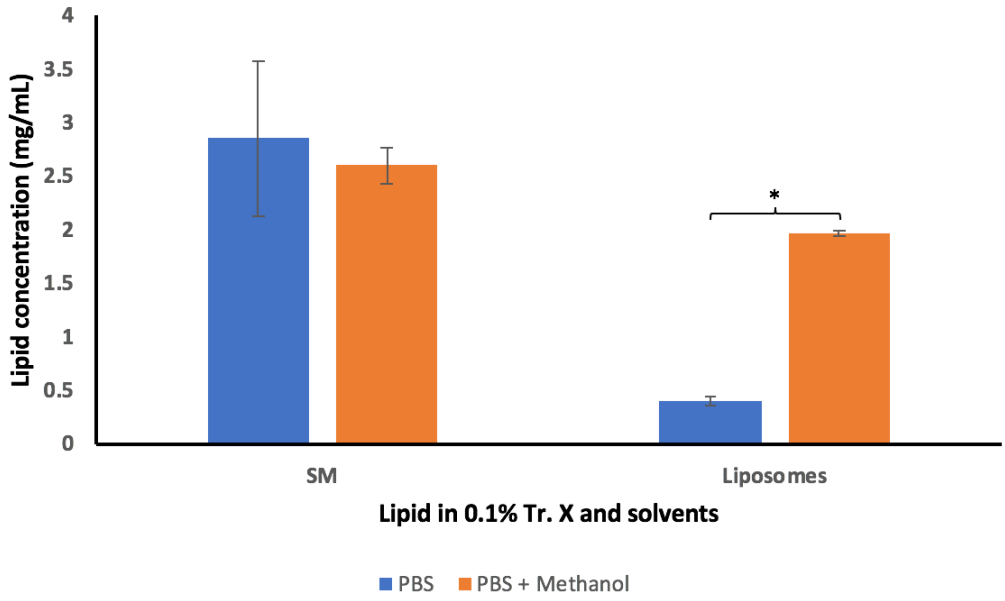

Figure 5.4: Wako assay lipid concentration of SM and liposomes in various solvents and 0.1% Tr X. *Bars show average ± SD (n=3) at a SM concentration of 3 mg/mL. Significance shown at a 5% confidence interval.*

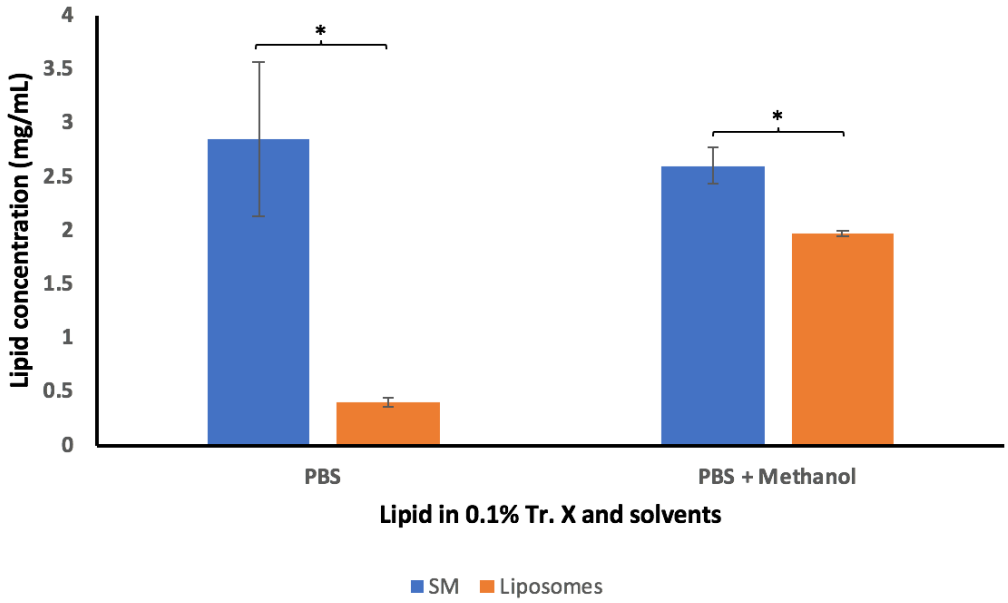

Figure 5.5: Wako assay lipid concentration of SM and liposomes in various solvents and 0.1% Tr X. *Bars show average ± SD (n=3) at a SM concentration of 3 mg/mL. Significance shown at a 5% confidence interval.*

5.6 Liposomes in different solvents in 0.1% Triton-X

Liposomal SM was most effectively dissolved in PBS + Me as shown in Figure 5.5, yet did not reflect the expected SM concentration in liposomes. Chl has been shown to enhance liposome lysis and SM dissolution. An assay was prepared with liposomes (3 mM total lipids) in PBS, PBS+Me and PBS+Me +Chl, in Tr X in order to determine if Chl is effective. Results showed lipid conc. of PBS, PBS+Me and PBS+Me+Chl to be 0.50, 0.78 and 0.87 (mg/mL) respectively (Figure 5.6). The use of both PBS+Me and PBS+Me+Chl resulted in significantly increased lipid concentration compared with PBS.

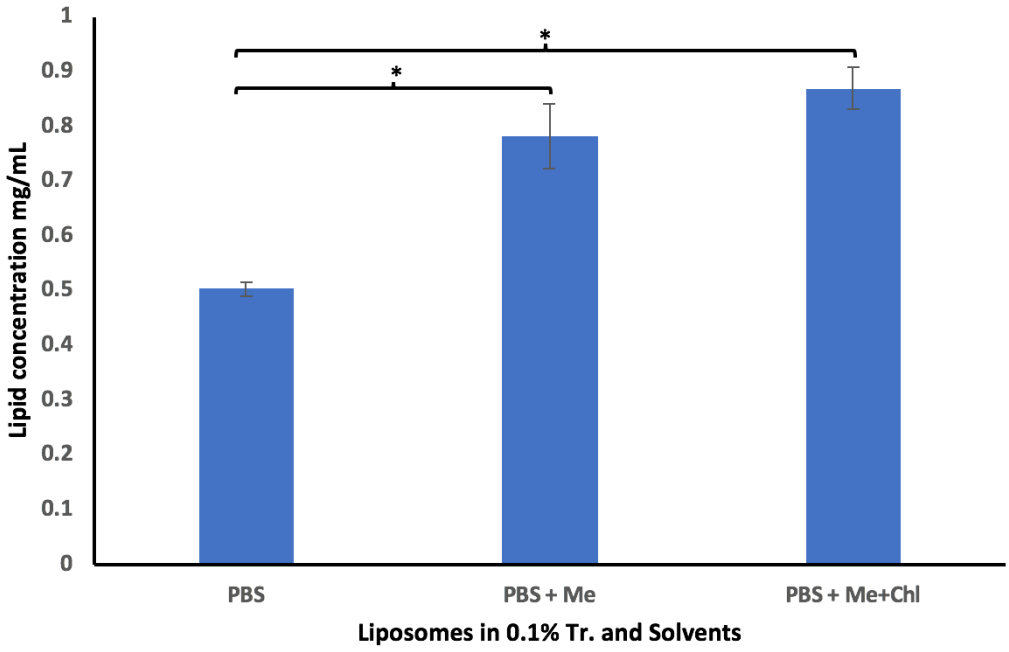

Figure 5.6: Wako assay lipid concentration of liposomes in various solvents and 0.1% Tr X. *The graph shows lipid concentration (mg/mL) on the x-axis and liposomes in PBS, PBS + Me and PBS + Me + Chl, and 0.1% Tr X on the y-axis. Bars show average ± SD (n=3) at a liposome concentration of 3mM. Significance shown at a 5% confidence interval.*

CHAPTER SIX – Cell Penetration Results

6.1 Cell penetration assay – Fluorescent microscopy

Tau aggregation occurs intracellularly, therefore anti-tau therapeutics must be able to penetrate into neuronal cells in order to inhibit or prevent this aggregation. There is some evidence that Aβ aggregation begins inside cells, suggesting that it may also be beneficial for Aβ therapeutics to penetrate into cells. As a result, an important feature of antibody loaded liposomes includes their ability to penetrate into neuronal cells. In the following assay, fluorescent BODIPY liposomes (100 nm) with various modifications were prepared at different lipid concentrations (50 μM, 100 μM and 200 μM). Modifications included: PEG-NLs, AB-NLs, RI-OR2-TAT-NLs and RI-OR2-TAT+AB-NLs. Prepared liposomes were incubated in standard mammalian cell culture conditions with SH-SY5Y neuroblastoma cells for 2 h and cell penetration was observed by confocal microscopy (LSM 510 – Laser Module – ZEISS). Different filters were used throughout the experimentation, including Dapi (blue), Bodipy (green), Alexa Fluor (Alexa) (red) and brightfield. These were used individually or in combination to portray results.

6.2 BODIPY liposomes and control

BODIPY-cholesterol is a fluorescent boron dipyrromethene difluoride linked to sterol carbon-24 and was used to identify the location and abundance of liposomes by fluorescent microscopy. BODIPY PEG-NLs were compared with a control (prepared with normal cholesterol) to confirm that there was no background fluorescence present. Figure 6.1 shows images of fluorescent liposomes and this negative control. The DAPI and brightfield confirm the presence of cells, which was evident in both samples. Little or no green fluorescence was

observed in the negative control, as expected. In some cases, the cells produce a weak signal due to auto-fluorescent properties.

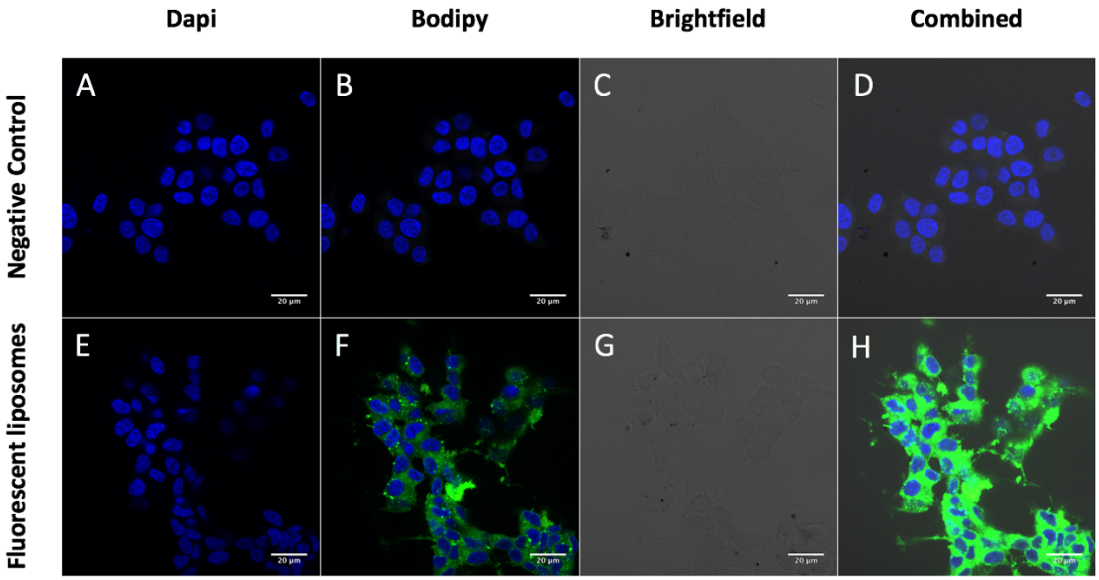

Figure 6.1: Comparison between PEG-NLs with and without BODIPY (100 μM). *Micrographs A-D show images of SH-SY5Y cells incubated with PEG-NLs (negative control) and E-H show images of SH-SY5Y cells incubated with BODIPY PEG-NLs (fluorescent liposomes). The columns represent the different filters. By comparing A-D to E-H, we can observe that both the fluorescent liposomes and negative control show cells on the brightfield that are stained by DAPI. The negative control did not show any fluorescence on the bodipy filter, as expected. Scales bar = 20 μm.*

6.3 PEGylated liposomes

SH-SY5Y cells were incubated with BODIPY PEG-NLs at different lipid concentrations (0 μM, 50 μM and 200 μM) to determine the impact of liposome concentration on cellular uptake, in absence of any additional modifications. Figure 6.2 shows that an increase in liposome concentration leads to a greater cellular uptake, as expected.

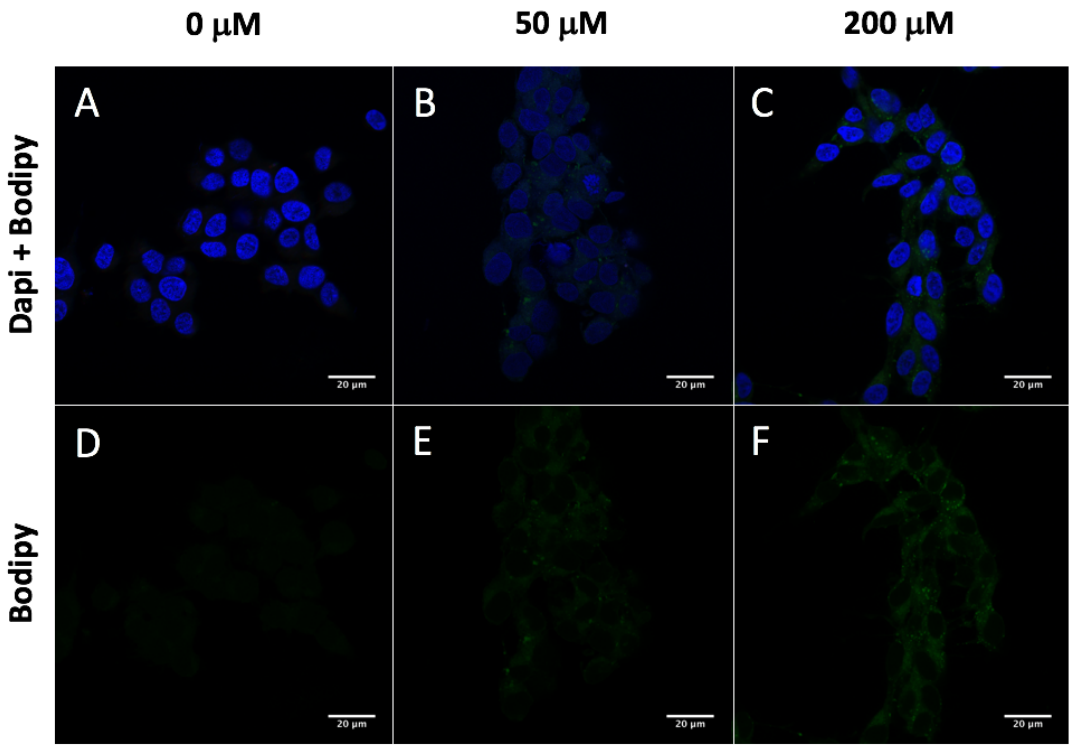

Figure 6.2: SH-SY5Y cells with BODIPY PEG-NLs at different concentrations. *A-C shows dapi + bodipy filter, D-F shows bodipy filter alone. A+D, B+E and C+F show liposome concentrations 0 μM, 50 μM and 200 μM respectively. By comparing AD, BE and CF, we can observe that PEG-NLs are able to penetrate cells, and 200 μM liposomes penetrate with greater efficiency than 50 μM. Scales bar = 20 μm.*

6.4 Alexa Fluor loaded liposomes

It is clear that liposomes can penetrate into SH-SY5Y neuroblastoma cells, as shown in the BODIPY PEG-NLs. The quantity of antibody that can be incorporated into liposomes and delivered into cells can now be determined, by incubating the SH-SY5Y cells with BODIPY AB-NLs (using Alexa Fluor). Alexa Fluor is a fluorescent conjugated monoclonal antibody that detects β-Actin in cells, and can be visualised by fluorescent microscopy. BODIPY AB-NLs were prepared at different lipid concentrations (50 μM and 200 μM) in order to observe cellular uptake. Figure 6.3 shows the BODIPY filter for the alexa fluor liposomes. The SH-SY5Y cells with 200 μM BODIPY AB-NLs had more intense bodipy fluorescence than the 50 μM, as expected. Figure 6.4 shows the Alexa filter, which exhibits no cellular uptake of Alexa Fluor for the 50 μM BODIPY AB-NLs and limited uptake at 200 μM.

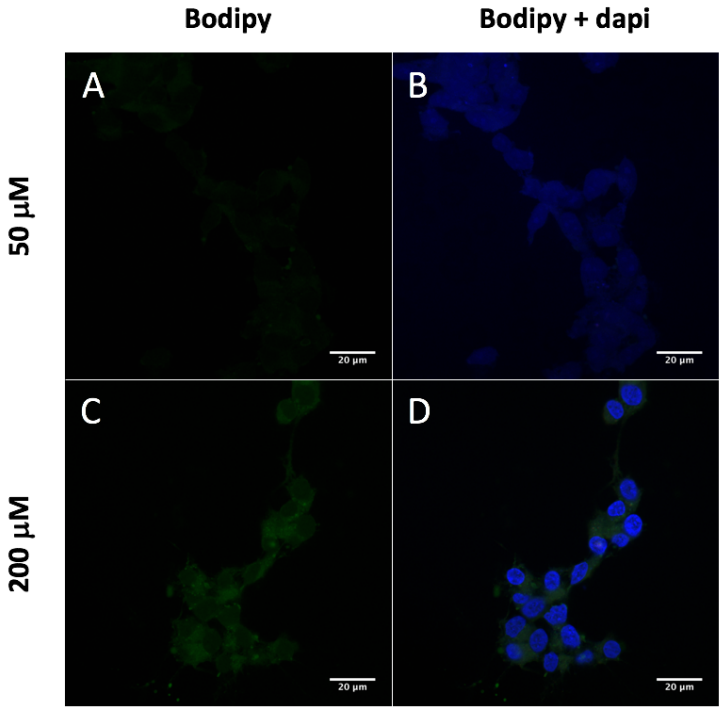

Figure 6.3: Bodipy micrograph - SH-SY5Y cells with BODIPY AB-NLs at different concentrations. *Columns show filters with bodipy and bodipy + dapi for comparison. A,B and C,D shows liposome concentrations 50 μM and 200 μM respectively. By comparing A,B and C,D, we can observe that BODIPY AB-NLs are able to penetrate cells, and 200 μM liposomes penetrate with greater efficiency than 50 μM. Scales bar = 20 μm.*

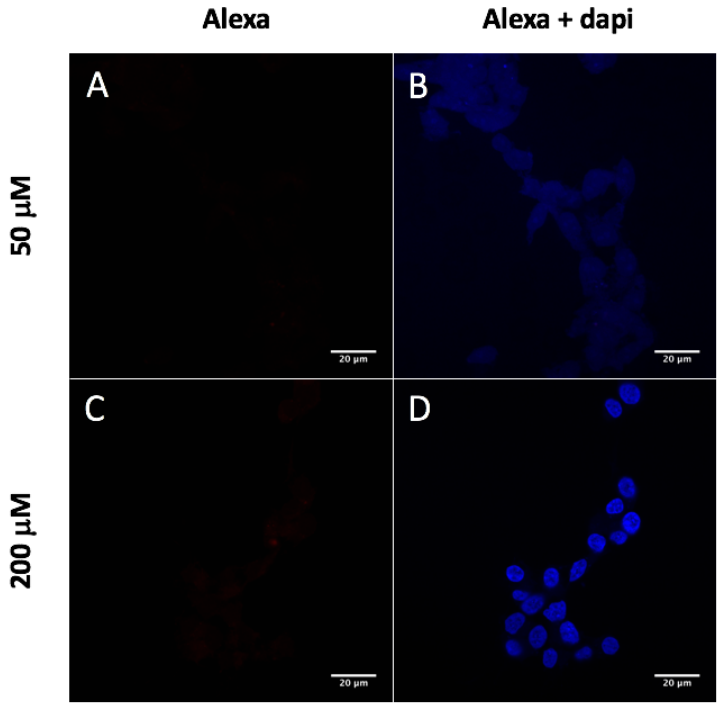

Figure 6.4: Alexa micrograph - SH-SY5Y cells with BODIPY AB-NLs at different concentrations. *Columns show filters with Alexa and Alexa + dapi for comparison. A,B and C,D shows liposome concentrations 50 µM and 200 µM respectively. By comparing A,B and C,D we can observed that limited antibody is present the cells. Scales bar = 20 µm.*

6.5 RI-OR2-TAT and RI-OR2-TAT+AB modified liposomes

RI-OR2-TAT peptide was attached to liposomes, producing to RI-OR2-TAT-NLs and RI-OR2-TAT+AB-NLs, to observe the impact on cellular uptake. RI-OR2-TAT is a CPP that has the ability to allow enhanced transport into cells. SH-SY5Y cells were incubated with these modified liposomes at different lipid concentrations (50 µM, 100 µM and 200 µM). Figure 6.5 and 6.6 shows SH-SY5Y cells incubated with RI-OR2-TAT-NLs and RI-OR2-TAT+AB-NLs respectively. The figures suggest that the SH-SY5Y cells have high affinity for liposomes with RI-OR2-TAT attached, shown by the bodipy micrographs. Alexa Fluor uptake is limited, but is increased at higher liposome concentrations.

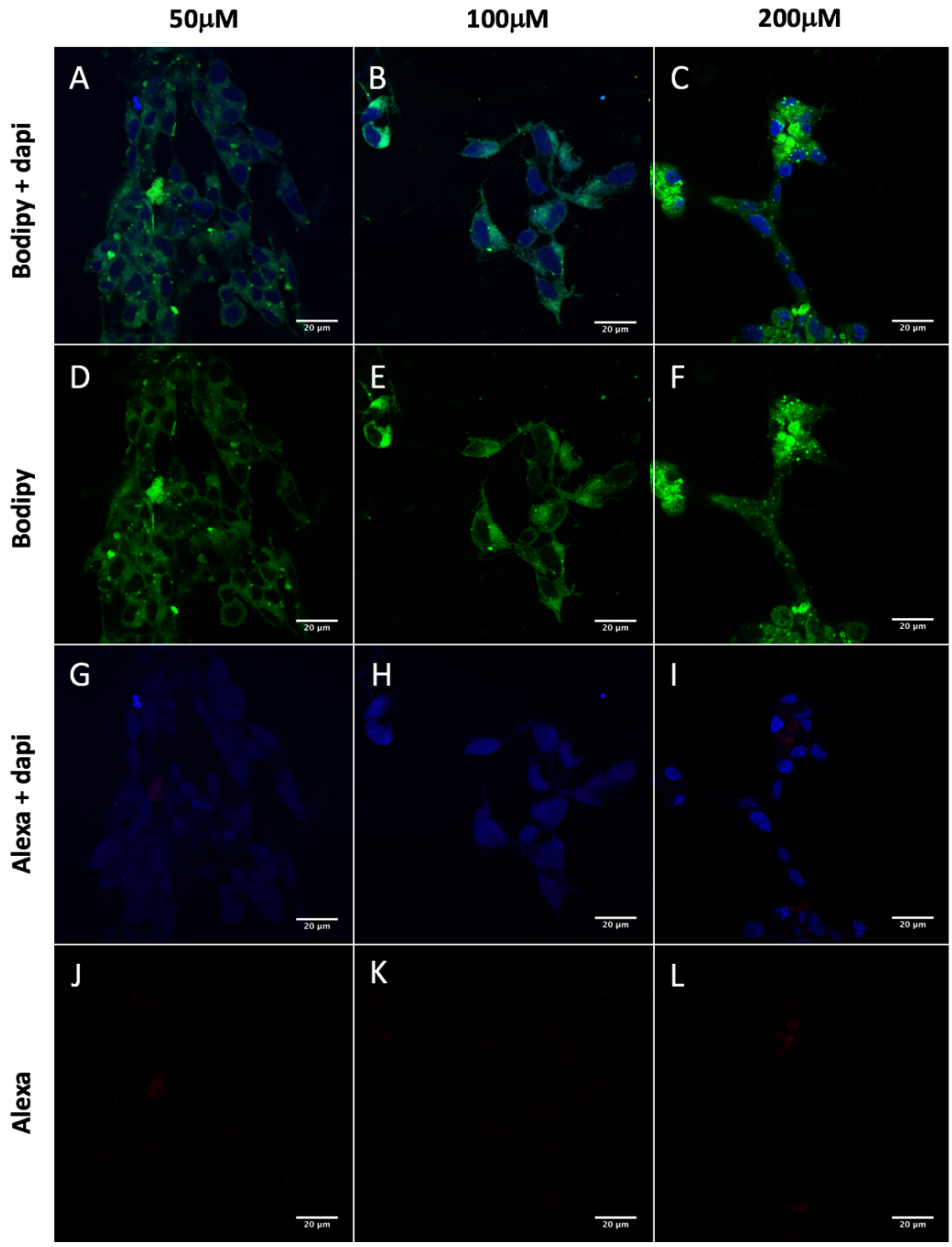

Figure 6.5: SH-SY5Y cells with RI-OR2-TAT-NLs at different concentrations. *A-C, D-F, G-I, J-L show different filters of 50 µM, 100 µM and 200 µM liposome concentrations. A-F shows cells have high affinity for liposomes, which is increased at higher concentrations. G-L shows cells have limited fluorescence from Alexa Fluor, as expected. Scale bar = 20 µm.*

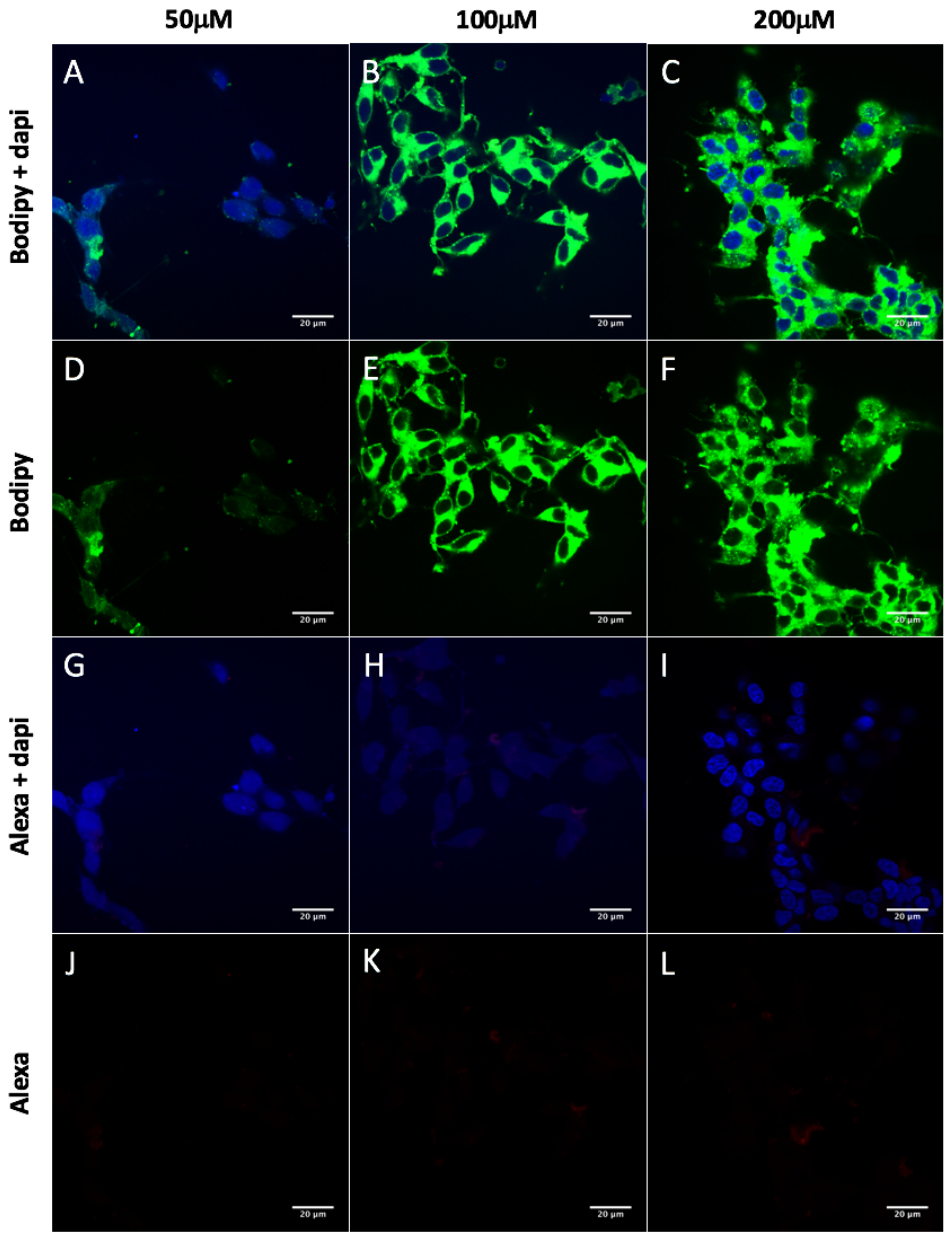

Figure 6.6: SH-SY5Y cells with RI-OR2-TAT+AB-NLs at different concentrations*. A-C, D-F, G-I, J-L show different filters of 50 µM, 100 µM and 200 µM liposome concentrations. A-F shows cells have high affinity for liposomes, which is increased at higher concentrations. G-L shows cells have limited fluorescence from Alexa Fluor at 50 µM liposomes, which is increased at higher concentrations. Scales bar = 20 µm.*

The micrographs obtained with SH-SY5Y cells incubated with RI-OR2-TAT-NLs and RI-OR2-TAT+AB-NLs were combined for comparison (Figure 6.7). The purpose of this was to observe the intensity of the bodipy and Alexa under the respective filters. BODIPY is more intense in both liposome types as the concentration is increased, as expected. There is small background of Alexa Fluor in RI-OR2-TAT-NLs. For RI-OR2-TAT+AB-NLs, Alexa Fluor is more intense as concentration increases.

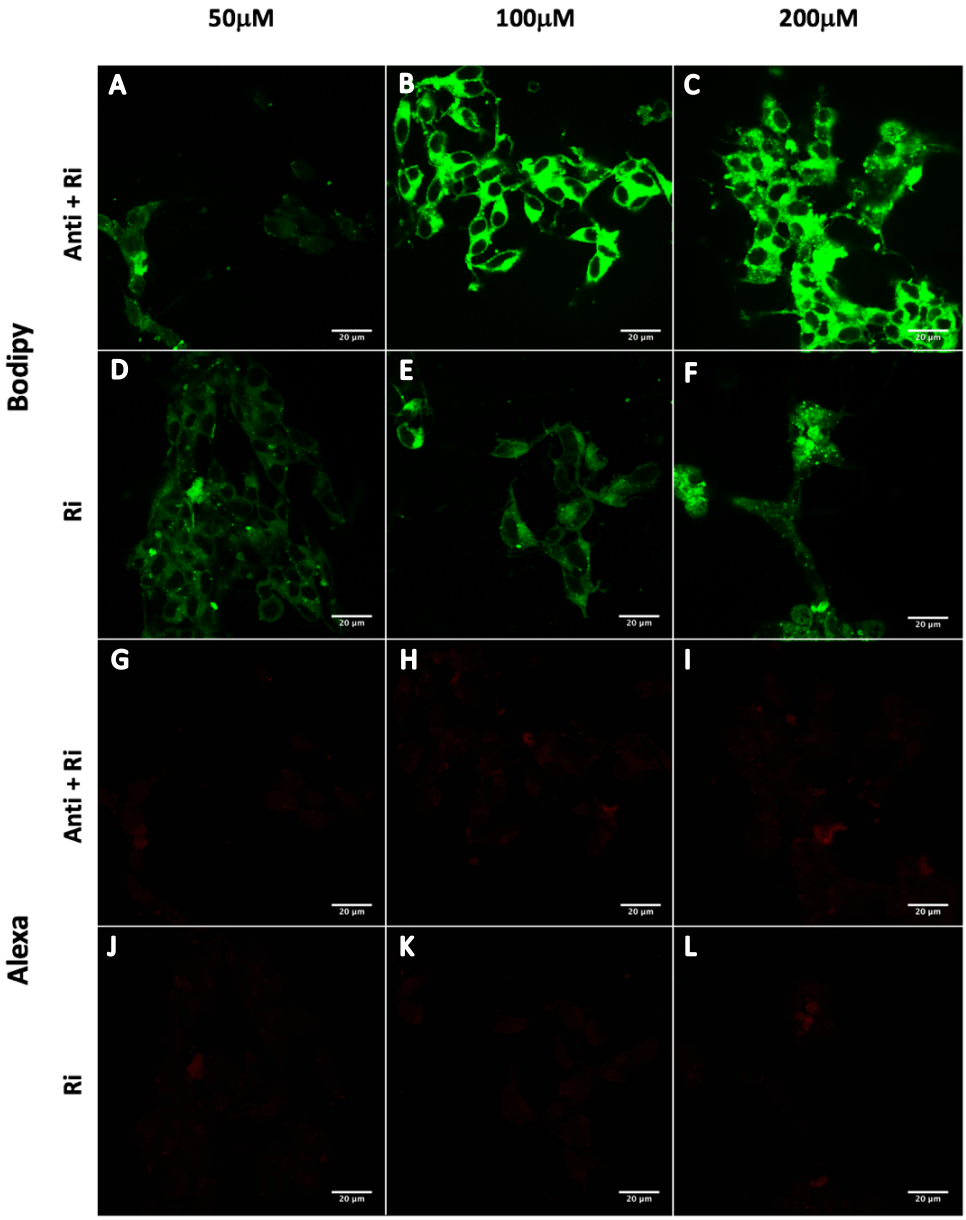

Figure 6.7: SH-SY5Y cells with RI-OR2-TAT-NLs and RI-OR2-TAT+AB-NLs*. A-F shows the bodipy filter for both liposome types, G-L shows the Alexa filter for both liposome types. A-F shows cells have high affinity for liposomes, which is increased at higher concentrations. J-L shows cells have a limited background on the Alexa filter. G-I suggests Alexa Fluor fluorescence is limited at 50 µM liposome concentration, yet the affinity is increased at higher concentrations. Scales bar = 20 µm.*

CHAPTER SEVEN – Discussion

7.1 Background

36 million people are affected by AD worldwide, and this number is set to rise to over 115 million by 2050, as populations age (WHO, 2006). AD is a neurodegenerative disorder that severely affects the functioning of the brain, triggering widespread neuronal and synaptic loss, memory impairment, and cognitive and behavioural disturbances (Prince *et al.,* 2016). The underlying cause of AD is accepted to be the progressive accumulation of extracellular senile plaques, containing Aβ, and NFTs, consisting of PHFs composed of hyper-phosphorylated Tau protein (Murphy and LeVine, 2010). The drugs currently available for the treatment of AD (acetylcholinesterase inhibitors, and the NMDA antagonist memantine) do not target any of these underlying disease mechanisms (Hansen *et al.,* 2008). and do not slow the long-term progression of the disorder. Liposomes are a biocompatible and highly flexible drug delivery system, with the potential for carrying many different types of bioactive molecules across the BBB. Their physiological composition facilitates numerous modifications, in comparison to other nano-carriers. These attractive properties of liposomes have provoked an interest in their development as a possible new and more effective therapy for AD than conventional small molecule drugs or biological agents.

RI-OR2-TAT is a peptide inhibitor with the capacity to inhibit Aβ aggregation. It contains a retro-inverso version of the TAT sequence, which substantially enhances transport across the BBB, a metabolic and transport barrier that prevents access to the brain of ~98% of neurotherapeutics. Amongst all CPPs, TAT is the best described with the greatest success. Despite the promising potential of RI-OR2-TAT, it only inhibits Aβ aggregation at relatively high concentrations, limiting its potential (Taylor *et al.,* 2010; Sherer *et al.,* 2015). The peptide was

then attached to stealth liposomes, which improved the potency of RI-OR2-TAT. Yet, i.v. injection in TG2576 mice showed that most of the dose accumulates in peripheral tissues which will be subject to clearance (Gregori *et al.,* 2017). These therapeutic entities known as PINPS could be improved by incorporation of alternative or additional modifications. The current study looks to see if antibodies can be delivered into cells using liposomes. This might be useful for highly functionalised multi-drug targeting systems in the future. Anti-Aβ and anti-Tau antibodies were not used for experimentation. Instead, various other types of monoclonal antibodies were used as a test system. The future use of antibody loaded liposomes can be determined through analyzing the ultrastructure, stability and cell penetration efficacy.

7.2 Antibody incorporation

The liposome preparation and characterization methods used were, in the majority, derived or adapted from previous studies. Modifications of the Bangham method were used to try and incorporate antibodies into both plain liposomes and PINPs. This preparation method is relatively straight forward and is routinely used in our laboratory, but antibody incorporation into our liposomes has not been attempted previously. PEGylated liposomes firstly underwent hydration of the thin lipid film with PBS, followed by the addition of antibodies. Immunogold (10 nm) conjugated goat anti-fluorescein antibody was used as a test system to see if this could be incorporated into the liposomes. This approach showed that the antibodies were randomly dispersed between the liposomes and the surrounding areas, as observed by TEM (Figure 4.5 and 4.6). The encapsulation efficacy was poor and required improvement if it were to be useful as a system to deliver antibodies.

It was hypothesised that the addition of antibodies to the lipid film before rehydration of PBS would lead to them interacting with the film so that sequential rehydration would ensure a good encapsulation efficacy (Figure 4.8). This was the case, the results before rehydration

showed that antibodies were situated around or in liposomes (Figure 4.9 and 4.10). Analysis of this data showed antibodies per liposomal area (μm^2) were significantly increased compared to antibodies per non-liposomal area (Figure 4.11), suggesting that adding antibodies before lipid film rehydration provided more effective encapsulation than adding them after rehydration. A drawback from TEM is the difficulty in determining whether the antibodies are encapsulated inside liposomes, integrated into the lipid bilayers, or resting on the outside of the vesicles. However, if they were solely in the membrane, they would most likely be grouped in the bilayers, so it is highly likely that they are inside the liposomes.

In order to improve the reliability of the TEM micrographs, a washing step was introduced to remove any free (non-bound) bound antibodies from the solution containing the liposomes. A series of steps involving centrifugation, discarding of supernatant, and resuspension of liposomes in PBS, was repeated three times and TEM micrographs were then produced (Figure 4.12 and 4.13). Results showed that all antibodies across 8 micrographs were situated within (or at least closely associated with) liposomal areas and none resided outside of the liposomes (Figure 4.14). There was no apparent clustering on liposomal membranes. Instead the antibodies were dispersed evenly within liposomes, suggesting that the bulk of the antibody is contained within the liposome core, rather than being contained within or attached to the lipid bilayers. Based on these images, it is clear that these liposomes have the potential to trap and deliver the antibodies to a therapeutic target.

7.3 DLS investigation

Characterisation of liposomes was conducted by DLS. Colloidal gold standards were first measured at optimum dilutions in order to calibrate and validate the technique for the liposome samples. The gold nanoparticles at the dilutions tested were expected to give peaks at their respective vesicle size, with low PDI and SD. Results gave the expected mean vesicle

diameter for each sized sample (Figure 3.1), but the SD was high, particularly at higher gold nanoparticle sizes. This is likely to be due to clumping in solution, producing varied particle sizes. This is unusual as DLS, when conducted at appropriate dilutions for each nanoparticle size, should give tight and accurate measurements. It is possible that the colloidal gold samples were aged, or unusually clumped in solution. Overall, the PDI remained stable and the mean peak values were as expected, so it was decided that the system was reliable enough for further experimentation. Additionally, the experimental liposome samples have a PEGylated lipid incorporated into their membranes, which should reduce attractive forces (van der Waals) between them, and increase repulsive forces (Kenworthy *et al.,* 1995a; Kenworthy *et al.,* 1995b), therefore reducing any clumping observed.

Following the system calibration, PEG-NLs of three distinct sizes (200 nm, 100 nm and 50 nm) were analysed by DLS at optimal dilutions (shown in Figure 3.3 and 3.4). Again it was expected that the DLS results would accurately reflect the anticipated diameters of the samples. The incorporation of the PEGylated lipid should result in an increased vesicle diameter compared with plain liposomes. Previous studies with PEG-DSPE at 7±2 molar % have suggested that a size increase of no more than 1.5 nm would be expected, yet an increase of 15 ± 5 nm was actually observed (Garbuzenko *et al.,* 2005). Consequently, a similar increase in the current study is a possibility. The 200 nm liposomes gave a mean size of 213.50 ± 9.30 nm, as expected. Yet, their wide size distribution makes them undesirable for antibody encapsulation. Also, liposomes of 100 nm and smaller are considered to be more suitable for BBB transportation, and so 200 nm liposomes are likely to have limited uptake and delivery. The 50 nm liposomes gave a mean size of 49.51 ± 0.49 nm, however, Figure 3.4 shows that a second peak at 220.70 nm was observed. This peak suggests the liposomes are aggregating, even at a high dilution factor (1:500 dilution) and so 50 nm liposomes are unlikely to be suitable for AD therapy, as aggregated 50 nm liposomes will have limited mobility, have reduced BBB uptake and be

susceptible for immune system degradation. Additionally, a small diameter will limit the antibody incorporation efficiency, reducing its therapeutic potential. The 100 nm liposomes had a mean diameter of 180.30 ± 5.16 nm, much larger than anticipated. They were more narrowly distributed than 200 nm or 50 nm liposome samples and remain the most suitable vesicle size for antibody incorporation and potential brain delivery based on DLS results. The increased diameter could be due to vesicles clumping together, or abnormally shaped vesicle formation.

AB-NLs were then analysed by DLS in order to evaluate the impact the antibody has on the size and stability of the vesicles. Since 50 nm vesicles are considered to be the least suitable for antibody incorporation and delivery, only 100 nm and 200 nm liposomes were produced for this purpose. There is limited data on AB-NLs, and so the expected results are not clear from the literature. It is thought, however, that 100 nm liposomes maintain the most stable size and distribution with antibody incorporation, a result shown in the PEG-NL results. It is possible that antibody incorporation could distort the vesicles, causing an increase in size or vesicle aggregation. Results showed that 200 nm AB-NLs had mean size of 196.7 ± 9.51 nm, and showed no significant difference to the PEG-NLs which had a diameter of 213.5 ± 9.30 nm (Figure 3.5). They also had greater intensity and lower PDI, suggesting that overall, they are more stable (Figure 3.6). The 100 nm AB-NLs were 213.5 ± 41.33 nm, and showed no significant difference to the PEG-NLs with a diameter of 180.3 ± 5.16 nm (Figure 3.7). However, the SD is increased, which could be as a result of the antibody incorporation. They had similar intensity but increased PDI, and some AB-NLs were as large as 250 nm in diameter (Figure 3.8). It is possible that antibody incorporation may have an impact on structure or cause liposomes to aggregate. Assuming the structure of AB-NLs is normal (determined by TEM) rather than forming large irregular vesicles, this is unlikely to be problematic for experimentation. The 200 nm liposomes would most likely be degraded quickly by the immune system, and are too large

for efficient BBB transportation. Based on this and TEM results, it was decided to use 100 nm liposomes for additional experimentation.

Subsequent studies involved the analysis of RI-OR2-TAT-NLs and RI-OR2-TAT+AB-NLs by DLS to assess the impact of attaching the peptide inhibitor to PEG-NLs and AB-NLs. Previous DLS studies have shown that RI-OR2-TAT-NLs are stable (Sherer *et al.,* 2015), and so it is expected that RI-OR2-TAT-NLs will be stable in size and PDI . RI-OR2-TAT+AB-NLs have not been studied previously, and the expected outcome was somewhat unknown. Yet, unexpectedly, RI-OR2-TAT-NLs had significantly increased diameter than PEG-NLs (Figure 3.9), and it is likely that the attachment of RI-OR2-TAT caused the vesicles to clump. RI-OR2-TAT+AB-NLs had a significantly increased diameter than PEG-NLs and AB-NLs. It appears that the attachment of RI-OR2-TAT, rather than the incorporation of antibodies, is causing the diameter to increase. Both of the RI-OR2-TAT modified liposomes are roughly twice the expected size. It is possible that the liposomes are aggregated in pairs, due to the process of RI-OR2-TAT attachment. This would have to be confirmed by further TEM studies.

7.4 Wako Assay investigation

The purpose of this investigation was to characterise the conditions required for the SM content of liposomes to be measured accurately, using the Wako Assay. After characterization, the assay could then be used in the future to accurately determine how much of the lipid weighed out is integrated into liposomes and how much is lost. A standard curve, using Wako assay standard solution, was initially produced in order to assess the accuracy of the Wako Assay kit (Figure 5.1). The phospholipid concentration (mg/mL) measured gave a good line of best fit with a high R^2 value (0.9998), which suggests that the assay kit is reliable.

Before experimentation, it was expected that strong organic solvents such as Me and Chl would be the most successful for measuring SM content as they have been shown previously to dissolve this lipid. As a detergent, Tr X lyses liposomes, and is therefore thought to be beneficial for the assay to detect SM in solution. Yet, the most effective combination of solvents and incubation conditions is likely to change for different SM concentrations and in different liposomal vesicles. As a result, SM was firstly assayed alone (non-liposome) in a variety solvents and incubation conditions to determine which of them can most effectively measure SM concentration. The assay could then be further characterised to measure SM concentration in liposomes. Results showed that, other than Chl alone, all combinations of solvents and their various incubation conditions gave increased lipid concentration compared to SM (3 mg/mL) dissolved in PBS alone (Figure 5.2). The Chl result was unexpectedly poor, and suggests that Chl is only effective when used in combination with Me. SM dissolved in PBS and Tr X (with no additional solvent) produced similar results to SM dissolved in Chl/Me, and 2% Tr X was not significantly increased compared with 0.1% Tr X. It would seem that 0.1% Tr X is sufficient to dissolve the 3mM SM in solution and there is no benefit of using an increased Tr X concentration.

Since both of these approaches have shown success, it would be worthwhile to repeat the assay with both Tr X and solvents like Me to see if the impact is additive or synergistic on yielding the expected SM concentration. Since Chl was somewhat poor in the previous study, it was not included in this experiment. Also, different Tr X concentrations had no significant impact on SM yield. The study was instead conducted with various ratios of Tr X in order to determine if the volume of Tr X had an effect on the SM yield (12 mg/mL). It is difficult to know what to expect from this experiment. If the current ratio of lipid to solvent/Tr X (50:50) is sufficient, then alteration will likely have little effect. Whereas if an increased SM yield is observed, then the solvent/Tr X volume would have previously been a limiting factor. Results

showed that the ratio had no significant impact on lipid concentration; it is therefore assumed that the concentration of solvent/Tr X is not limiting the ability for the assay to detect SM.

Apart from a few unexpected results (e.g. 40:60 ratio of 2% Tr X in Me), the concentration of lipid yielded from the assay ranges from approximately 75-90% of the total SM that was added to the solution. This is sufficient to assume that the majority of lipid is being detected by the assay under optimised conditions and the assay can now be used to detect SM in liposome samples.

Liposomes must be lysed in order to effectively measure their lipid concentration. Tr X is known to lyse liposomes and is almost certainly required for the assay to be successful. The solvent/Tr X conditions optimised for previous experiments on SM will be used for liposomes in order to observe if these conditions are effective. It would be expected that the use of a strong solvent such as Me and Chl would be more effective than PBS alone. While SM samples may effectively dissolve in PBS alone, liposomes often require additional solvents in order to dissolve all the lipid formed in bilayers. As expected, Figure 5.4 and 5.5 shows that the lipid concentration yielded from liposomes is significantly increased in PBS + Me compared with PBS alone. This is not the case in the SM sample, where both PBS and PBS + Me both show concentrations close to 3 mg/mL. This confirms that a solvent is important to dissolve liposomes, yet not important for dissolving free SM in solution. For this sample, it is likely that the processes of heating and sonication as well as Tr X are sufficient to dissolve the majority of the lipid. Figure 5.5 confirms that liposomes in PBS + Me still yield a significantly lower lipid concentration than SM in the same conditions. This suggests that there could be SM in liposomes still not dissolved in PBS + Me. Since a ratio of Me to Chl (1:1) has proven successful in previous experimentation as well as in above results, this is a good strategy to improve accuracy of measuring the lipid concentration of liposomes.

Figure 5.6 shows a comparison between liposomes treated in PBS, PBS + Me and PBS + Me + Chl (1:1). The greatest lipid concentration observed was those treated with PBS + Me + Chl (0.87 mg/mL), which was significantly different from PBS (0.5 mg/mL). Yet, there was no significance with PBS + Me, regardless of the higher lipid concentration. The total lipid concentration for this study was expected to be ~3 mM, which was calculated based on the volumes of lipid weighed out during liposome preparation. When converted to millimolar, the 0.87 mg/mL of SM observed in this study is the equivalent of 1.34 mM. The SM content in these liposomes is only ~50 molar % of the total lipid content, so 1.34 mM can be doubled, producing 2.67 mM, to produce an estimate of total lipid in liposomes. Based on the total lipid weighed into solution, the total lipid conc. was expected to be ~3 mM, which suggests that there is a 10.9% loss of lipid in liposomes compared with the original lipid weighed. Taking into account that there will be loss of lipid dehydration and rehydration and also in the final solution where some lipid won't have formed liposomes, the concentration observed in the assay has detected the large majority of lipid in solution and any lipid loss is likely to be due to these factors involving liposome preparation.

This Wako Assay method and the refined treatment conditions can now be used in the future to determine the actual concentration of lipid in solution and therefore effectively estimate the overall lipid content of liposomes.

7.5 TEM investigation

TEM not only compliments DLS by providing additional information on the size, shape and ultrastructure of nanoliposomes, but it was essential in order to observe antibody encapsulation. Many characteristics that were not revealed by DLS were shown by TEM. For example, key observations included the impact that antibody encapsulated has on the

liposome structure. The ability to visualise liposomes by TEM also allowed quantitative data to be produced and analysed to refine encapsulation techniques to improve efficiency. Four types of nanoliposome (PEG-NL, AB-NL, RI-OR2-TAT-NLs and RI-OR2-TAT+AB-NLs) of different sizes (50 nm, 100 nm and 200 nm) were imaged and analysed.

Other than size and general structure, one key structural characteristic revealed by TEM is the lamellarity of all liposome types. The freeze thawing and sonication preparation methods used here should produce unilamellar vesicles rather than multilamellar vesicles (Traïkia *et al.,* 2000). In addition to observing if the preparation methods used here produce unilamellar PEG-NLs, it was also worthwhile to investigate if any other liposome types, with attached peptide inhibitor or incorporated antibody, have altered lamellarity. Figures 4.1-4 show TEM micrographs of various sizes of PEG-NLs. Depending on the particular micrograph, some show clear unilamellar vesicles, e.g. Figure 4.1 and 4.3, and all micrographs produced liposomes with vesicles that varied slightly in size, but were in the large majority, stable in size and structure. Based on this, it is clear that the current preparation method produces desired vesicles, most of which are unilamellar.

The study involving the incorporation of gold-conjugated antibodies did not require negative staining, and so the resulting micrographs (Figure 4.5-6 and 4.9-10) are not ideal for determining lamellarity. However, results show the characterization of RI-OR2-TAT and AB modified liposomes, which shows unilamellarity in AB-NLs (Figure 4.16), RI-OR2-TAT-NLs (Figure 4.18) and RI-OR2-TAT+AB-NLs (Figure 4.19) in some high magnification micrographs. RI-OR2-TAT-NLs and RI-OR2-TAT+AB-NLs also show some liposomes that are multilamellar. It is possible that the modification has caused a change in the ultrastructure and so some multilamellar vesicles are formed. Yet, the majority remain unilamellar and those that are

multilamellar have only 2-3 layers. Overall, it would seem that the lamellarity is fairly stable for all the liposome types.

7.6 Cell penetration investigation

An important characteristic of AB-NLs is their ability to penetrate cells. In order to do this, 100 nm bodipy liposomes with modifications: NLs, AB-NLs, RI-OR2-TAT-NLs and RI-OR2-TAT+AB-NLs were produced, and tested at various concentrations on neuroblastoma SH-SY5Y cells and measured for cellular uptake. Alexa Fluor antibodies were used for fluorescence observation and were observed under the red filter (referred as Alexa). BODIPY chl also used and was observed under the green filter (referred as Bodipy). The Alexa filter was likely to give insight into situation and quantity of antibodies in cells, whereas the BODIPY chl will track what happens to the liposome once entering the cells. The two filters together were thought to give insight into whether it is possible to transport antibodies into cells using liposomes, and also what happens to them once inside (Holtta-Vuori *et al.,* 2008).

An initial study showed the effectiveness of this experiment (Figure 6.1), showing that liposomes with and without bodipy cholesterol give clear differences under the Bodipy filter. PEG-NLs of different concentrations showed a clear gradient in terms of their intensity under the Bodipy filter, suggesting that higher concentrations of simple PEG-NLs are more likely to penetrate SH-SY5Y cells. This was an observation that was also shown in AB-NLs (Figure 6.3), whereby an increase in liposome concentration appeared to increase cellular uptake. However, the Alexa fluorescence was unexpectedly poor, and there was only a very slight visual increase in fluorescence in the 200 μM compared with the 50 μM. The microscope was also set at maximum sensitively to detect the slightest fluorescent signal. It is likely that the amount of Alexa Fluor incorporated in the AB-NLs is insufficient to produce a greater signal, certainly in these liposomes that do not have RI-OR2-TAT attachment.

As previously discussed, RI-OR2-TAT is a modified CPP that is known to enhance cellular uptake. RI-OR2-TAT-NLs and RI-OR2-TAT+AB-NLs of various concentrations were produced to observe the impact RI-OR2-TAT has on cellular uptake in terms of the BODIPY and Alexa Fluor fluorescent markers that are observed. Figures 6.5 and 6.6 show that the BODIPY intensity is increased as the concentration increased, as expected. However, the overall intensity is far greater than the NL and AB-NLs, suggesting that the addition of RI-OR2-TAT has successfully increased the cellular uptake, without killing the cells. Figure 6.7 shows a comparison between RI-OR2-TAT-NLs and RI-OR2-TAT+AB-NLs. Alexa Fluor is only expected to be seen in the RI-OR2-TAT+AB-NLs, however there appears to be red fluorescence also observed in RI-OR2-TAT-NLs. Whilst this is unexpected, there are a few observations that can be used for evaluation. Firstly, the intensity in the RI-OR2-TAT+AB-NLs increased as the concentration increased, whilst in the RI-OR2-TAT-NLs, there remained a consistent intensity throughout all concentrations. This suggests that the fluorescence observed in the later, is background fluorescence from the liposomes, or the bodipy cholesterol, which can be backed up by the fact the spots of fluorescence on the red filter match up with that of the green, something not observed on the RI-OR2-TAT+AB-NLs. Overall, there is evidence to suggest that RI-OR2-TAT+AB-NLs do transport antibodies into cells with greater success than AB-NLs alone. However, the quantity of antibody reaching the cells is likely still to be low.

7.7 Future studies

The production of these types of liposome carriers for brain delivery is still in its early stages of development. As a result, there are many types of studies that should be performed in order for this system to improve. A variety of different lipids should be trialled in all of the liposome types to observe the impact on liposome stability, which can be confirmed by DLS and TEM. Characteristics such as their shape, size, lamellarity and interaction with other molecules will

differ depending on the lipid composition of liposomes, and this is something that should be measured for vesicle optimisation.

The key study that can be improved is the cell penetration investigation. The current study was informative, showed that antibodies can be delivered into neuronal cells, which was enhanced by the attachment of TAT. However, the uptake of the antibody was likely to be poor. There can be continuous re-evaluation of the antibody incorporation method in order to increase the incorporation efficiency, which will in theory allow the uptake of more antibodies into cells. The antibodies used for the current study were solely used to show that they could be transported into cells, and were not specific towards any AD pathologies. Additional studies could incorporate anti-Tau or anti-Aβ antibodies into liposomes, and transport them into a cell line expressing Tau or Aβ respectively. This would not only demonstrate the uptake efficiency but also the potential for using anti-Tau or anti-Aβ antibodies therapeutically. A final study could also utilise a BBB model, by producing various types of liposomes and observing their ability to penetrate the BBB, which prevents 98% of potential neurotherapeutics from entering the brain. This will particularly highlight the effectiveness of CPPs such as TAT, and if their attachment can enhance the BBB penetrate.

Overall, if studies can show that produced AB-NLs are stable and safe, can penetrate the BBB with the aid of various attachments and can be delivered into cells expressing AD pathologies and have a positive impact on these cells, then this system will have great potential to progress to clinical trials and therapeutic use.

7.8 Conclusion

Compared with plain liposomes, antibody loaded liposomes often had a tendency to clump. Other than this, there was no great impact size or ultrastructure of the vesicles and antibodies

have been shown to be effectively incorporated. However, the incorporation efficiency is likely to have been poor, and development of current antibody incorporation techniques is essential for improved uptake. Modified antibody loaded liposomes were also successfully delivered into SH-SY5Y cells, enhanced by the attachment of TAT. Fluorescence showed that antibody was also delivered into the cells by liposomes. This demonstrates the potential of antibody loaded liposomes for the treatment of AD. Extensive research is still required to improve and refine the technique, in order be used therapeutically.

References

1. Abbott, N. J., Patabendige, A. A. K., Dolman, D. E. M., Yusof, S. R. & Begley, D. J. 2010. Structure and Function of the Blood-Brain Barrier. *Neurobiology of Disease,* 37(1)**,** 13-25.

2. Abra, R. M. & Hunt, C. A. 1981. Liposome Disposition Invivo .3. Dose and Vesicle-Size Effects. *Biochimica Et Biophysica Acta,* 666(3)**,** 493-503.

3. Agrawal, M., Ajazuddin, Tripathi, D. K., Saraf, S., Antimisiaris, S. G., Mourtas, S., Hammarlund-Udenaes, M. & Alexander, A. 2017. Recent Advancements in Liposomes Targeting Strategies to Cross Blood-Brain Barrier (Bbb) for the Treatment of Alzheimer's Disease. *Journal of Controlled Release,* 260**,** 61-77.

4. Akbarzadeh, A., Rezaei-Sadabady, R., Davaran, S., Joo, S. W., Zarghami, N., Hanifehpour, Y., Samiei, M., Kouhi, M. & Nejati-Koshki, K. 2013. Liposome: Classification, Preparation, and Applications. *Nanoscale Research Letters,* 8**,** 9.

5. Allen, T. M. 1997. Liposomes - Opportunities in Drug Delivery. *Drugs,* 54**,** 8-14.

6. Allsop, D. & Mayes, J. 2014. Amyloid Beta-Peptide and Alzheimer's Disease. *In:* PERRETT, S. (ed.) *Amyloids in Health and Disease.* London: Portland Press Ltd.

7. Alonso, A. D., Grundkeiqbal, I., Barra, H. S. & Iqbal, K. 1997. Abnormal Phosphorylation of Tan and the Mechanism of Alzheimer Neurofibrillary Degeneration: Sequestration

of Microtubule-Associated Proteins 1 and 2 and the Disassembly of Microtubules by the Abnormal Tau. *Proceedings of the National Academy of Sciences of the United States of America,* 94(1)**,** 298-303.

8. Alonso, A. D., Grundkeiqbal, I. & Iqbal, K. 1996. Alzheimer's Disease Hyperphosphorylated Tau Sequesters Normal Tau into Tangles of Filaments and Disassembles Microtubules. *Nature Medicine,* 2(7)**,** 783-787.

9. Areosa, A. A. S. 2004. Glutamate Antagonist for Dementia. *European Neuropsychopharmacology,* 14**,** S114-S115.

10. Atamna, H., Nguyen, A., Schultz, C., Boyle, K., Newberry, J., Kato, H. & Ames, B. N. 2008. Methylene Blue Delays Cellular Senescence and Enhances Key Mitochondrial Biochemical Pathways. *Faseb Journal,*22(3)**,** 703-712.

11. Austen, B. M., Paleologou, K. E., Ali, S. A. E., Qureshi, M. M., Allsop, D. & El-Agnaf, O. M. A. 2008. Designing Peptide Inhibitors for Oligomerization and Toxicity of Alzheimer's Beta-Amyloid Peptide. *Biochemistry,* 47(7)**,** 1984-1992.

12. Bangham, A. D., Standish, M. M. & Watkins, J. C. 1965. Diffusion of Univalent Ions across Lamellae of Swollen Phospholipids. *Journal of Molecular Biology,* 13(1)**,** 238-&.

13. Barnham, K. J., Mckinstry, W. J., Multhaup, G., Galatis, D., Morton, C. J., Curtain, C. C., Williamson, N. A., White, A. R., Hinds, M. G., Norton, R. S., Beyreuther, K., Masters, C. L., Parker, M. W. & Cappai, R. 2003. Structure of the Alzheimer's Disease Amyloid Precursor Protein Copper Binding Domain - a Regulator of Neuronal Copper Homeostasis. *Journal of Biological Chemistry,* 278(19)**,** 17401-17407.

14. Bhowmik, A., Khan, R. & Ghosh, M. K. 2015. Blood Brain Barrier: A Challenge for Effectual Therapy of Brain Tumors. *Biomed Research International***,** 20.

15. Bird, T. D. 2008. Genetic aspects of Alzheimer's disease. *Genetics in Medicine.* 10, 231-239.

16. Blennow, K., De Leon, M. J. & Zetterberg, H. 2006. Alzheimer's Disease. *Lancet*, 364(9533), 387-403.

17. Blennow, K., Wallin, A. & Gottfries, C. G. 1991. Presence of Parietotemporal Symptomatology Distinguishes Early and Late Onset Alzheimers-Disease. *International Journal of Geriatric Psychiatry,* 6(3)**,** 147-154.

18. Bozzuto, G. & Molinari, A. 2015. Liposomes as Nanomedical Devices. *International Journal of Nanomedicine,*10**,** 975-999.

19. Braak, H., Braak, E., Grundkeiqbal, I. & Iqbal, K. 1986. Occurrence of Neuropil Threads in the Senile Human-Brain and in Alzheimers-Disease - a 3rd Location of Paired Helical Filaments Outside of Neurofibrillary Tangles and Neuritic Plaques. *Neuroscience Letters,* 65(3)**,** 351-355.

20. Bullock, R. & Dengiz, A. 2005. Cognitive Performance in Patients with Alzheimer's Disease Receiving Cholinesterase Inhibitors for up to 5 Years. *International Journal of Clinical Practice,* 59(7)**,** 817-822.

21. Butner, K. A. & Kirschner, M. W. 1991. Tau-Protein Binds to Microtubules through a Flexible Array of Distributed Weak Sites. *Journal of Cell Biology,* 115(3)**,** 717-730.

22. Corder, E. H., Saunders, A. M., Strittmatter, W. J., Schmechel, D. E., Gaskell, P. C., Small, G. W., Roses, A. D., Haines, J. L. & Pericakvance, M. A. 1993. Gene Dose of Apolipoprotein-E Type-4 Allele and the Risk of Alzheimers-Disease in Late-Onset Families. *Science,* 261(5123)**,** 921-923.

23. Davies, L., Wolska, B., Hilbich, C., Multhaup, G., Martins, R., Simms, G., Beyreuther, K. & Masters, C. L. 1988. A4 Amyloid Protein Deposition and the Diagnosis of Alzheimers-Disease - Prevalence in Aged Brains Determined by Immunocytochemistry Compared with Conventional Neuropathologic Techniques. *Neurology,* 38(11)**,** 1688-1693.

24. De Coupade, C., Fittipaldi, A., Chagnas, V., Michel, M., Carlier, S., Tasciott, E., Darmon, A., Ravel, D., Kearsey, J., Giacca, M. & Cailler, F. 2005. Novel Human-Derived Cell-Penetrating Peptides for Specific Subcellular Delivery of Therapeutic Biomolecules. *Biochemical Journal,* 390**,** 407-418.

25. Deamer, D. & Bangham, A. D. 1976. Large Volume Liposomes by an Ether Vaporization Method. *Biochimica Et Biophysica Acta,* 443(3)**,** 629-634.

26. Derossi, D., Joliot, A. H., Chassaing, G. & Prochiantz, A. 1994. The 3rd Helix of the Antennapedia Homeodomain Translocates through Biological-Membranes. *Journal of Biological Chemistry,* 269(14)**,**10444-10450.

27. Eisenberg, D. & Jucker, M. 2012. The Amyloid State of Proteins in Human Diseases. *Cell,* 148(6)**,** 1188-1203.

28. Fanciullino, R. & Ciccolini, J. 2009. Liposome-Encapsulated Anticancer Drugs: Still Waiting for the Magic Bullet? *Current Medicinal Chemistry,* 16(33)**,** 4361-4373.

29. Fillebeen, C., Descamps, L., Dehouck, M. P., Fenart, L., Benaissa, M., Spik, G., Cecchelli, R. & Pierce, A. 1999. Receptor-Mediated Transcytosis of Lactoferrin through the Blood-Brain Barrier. *Journal of Biological Chemistry,* 274(11)**,** 7011-7017.

30. Fu, H. J., Liu, B., Frost, J. L. & Lemere, C. A. 2010. Amyloid-Beta Immunotherapy for Alzheimer's Disease. *Cns & Neurological Disorders-Drug Targets,* 9(2)**,** 197-206.

31. Futaki, S., Ohashi, W., Suzuki, T., Niwa, M., Tanaka, S., Ueda, K., Harashima, H. & Sugiura, Y. 2001. Stearylated Arginine-Rich Peptides: A New Class of Transfection Systems. *Bioconjugate Chemistry,*12(6)**,** 1005-1011.

32. Gabizon, A., Goren, D., Cohen, R. & Barenholz, Y. 1998. Development of Liposomal Anthracyclines: From Basics to Clinical Applications. *Journal of Controlled Release,* 53(1-3)**,** 275-279.

33. Gaillard, P. J., Appeldoorn, C. C. M., Dorland, R., Van Kregten, J., Manca, F., Vugts, D. J., Windhorst, B., Van Dongen, G., De Vries, H. E., Maussang, D. & Van Tellingen, O. 2014. Pharmacokinetics, Brain Delivery, and Efficacy in Brain Tumor-Bearing Mice of Glutathione Pegylated Liposomal Doxorubicin (2b3-101). *Plos One,* 9(1)**,** 10.

34. Gandy, S. 2005. The Role of Cerebral Amyloid Beta Accumulation in Common Forms of Alzheimer Disease. *Journal of Clinical Investigation,* 115(5)**,** 1121-1129.

35. Gao, C. S., Mao, S. L., Ditzel, H. J., Farnaes, L., Wirsching, P., Lerner, R. A. & Janda, K. D. 2002. A Cell-Penetrating Peptide from a Novel Pvii-Pix Phage-Displayed Random Peptide Library. *Bioorganic & Medicinal Chemistry,* 10(12)**,** 4057-4065.

36. Gao, H. L. 2016. Progress and Perspectives on Targeting Nanoparticles for Brain Drug Delivery. *Acta Pharmaceutica Sinica B,* 6(4)**,** 268-286.

37. Garbuzenko, O., Barenholz, Y. & Priev, A. 2005. Effect of Grafted Peg on Liposome Size and on Compressibility and Packing of Lipid Bilayer. *Chemistry and Physics of Lipids,* 135(2)**,** 117-129.

38. Gauthier, S., Reisberg, B., Zaudig, M., Petersen, R. C., Ritchie, K., Broich, K., Belleville, S., Brodaty, H., Bennett, D., Chertkow, H., Cummings, J. L., De Leon, M., Feldman, H., Ganguli, M., Hampel, H., Scheltens, P., Tierney, M. C., Whitehouse, P., Winblad, B. & Int Psychogeriatric Assoc Expert, C. 2006. Mild Cognitive Impairment. *Lancet,* 367(9518)**,** 1262-1270.

39. Ghanta, J., Shen, C. L., Kiessling, L. L. & Murphy, R. M. 1996. A Strategy for Designing Inhibitors of Beta-Amyloid Toxicity. *Journal of Biological Chemistry,* 271(47)**,** 29525-29528.

40. Gilman, S., Koller, M., Black, R. S., Griffith, S. G., Fox, N. C., Eisner, L., Kirby, L., Rovira, M. B., Forette, F., Orgogozo, J. M. 2005. Clinical effects of Abeta immunization (AN1792) in patients with AD in an interrupted trial. *Neurology,* 64(9), 1553-1562.

41. Glenner, G. G. & Wong, C. W. 2012. Alzheimer's Disease: Initial Report of the Purification and Characterization of a Novel Cerebrovascular Amyloid Protein (Reprinted from Biochemical and Biophysical Research Communications, Vol 120, Pg 885-890, 1984). *Biochemical and Biophysical Research Communications,* 425(3)**,** 534-539.

42. Goedert, M., Spillantini, M. G., Jakes, R., Rutherford, D. & Crowther, R. A. 1989. Multiple Isoforms of Human Microtubule-Associated Protein-Tau - Sequences and Localization in Neurofibrillary Tangles of Alzheimers-Disease. *Neuron,* 3(4)**,** 519-526.

43. Gomez-Hens, A. & Fernandez-Romero, J. M. 2006. Analytical Methods for the Control of Liposomal Delivery Systems. *Trac-Trends in Analytical Chemistry,* 25(2)**,** 167-178.

44. Gregori, M., Taylor, M., Salvati, E., Re, F., Mancini, S., Balducci, C., Forloni, G., Zambelli, V., Sesana, S., Michael, M., Michail, C., Tinker-Mill, C., Kolosov, O., Sherer, M., Harris, S., Fullwood, N. J., Masserini, M. & Allsop, D. 2017. Retro-Inverso Peptide Inhibitor Nanoparticles as Potent Inhibitors of Aggregation of the Alzheimer's a Beta Peptide. *Nanomedicine-Nanotechnology Biology and Medicine,* 13(2)**,** 723-732.

45. Grundkeiqbal, I., Iqbal, K., Tung, Y. C., Quinlan, M., Wisniewski, H. M. & Binder, L. I. 1986. Abnormal Phosphorylation of the Microtubule-Associated Protein-Tau (Tau) in Alzheimer Cytoskeletal Pathology. *Proceedings of the National Academy of Sciences of the United States of America,* 83(13)**,** 4913-4917.

46. Guo, L., Ren, J. & Jiang, X. 2012. Perspectives on Brain-Targeting Drug Delivery Systems. *Current Pharmaceutical Biotechnology,* 13(12)**,** 2310-2318.

47. Haass, C. & Selkoe, D. J. 2007. Soluble Protein Oligomers in Neurodegeneration: Lessons from the Alzheimer's Amyloid Beta-Peptide. *Nature Reviews Molecular Cell Biology,* 8(2)**,** 101-112.

48. Hansen, R. A., Gartlehner, G., Webb, A. P., Morgan, L. C., Moore, C. G. & Jonas, D. E. 2008. Efficacy and Safety of Donepezil, Galantamine, and Rivastigmine for the Treatment of Alzheimer's Disease: A Systematic Review and Meta-Analysis. *Clinical Interventions in Aging,* 3(2)**,** 211-225.

49. Harashima, H. & Kiwada, H. 1996. Liposomal Targeting and Drug Delivery: Kinetic Consideration. *Advanced Drug Delivery Reviews,* 19(3)**,** 425-444.

50. Hardy, J. & Allsop, D. 1991. Amyloid Deposition as the Central Event in the Etiology of Alzheimers-Disease. *Trends in Pharmacological Sciences,* 12(10)**,** 383-388.

51. Hardy, J. & Selkoe, D. J. 2002. Medicine - the Amyloid Hypothesis of Alzheimer's Disease: Progress and Problems on the Road to Therapeutics. *Science,* 297(5580)**,** 353-356.

52. Henriques, S. T. & Castanho, M. 2008. Translocation or Membrane Disintegration? Implication of Peptide-Membrane Interactions in Pep-1 Activity. *Journal of Peptide Science,* 14(4)**,** 482-487.

53. Hersh, D. S., Wadajkar, A. S., Roberts, N. B., Perez, J. G., Connolly, N. P., Frenkel, V., Winkles, J. A., Woodworth, G. F. & Kim, A. J. 2016. Evolving Drug Delivery Strategies

to Overcome the Blood Brain Barrier. *Current Pharmaceutical Design,* 22(9)**,** 1177-1193.

54. Himmler, A., Drechsel, D., Kirschner, M. W. & Martin, D. W. 1989. Tau Consists of a Set of Proteins with Repeated C-Terminal Microtubule-Binding Domains and Variable N-Terminal Domains. *Molecular and Cellular Biology,* 9(4)**,** 1381-1388.

55. Hoff, P. & Hippius, H. 1990. The Life of Alzheimer,Alois. *Psychiatry : a World Perspective, Vol 4: Social Psychiatry ; Ethics and Law ; History of Psychiatric Education,* 900**,** 1061-1065.

56. Hölttä-Vuori M., Uronen R.L., Repakova J., Salonen E., Vattulainen I., Panula P., Li Z., Bittman R. & Ikonen E. 2008. BODIPY-cholesterol: a new tool to visualize sterol trafficking in living cells and organisms. *Traffic.* 3: 221-235.

57. Hutton, M., Lendon, C. L., Rizzu, P., Baker, M., Froelich, S., Houlden, H., Pickering-Brown, S., Chakraverty, S., Isaacs, A., Grover, A., Hackett, J., Adamson, J., Lincoln, S., Dickson, D., Davies, P., Petersen, R. C., Stevens, M., De Graaff, E., Wauters, E., Van Baren, J., Hillebrand, M., Joosse, M., Kwon, J. M., Nowotny, P., Che, L. K., Norton, J., Morris, J. C., Reed, L. A., Trojanowski, J., Basun, H., Lannfelt, L., Neystat, M., Fahn, S., Dark, F., Tannenberg, T., Dodd, P. R., Hayward, N., Kwok, J. B. J., Schofield, P. R., Andreadis, A., Snowden, J., Craufurd, D., Neary, D., Owen, F., Oostra, B. A., Hardy, J., Goate, A., Van Swieten, J., Mann, D., Lynch, T. & Heutink, P. 1998. Association of Missense and 5 '-Splice-Site Mutations in Tau with the Inherited Dementia Ftdp-17. *Nature,* 393(6686)**,** 702-705.

58. Illum, L. 2012. Nasal Drug Delivery - Recent Developments and Future Prospects. *Journal of Controlled Release,* 161(2)**,** 254-263.

59. Immordino, M. L., Dosio, F. & Cattel, L. 2006. Stealth Liposomes: Review of the Basic Science, Rationale, and Clinical Applications, Existing and Potential. *International Journal of Nanomedicine,* 1(3)**,** 297-315.

60. Jicha, G. A., Lane, E., Vincent, I., Otvos, L., Hoffmann, R. & Davies, P. 1997. A Conformation- and Phosphorylation-Dependent Antibody Recognizing the Paired Helical Filaments of Alzheimer's Disease. *Journal of Neurochemistry,* 69(5)**,** 2087-2095.

61. Johansson, H. J., El-Andaloussi, S., Holm, T., Mae, M., Janes, J., Maimets, T. & Langel, U. 2008. Characterization of a Novel Cytotoxic Cell-Penetrating Peptide Derived from P14arf Protein. *Molecular Therapy,* 16(1)**,** 115-123.

62. Kamei, N., Tanaka, M., Choi, H., Okada, N., Ikeda, T., Itokazu, R. & Takeda-Morishita, M. 2017. Effect of an Enhanced Nose-to-Brain Delivery of Insulin on Mild and Progressive Memory Loss in the Senescence-Accelerated Mouse. *Molecular Pharmaceutics,* 14(3)**,** 916-927.

63. Kenworthy, A. K., Hristova, K., Needham, D. & Mcintosh, T. J. 1995a. Range and Magnitude of the Steric Pressure between Bilayers Containing Phospholipids with Covalently Attached Poly(Ethylene Glycol). *Biophysical Journal,* 68(5)**,** 1921-1936.

64. Kenworthy, A. K., Simon, S. A. & Mcintosh, T. J. 1995b. Structure and Phase-Behavior of Lipid Suspensions Containing Phospholipids with Covalently Attached Poly(Ethylene Glycol). *Biophysical Journal,* 68(5)**,**1903-1920.

65. Khatoon, S., Grundkeiqbal, I. & Iqbal, K. 1992. Brain Levels of Microtubule-Associated Protein-Tau Are Elevated in Alzheimers-Disease - a Radioimmuno-Slot-Blot Assay for Nanograms of the Protein. *Journal of Neurochemistry,* 59(2)**,** 750-753.

66. Kopke, E., Tung, Y. C., Shaikh, S., Alonso, A. D., Iqbal, K. & Grundkeiqbal, I. 1993. Microtubule-Associated Protein-Tau - Abnormal Phosphorylation of a Non-Paired Helical Filament Pool in Alzheimer-Disease. *Journal of Biological Chemistry,* 268(32)**,** 24374-24384.

67. Koren, E. & Torchilin, V. P. 2012. Cell-Penetrating Peptides: Breaking through to the Other Side. *Trends in Molecular Medicine,* 18(7)**,** 385-393.

68. Lai, F., Fadda, A. M. & Sinico, C. 2013. Liposomes for Brain Delivery. *Expert Opinion on Drug Delivery,* 10(7)**,**1003-1022.

69. Lasch, J., Weissig, V. & Brandl, M. 2003. Preparation of liposomes. In: Torchilin B, Weissig V, editors. Liposomes: A Practical Approach. *New York: Oxford University Press.*

70. Lee, V. M. Y., Goedert, M. & Trojanowski, J. Q. 2001. Neurodegenerative Tauopathies. *Annual Review of Neuroscience,* 24**,** 1121-1159.

71. Levylahad, E., Wasco, W., Poorkaj, P., Romano, D. M., Oshima, J., Pettingell, W. H., Yu, C. E., Jondro, P. D., Schmidt, S. D., Wang, K., Crowley, A. C., Fu, Y. H., Guenette, S. Y., Galas, D., Nemens, E., Wijsman, E. M., Bird, T. D., Schellenberg, G. D. & Tanzi, R. E. 1995. Candidate Gene for the Chromosome-1 Familial Alzheimers-Disease Locus. *Science,* 269(5226)**,** 973-977.

72. Li, J. F., Zhou, L., Ye, D. Y., Huang, S. X., Shao, K., Huang, R. Q., Han, L., Liu, Y., Liu, S. H., Ye, L. Y., Lou, J. N. & Jiang, C. 2011. Choline-Derivate-Modified Nanoparticles for Brain-Targeting Gene Delivery. *Advanced Materials,* 23(39)**,** 4516-+.

73. Li, W. Z., Zhou, Y. Q., Zhao, N., Hao, B. H., Wang, X. N. & Kong, P. 2012. Pharmacokinetic Behavior and Efficiency of Acetylcholinesterase Inhibition in Rat Brain after Intranasal Administration of Galanthamine Hydrobromide Loaded Flexible Liposomes. *Environmental Toxicology and Pharmacology,* 34(2)**,** 272-279.

74. Lindgren, M., Hallbrink, M., Prochiantz, A. & Langel, U. 2000. Cell-Penetrating Peptides. *Trends in Pharmacological Sciences,* 21(3)**,** 99-103.

75. Lu, W., Zhang, Y., Tan, Y. Z., Hu, K. L., Jiang, X. G. & Fu, S. K. 2005. Cationic Albumin-Conjugated Pegylated Nanoparticles as Novel Drug Carrier for Brain Delivery. *Journal of Controlled Release,* 107(3)**,** 428-448.

76. Mackenzie, I. R. A. & Neumann, M. 2016. Molecular Neuropathology of Frontotemporal Dementia: Insights into Disease Mechanisms from Postmortem Studies. *Journal of Neurochemistry,* 138**,** 54-70.

77. Magzoub, M., Sandgren, S., Lundberg, P., Oglecka, K., Lilja, J., Wittrup, A., Eriksson, L. E. G., Langel, U., Belting, M. & Graslund, A. 2006. N-Terminal Peptides from Unprocessed Prion Proteins Enter Cells by Macropinocytosis. *Biochemical and Biophysical Research Communications,* 348(2)**,** 379-385.

78. Mahley, R. W. 2016. Central Nervous System Lipoproteins Apoe and Regulation of Cholesterol Metabolism. *Arteriosclerosis Thrombosis and Vascular Biology,* 36(7)**,** 1305-1315.

79. Malam, Y., Loizidou, M. & Seifalian, A. M. 2009. Liposomes and Nanoparticles: Nanosized Vehicles for Drug Delivery in Cancer. *Trends in Pharmacological Sciences,* 30(11)**,** 592-599.

80. Mangialasche, F., Solomon, A., Winblad, B., Mecocci, P. & Kivipelto, M. 2010. Alzheimer's Disease: Clinical Trials and Drug Development. *Lancet Neurology,* 9(7)**,** 702-716.

81. Martin, J. B. 1999. Molecular Basis of the Neurodegenerative Disorders. *New England Journal of Medicine,*340(25)**,** 1970-1980.

82. Masserini, M. 2013. Nanoparticles for brain drug delivery. *ISRN Biochemistry*, 2013, 18.

83. Mckeith, I., Mintzer, J., Aarsland, D., Burn, D., Chiu, H., Cohen-Mansfield, J., Dickson, D., Dubois, B., Duda, J. E., Feldman, H., Gauthier, S., Halliday, G., Lawlor, B., Lippa, C.,

Lopez, O. L., Machado, J. C., O'brien, J., Playfer, J., Reid, W. & Int Psychogeriatric Assoc Expert, M. 2004. Dementia with Lewy Bodies. *Lancet Neurology,* 3(1)**,** 19-28.

84. Merchant, C., Tang, M. X., Albert, S., Manly, J., Stern, Y. & Mayeux, R. 1999. The Influence of Smoking on the Risk of Alzheimer's Disease. *Neurology,* 52(7)**,** 1408-1412.

85. Moller, H. J. & Graeber, M. B. 1998. The Case Described by Alois Alzheimer in 1911 - Historical and Conceptual Perspectives Based on the Clinical Record and Neurohistological Sections. *European Archives of Psychiatry and Clinical Neuroscience,* 248(3)**,** 111-122.

86. Morris, M. C., Deshayes, S., Heitz, F. & Divita, G. 2008. Cell-Penetrating Peptides: From Molecular Mechanisms to Therapeutics. *Biology of the Cell,* 100(4)**,** 201-217.

87. Morrison, J. H. & Hof, P. R. 1997. Life and Death of Neurons in the Aging Brain. *Science,* 278(5337)**,** 412-419.

88. Murphy, M. P. & Levine, H. 2010. Alzheimer's Disease and the Amyloid-Beta Peptide. *Journal of Alzheimers Disease,* 19(1)**,** 311-323.

89. Nicolas, M. & Hassan, B. A. 2014. Amyloid Precursor Protein and Neural Development. *Development,* 141(13)**,**2543-2548.

90. Noble, G. T., Stefanick, J. F., Ashley, J. D., Kiziltepe, T. & Bilgicer, B. 2014. Ligand-Targeted Liposome Design: Challenges and Fundamental Considerations. *Trends in Biotechnology,* 32(1)**,** 32-45.

91. Nordberg, A., Hellstrom-Lindahl, E., Lee, M., Johnson, M., Mousavi, M., Hall, R., Perry, E., Bednar, I. & Court, J. 2002. Chronic Nicotine Treatment Reduces Beta-Amyloidosis in the Brain of a Mouse Model of Alzheimer's Disease (Appsw). *Journal of Neurochemistry,* 81(3)**,** 655-658.

92. Novak, M., Jakes, R., Edwards, P. C., Milstein, C. & Wischik, C. M. 1991. Difference between the Tau-Protein of Alzheimer Paired Helical Filament Core and Normal Tau Revealed by Epitope Analysis of Monoclonal Antibodies-423 and Antibodies-7.51. *Proceedings of the National Academy of Sciences of the United States of America,* 88(13)**,** 5837-5841.

93. Oehlke, J., Krause, E., Wiesner, B., Beyermann, M. & Bienert, M. 1997. Extensive Cellular-Uptake into Endothelial Cells of an Amphipathic Beta-Sheet Forming Peptide. *Febs Letters,* 415(2)**,** 196-199.

94. Orgogozo, J. M., Dartigues, J. F., Lafont, S., Letenneur, L., Commenges, D., Salamon, R., Renaud, S. & Breteler, M. 1997. Wine Consumption and Dementia in the Elderly: A Prospective Community Study in the Bordeaux Area. *Revue Neurologique,* 153(3)**,** 185-192.

95. Palchetti, S., Colapicchioni, V., Digiacomo, L., Caracciolo, G., Pozzi, D., Capriotti, A. L., La Barbera, G. & Lagana, A. 2016. The Protein Corona of Circulating Pegylated Liposomes. *Biochimica Et Biophysica Acta-Biomembranes,* 1858(2)**,** 189-196.

96. Pardridge, W. M. 2007. Brain Drug Development and Brain Drug Targeting. *Pharmaceutical Research,* 24(9)**,**1729-1732.

97. Parthsarathy, V., Mcclean, P. L., Holscher, C., Taylor, M., Tinker, C., Jones, G., Kolosov, O., Salvati, E., Gregori, M., Masserini, M. & Allsop, D. 2013. A Novel Retro-Inverso Peptide Inhibitor Reduces Amyloid Deposition, Oxidation and Inflammation and Stimulates Neurogenesis in the Appswe/Ps1 Delta E9 Mouse Model of Alzheimer's Disease. *Plos One,* 8(1)**,** 11.

98. Petersen, R. C. 2004. Mild Cognitive Impairment as a Diagnostic Entity. *Journal of Internal Medicine,* 256(3)**,**183-194.

99. Petit, A., Bihel, F., Da Costa, C. A., Pourquie, O., Checler, F. & Kraus, J. L. 2001. New Protease Inhibitors Prevent Gamma-Secretase-Mediated Production of a Beta 40/42 without Affecting Notch Cleavage. *Nature Cell Biology,* 3(5)**,** 507-511.

100. Pfrieger, F. W. 2003. Cholesterol Homeostasis and Function in Neurons of the Central Nervous System. *Cellular and Molecular Life Sciences,* 60(6)**,** 1158-1171.

101. Pooga, M., Hallbrink, M., Zorko, M. & Langel, U. 1998. Cell Penetration by Transportan. *Faseb Journal,* 12(1)**,**67-77.

102. Prince, M., Ali, G. C., Guerchet, M., Prina, A. M., Albanese, E. & Wu, Y. T. 2016. Recent Global Trends in the Prevalence and Incidence of Dementia, and Survival with Dementia. *Alzheimers Research & Therapy,* 8**,**13.

103. Qian, Z. M., Li, H. Y., Sun, H. Z. & Ho, K. 2002. Targeted Drug Delivery Via the Transferrin Receptor-Mediated Endocytosis Pathway. *Pharmacological Reviews,* 54(4)**,** 561-587.

104. Raymond, L. A., Andre, V. M., Cepeda, C., Gladding, C. M., Milnerwood, A. J. & Levine, M. S. 2011. Pathophysiology of Huntington's Disease: Time-Dependent Alterations in Synaptic and Receptor Function. *Neuroscience,* 198**,** 252-273.

105. Rhee, M. & Davis, P. 2006. Mechanism of Uptake of C105y, a Novel Cell-Penetrating Peptide. *Journal of Biological Chemistry,* 281(2)**,** 1233-1240.

106. Rogaev, E. I., Sherrington, R., Rogaeva, E. A., Levesque, G., Ikeda, M., Liang, Y., Chi, H., Lin, C., Holman, K., Tsuda, T., Mar, L., Sorbi, S., Nacmias, B., Piacentini, S., Amaducci, L., Chumakov, I., Cohen, D., Lannfelt, L., Fraser, P. E., Rommens, J. M. & Stgeorgehyslop, P. H. 1995. Familial Alzheimers-Disease in Kindreds with Missense Mutations in a Gene on Chromosome-1 Related to the Alzheimers-Disease Type-3 Gene. *Nature,* 376(6543)**,** 775-778.

107. Roth, M. 1986. The Association of Clinical and Neurological Findings and Its Bearing on the Classification and Etiology of Alzheimers-Disease. *British Medical Bulletin,* 42(1)**,** 42-50.

108. Rotman, M., Welling, M. M., Bunschoten, A., De Backer, M. E., Rip, J., Nabuurs, R. J. A., Gaillard, P. J., Van Buchem, M. A., Van Der Maarel, S. M. & Van Der Weerd, L. 2015. Enhanced Glutathione Pegylated Liposomal Brain Delivery of an Anti-Amyloid Single

Domain Antibody Fragment in a Mouse Model for Alzheimer's Disease. *Journal of Controlled Release,* 203**,** 40-50.

109. Ruitenberg, A., Van Swieten, J. C., Witteman, J. C. M., Mehta, K. M., Van Duijn, C. M., Hofman, A. & Breteler, M. M. B. 2002. Alcohol Consumption and Risk of Dementia: The Rotterdam Study. *Lancet,* 359(9303)**,**281-286.

110. Rumble, B., Retallack, R., Hilbich, C., Simms, G., Multhaup, G., Martins, R., Hockey, A., Montgomery, P., Beyreuther, K. & Masters, C. L. 1989. Amyloid A4 Protein and Its Precursor in Downs-Syndrome and Alzheimers-Disease. *New England Journal of Medicine,* 320(22)**,** 1446-1452.

111. Sadler, K., Eom, K. D., Yang, J. L., Dimitrova, Y. & Tam, J. P. 2002. Translocating Proline-Rich Peptides from the Antimicrobial Peptide Bactenecin 7. *Biochemistry,* 41(48)**,** 14150-14157.

112. Sanchez-Navarro, M., Giralt, E. & Teixido, M. 2017. Blood-Brain Barrier Peptide Shuttles. *Current Opinion in Chemical Biology,* 38**,** 134-140.

113. Saunders, A. M., Strittmatter, W. J., Schmechel, D., Georgehyslop, P. H. S., Pericakvance, M. A., Joo, S. H., Rosi, B. L., Gusella, J. F., Crappermaclachlan, D. R., Alberts, M. J., Hulette, C., Crain, B., Goldgaber, D. & Roses, A. D. 1993. Association of Apolipoprotein-E Allele Epsilon-4 with Late-Onset Familial and Sporadic Alzheimers-Disease. *Neurology,* 43(8)**,** 1467-1472.

114. Schuber, F., Said Hassane, F. & Frisch, B. 2007. Coupling of peptides to the surface of liposomes – Application to liposome-based synthetic vaccines. *Informa Healthcare, New York,* 111-130.

115. Schupf, N., Kapell, D., Nightingale, B., Lee, J. H., Mohlenhoff, J., Bewley, S., Ottman, R. & Mayeux, R. 2001. Specificity of the Fivefold Increase in Ad in Mothers of Adults with Down Syndrome. *Neurology,* 57(6)**,**979-984.

116. Selkoe, D. J. 2001. Alzheimer's Disease: Genes, Proteins, and Therapy. *Physiological Reviews,* 81(2)**,** 741-766.

117. Selkoe, D. J. 2011. Alzheimer's Disease. *Cold Spring Harbor Perspectives in Biology,* 3(7)**,** 16.

118. Shaw, P. J. 2005. Molecular and Cellular Pathways of Neurodegeneration in Motor Neurone Disease. *Journal of Neurology Neurosurgery and Psychiatry,* 76(8)**,** 1046-1057.

119. Sherer, M., Fullwood, N. J., Taylor, M., Allsop, D. & Iop. 2015. A Preliminary Electron Microscopic Investigation into the Interaction between a Beta(1-42) Peptide and a Novel Nanoliposome-Coupled Retro-Inverso Peptide Inhibitor, Developed as a Potential Treatment for Alzheimer's Disease. Electron Microscopy and Analysis Group Conference (EMAG), Jun 02-Jul 02 2015 Manchester, ENGLAND. BRISTOL: Iop Publishing Ltd.

120. Shulman, J. M., De Jager, P. L. & Feany, M. B. 2011. Parkinson's Disease: Genetics and Pathogenesis. *In:*ABBAS, A. K., GALLI, S. J. & HOWLEY, P. M. (eds.) *Annual Review of Pathology: Mechanisms of Disease, Vol 6.* Palo Alto: Annual Reviews.

121. Soto, C. 2003. Unfolding the Role of Protein Misfolding in Neurodegenerative Diseases. *Nature Reviews Neuroscience,* 4(1)**,** 49-60.

122. Stern, Y. 2012. Cognitive reserve in ageing and Alzheimer's Disease. *Neurology,* 11(11), 1006-1012

123. Sudimack, J. & Lee, R. J. 2000. Targeted Drug Delivery Via the Folate Receptor. *Advanced Drug Delivery Reviews,* 41(2)**,** 147-162.

124. Szoka, F. & Papahadjopoulos, D. 1978. Procedure for Preparation of Liposomes with Large Internal Aqueous Space and High Capture by Reverse-Phase Evaporation. *Proceedings of the National Academy of Sciences of the United States of America,* 75(9)**,** 4194-4198.

125. Tabner, B. J., El-Agnaf, O. M. A., Turnbull, S., German, M. J., Paleologou, K. E., Hayashi, Y., Cooper, L. J., Fullwood, N. J. & Allsop, D. 2005. Hydrogen Peroxide Is Generated During the Very Early Stages of Aggregation of the Amyloid Peptides Implicated in Alzheimer Disease and Familial British Dementia. *Journal of Biological Chemistry,* 280(43)**,** 35789-35792.

126. Taylor, B. N., Mehta, R. R., Yamada, T., Lekmine, F., Christov, K., Chakrabarty, A. M., Green, A., Bratescu, L., Shilkaitis, A., Beattie, C. W. & Gupta, T. K. D. 2009. Noncationic

Peptides Obtained from Azurin Preferentially Enter Cancer Cells. *Cancer Research,* 69(2)**,** 537-546.

127. Taylor, M., Moore, S., Mayes, J., Parkin, E., Beeg, M., Canovi, M., Gobbi, M., Mann, D. M. A. & Allsop, D. 2010. Development of a Proteolytically Stable Retro-Inverso Peptide Inhibitor of Beta-Amyloid Oligomerization as a Potential Novel Treatment for Alzheimer's Disease. *Biochemistry,* 49(15)**,** 3261-3272.

128. Tjernberg, L. O., Naslund, J., Lindqvist, F., Johansson, J., Karlstrom, A. R., Thyberg, J., Terenius, L. & Nordstedt, C. 1996. Arrest of Beta-Amyloid Fibril Formation by a Pentapeptide Ligand. *Journal of Biological Chemistry,* 271(15)**,** 8545-8548.

129. Tokuda, T., Fukushima, T., Ikeda, S., Sekijima, Y., Shoji, S., Yanagisawa, N. & Tamaoka, A. 1997. Plasma Levels of Amyloid Beta Proteins a Beta 1-40 and a Beta 1-42(43) Are Elevated in Down's Syndrome. *Annals of Neurology,* 41(2)**,** 271-273.

130. Traïkia, M., Warschawski, D. E., Recouvreur, M., Cartaud J. & Devaux, P. F. 2000. Formation of unilamellar vesicles by repetitive freeze-thaw cycles: Characterization by electron microscopy and 31P-nuclear magnetic resonance. *European Biophysics Journal,* 29, 184-195.

131. Trevitt, C. R. & Singh, P. N. 2003. Variant Creutzfeldt-Jakob Disease: Pathology, Epidemiology, and Public Health Implications. *American Journal of Clinical Nutrition,* 78(3)**,** 651S-656S.

132. Tseng, Y. L., Liu, J. J. & Hong, R. L. 2002. Translocation of Liposomes into Cancer Cells by Cell-Penetrating Peptides Penetratin and Tat: A Kinetic and Efficacy Study. *Molecular Pharmacology,* 62(4)**,** 864-872.

133. Van Dyck, C. H. 2018. Anti-Amyloid-Beta Monoclonal Antibodies for Alzheimer's Disease: Pitfalls and Promise. *Biological Psychiatry,* 83(4)**,** 311-319.

134. Vemuri, S. & Rhodes, C. T. 1995. Preparation and characterization of liposomes as therapeutic delivery systems: a review. *Pharmaceutica Acta Helvetiae,* 70, 95-111.

135. Verdile, G., Fuller, S., Atwood, C. S., Laws, S. M., Gandy, S. E. & Martins, R. N. 2004. The Role of Beta Amyloid in Alzheimer's Disease: Still a Cause of Everything or the Only One Who Got Caught? *Pharmacological Research,* 50(4)**,** 397-409.

136. Veronese, F. M. & Mero, A. 2008. The Impact of Pegylation on Biological Therapies. *Biodrugs,* 22(5)**,** 315-329.

137. Vieira, D. B. & Gamarra, L. F. 2016. Getting into the Brain: Liposome-Based Strategies for Effective Drug Delivery across the Blood-Brain Barrier. *International Journal of Nanomedicine,* 11**,** 5381-5414.

138. Visser, P. J., Scheltens, P. & Verhey, F. R. J. 2005. Do Mci Criteria in Drug Trials Accurately Identify Subjects with Predementia Alzheimer's Disease? *Journal of Neurology Neurosurgery and Psychiatry,* 76(10)**,**1348-1354.

139. Vives, E., Richard, J. P., Rispal, C. & Lebleu, B. 2003. Tat Peptide Internalization: Seeking the Mechanism of Entry. *Current Protein & Peptide Science,* 4(2)**,** 125-132.

140. Wagner, A., Vorauer-Uhl, K. 2011. Liposome technology for industrial purposes. *Journal of Drug Delivery,* 2011, 591325.

141. Walsh, D. M. & Selkoe, D. J. 2007. A Beta Oligomers - a Decade of Discovery. *Journal of Neurochemistry,*101(5)**,** 1172-1184.

142. Wender, P. A., Mitchell, D. J., Pattabiraman, K., Pelkey, E. T., Steinman, L. & Rothbard, J. B. 2000. The Design, Synthesis, and Evaluation of Molecules That Enable or Enhance Cellular Uptake: Peptoid Molecular Transporters. *Proceedings of the National Academy of Sciences of the United States of America,* 97(24)**,**13003-13008.

143. Wischik, C. M., Bentham, P., Wischik, D. J., Seng, K. M. 2008. Tau aggregation inhibitor (TAI) therapy with rember™ arrests disease progression in mild and moderate Alzheimer's disewase over 50 weeks. *Alzheimer's and Dementia,* 4, T167.

144. World Alzheimer Report. 2016. Improving healthcare for people living with dementia. *Alzheimer's Disease International.*

145. World Health Organisation. 2006. Neurological Disorders: Public Health Challenges. *Geneva: WHO.*

146. Xie, F. L., Yao, N., Qin, Y., Zhang, Q. Y., Chen, H. L., Yuan, M. Q., Tang, J., Li, X. K., Fan, W., Zhang, Q., Wu, Y., Hai, L. & He, Q. 2012. Investigation of Glucose-Modified

Liposomes Using Polyethylene Glycols with Different Chain Lengths as the Linkers for Brain Targeting. *International Journal of Nanomedicine,*7**,** 163-175.

147. Yanamandra, K., Patel, T. K., Jiang, H., Schindler, S., Ulrich, J. D., Boxer, A. L., Miller, B. L., Kerwin, D. R., Gallardo, G., Stewart, F., Finn, M. B., Cairns, N. J., Verghese, P. B., Fogelman, I., West, T., Braunstein, J., Robinson, G., Keyser, J., Roh, J., Knapik, S. S., Hu, Y. & Holtzman, D. M. 2017. Anti-Tau Antibody Administration Increases Plasma Tau in Transgenic Mice and Patients with Tauopathy. *Science Translational Medicine,* 9(386)**,** 11.

148. Yiannopoulou, K. G. & Papageorgiou, S. G. 2013. Current and Future Treatments for Alzheimer's Disease. *Therapeutic Advances in Neurological Disorders,* 6(1)**,** 19-33.

149. Zheng, X. Y., Shao, X. Y., Zhang, C., Tan, Y. Z., Liu, Q. F., Wan, X., Zhang, Q. Z., Xu, S. M. & Jiang, X. G. 2015. Intranasal H102 Peptide-Loaded Liposomes for Brain Delivery to Treat Alzheimer's Disease. *Pharmaceutical Research,* 32(12)**,** 3837-3849.

Websites

https://avantilipids.com/divisions/equipment-products

International Journal of Nanomedicine

Dovepress
open access to scientific and medical research

Open Access Full Text Article

REVIEW

Liposome delivery systems for the treatment of Alzheimer's disease

This article was published in the following Dove Press journal:
International Journal of Nanomedicine

Callum Ross
Mark Taylor
Nigel Fullwood
David Allsop

Division of Biomedical and Life Sciences, Faculty of Health and Medicine, Lancaster University, Lancaster LA1 4YQ, UK

Abstract: Alzheimer's disease (AD) will affect around 115 million people worldwide by the year 2050. It is associated with the accumulation of misfolded and aggregated proteins (β-amyloid and tau) in the senile plaques and neurofibrillary tangles found in the brain. Currently available drugs for AD only temporarily alleviate symptoms and do not slow the inevitable progression of this disease. New drugs are required that act on key pathologies in order to arrest or reverse cognitive decline. However, there has been a spectacular failure rate in clinical trials of conventional small molecule drugs or biological agents. Targeted nanoliposomes represent a viable and promising drug delivery system for AD that have not yet reached clinical trials. They are biocompatible, highly flexible, and have the potential to carry many different types of therapeutic molecules across the blood–brain barrier (BBB) and into brain cells. They can be tailored to extend blood circulation time and can be directed against individual or multiple pathological targets. Modifications so far have included the use of brain-penetrating peptides, together with Aβ-targeting ligands, such as phosphatidic acid, curcumin, and a retro-inverted peptide that inhibits Aβ aggregation. Combining several modifications together into multifunctional liposomes is currently a research area of great interest. This review focuses on recent liposomal approaches to AD therapy, including mechanisms involved in facilitating their passage across the BBB, and the evaluation of new therapeutic agents for blocking Aβ and/or tau aggregation.

Keywords: amyloid, blood–brain barrier, cell-penetrating peptides, neurofibrillary tangles, senile plaques, tau

Introduction

Alzheimer's disease (AD) affects 36 million people worldwide, and this number is set to rise to over 115 million by 2050, as populations age.[1] AD is a neurodegenerative disorder that severely affects the functioning of the brain, triggering widespread neuronal and synaptic loss, memory impairment, and cognitive and behavioral disturbances.[2] A major hypothesis regarding the underlying cause of AD is that the progressive accumulation of protein aggregates in the brain leads to neurodegeneration and dementia[3] (see Karran and de Strooper[4] for a critical review). These protein aggregates include extracellular senile plaques, containing the β-amyloid (Aβ) peptide, and neurofibrillary tangles (NFTs), consisting of intra-neuronal paired helical filaments (PHFs) composed of hyper-phosphorylated tau protein.[5] Aβ spontaneously and progressively aggregates to form oligomers and amyloid fibrils, with oligomers being a strong candidate for inducing synaptic damage and memory deficits in AD.[6] However, AD is likely to be a multifactorial disorder, with many mechanisms, including NFT formation, contributing to neuronal cell damage.

It is well established that Aβ and tau underlie the neuropathology of AD, but many aspects of the neuropathogenesis of this disease remain unanswered. There is

Correspondence: David Allsop
Division of Biomedical and Life Sciences, Faculty of Health and Medicine, Lancaster University, Room B75, Furness College, Lancaster LA1 4YQ, UK
Tel +44 1524 592122
Email d.allsop@lancaster.ac.uk

submit your manuscript | www.dovepress.com
Dovepress
http://dx.doi.org/10.2147/IJN.S183117

good evidence that aggregation and accumulation of these molecules induce membrane damage and oxidative damage through an increase in free radical production and promotion of pro-inflammatory processes.[7–9] NFT formation is also likely to interfere with axonal transport systems. The drugs currently available for the treatment of AD (acetylcholinesterase inhibitors [AChEIs] and the NMDA antagonist memantine) do not target any of these underlying disease mechanisms[10] and do not slow down the long-term progression of the disorder. Instead, they provide only temporarily improved cognition by counterbalancing neurotransmitter disturbances, in addition to having many limitations and side effects.[11] It is therefore essential to develop alternative therapies, with minimal adverse side effects, which aim to prevent, slow or reverse the neurodegeneration responsible for AD. Unfortunately, clinical trials on >200 drugs, with different molecular targets, have so far failed to find a therapeutic approach that arrests or reverses cognitive decline in patients with AD.[12–14]

Any effective treatment for AD would most likely require the therapeutic agent concerned to be transported across the blood–brain barrier (BBB),[15] which prevents access to the brain of around 98% of potential neuropharmaceuticals.[16] Liposomes are a biocompatible and highly flexible drug delivery system, with the potential for carrying many different types of bioactive molecules across the BBB. The therapeutic potential of liposomes was recognized shortly after their development in 1961, but only recently they have been considered as a suitable vehicle for the delivery of drugs that act on the central nervous system (CNS).[17,18] Their physiological composition facilitates numerous modifications, in comparison with other nano-carriers. Simple "non-targeted" liposomes can carry a drug cargo into the brain (eg, via the olfactory route, see "Intranasal delivery" section), but modified "targeted" liposomes are required for effective delivery across the BBB and can also be designed to interact with specific molecular targets relevant to the treatment or prevention of AD. Liposomes can incorporate hydrophilic or lipophilic/hydrophobic therapeutic agents, where hydrophilic drugs are entrapped in the aqueous core, and lipophilic compounds are contained in the hydrophobic region of the lipid bilayer.[19] Moreover, various types of therapeutic agent can be attached to the surface of the liposomes. These various configurations can be combined to give a targeted multi-drug delivery system, which is particularly relevant for the treatment of any multifactorial disease. These attractive properties of liposomes have provoked an interest in their development as a possible new and effective therapy for AD. This narrative review presents our own perspective on recent and promising liposome approaches to AD therapy, including mechanisms involved in facilitating their passage across the BBB, and the evaluation of new therapeutic agents for blocking Aβ and/or tau aggregation.

The BBB

The BBB is a metabolic and transport barrier that protects the brain from harmful stimuli. It comprises brain capillary endothelial cells that are attached to each other through tight junctions, resulting in restricted paracellular transport.[20,21] Degrading enzymes are also present at the BBB, which can destroy molecules during their attempted passage into the brain.[22] However, specific mechanisms are in place for the BBB transport of molecules that are essential for brain function,[23] and these can be exploited for therapeutic drug delivery.

Early strategies for BBB transportation

Passive diffusion permits the passage of some small lipophilic compounds across the BBB, such as certain amino acids, nucleosides, and small peptides. An early strategy utilized this simple mechanism by developing small lipophilic drugs that might pass through the endothelial cells. However, this excluded the vast majority of potential therapeutic molecules. A second approach was to develop small water-soluble drugs, in order to facilitate BBB transport via the paracellular hydrophilic diffusion pathway. However, most of these potential molecules could not penetrate past the tight endothelial cell junctions.[24]

Alternatives

Intracerebral or intracerebroventricular injection of drugs provides a strategy that avoids the BBB, but these procedures are highly invasive, and so are not widely used. Drugs administered by any peripheral route (eg, orally or by intravenous injection) will encounter the BBB.[25] Alternative methods, such as bypassing the BBB by delivery through the olfactory region (eg, as a nasal spray) have some potential.[26–28] Another strategy looks to utilize existing active BBB transport mechanisms, namely carrier-mediated transcytosis (also known as transporter-mediated transcytosis), receptor-mediated transcytosis, cell-mediated endocytosis, and adsorptive transcytosis (Table 1).[29]

Liposomal approaches to AD therapy

Several different types of nanoparticles (eg, solid lipid, magnetic, dendrimers, and liposomes) are under development

Table 1 Transport mechanisms for BBB transit and brain delivery

Transport mechanism	Explanation	Examples
Carrier-mediated transcytosis	Some essential materials required in the brain have specific transporters for active uptake across the BBB. Drugs can exploit these transporters for brain delivery	Glutathione[46] Glucose[49]
Receptor-mediated transcytosis	Receptors on the BBB endothelium can bind specifically with corresponding ligands and trigger internalization. Drugs can incorporate these ligands, or their modified forms, for enhanced brain penetration	Transferrin receptor[104] Insulin receptor[105] Lactoferrin receptor[106]
Cell-mediated endocytosis	Endocytosis into endothelial cells can deliver drugs across the BBB. This mechanism is almost unique to the action of CPPs which exhibit various features to trigger transportation, and they are often highly positively charged	TAT[64] Penetratin[107] Polyarginines[108]
Adsorptive transcytosis	Adsorptive-mediated targeting utilizes a modified, positively charged biological macromolecule for interaction with the negatively charged BBB, based on electrostatic attraction	Cationized bovine serum albumin[109] Cationized immunoglobulins/monoclonal antibodies[105]

Abbreviations: BBB, blood–brain barrier; CPPs, cell-penetrating peptides; TAT, transactivator of transcription of human immunodeficiency virus.

as possible vectors for AD therapy. A popular strategy is to aim for optimum brain selectivity by targeting receptors or transporters that are highly expressed at the BBB, and improving stability, for example, by using non-natural amino acids in the case of peptide drugs, so that they are resistant to proteolysis.[30] A second route considers intranasal administration of the active compounds, without any BBB interruption. Recent studies have begun to focus on liposomes as a possible carrier of drugs for the treatment of AD.[31–33]

BBB transport

Possible mechanisms for the transport of liposomes across the BBB have been highly debated.[25] An initial theory was that the phospholipid bilayer of the liposomes on its own might facilitate transportation across various biological membranes, including the BBB, but this simple mechanism proved to be ineffective. Modifications proposed for enhancing the transport of liposome carriers across the BBB utilize the existing active transport mechanisms, involving absorptive, carrier- or receptor-mediated transcytosis.[34] Absorptive methods take advantage of the BBB's negative charge. Cationic liposomal drug vehicles have been developed that can trigger cell internalization through electrostatic interactions. However, the nonspecific uptake of the cationic liposomes by peripheral tissues and their binding to serum proteins has meant that a toxic dose would often be required to reach therapeutic efficacy,[35] thus limiting therapeutic potential. Carrier-mediated transcytosis utilizes nutrients capable of passing across the BBB, such as glucose and glutathione (GSH), that can be attached to the surface of liposomes and facilitate translocation.[19] Ultimately, receptor-mediated transcytosis has great potential for success, since there are possibilities to target one or more of the many different receptors at the BBB by using their respective ligands. Yet there is still substantial interest in direct penetration of the BBB membrane, which has been achieved largely through the use of cell-penetrating peptides (CPPs) (Figure 1).

Intranasal delivery

A second route involves the intranasal administration of liposomes. This strategy avoids the BBB by offering direct nose-to-brain absorption through the olfactory and trigeminal nerves. Liposomal encapsulation of compounds can result in improved penetration via this route, by protecting them from degradation and facilitating their transport across the mucosal barrier. A recent study has demonstrated effective administration of a liposome-encapsulated "β-breaker" peptide, known as H102, using this strategy.[27] Results showed satisfactory drug concentrations in the brain, with limited toxicity. Thus, the intranasal route offers a promising alternative to BBB transport and delivery.

Vesicle optimization

Liposome size

Liposome size, as well as lipid composition, affects their circulation in the bloodstream and uptake into the brain.[36,37] Brain delivery requires liposomes to be roughly nano- or microsized and consists of one or more lipid bilayers surrounding an aqueous core. Only certain sizes will allow passage across the BBB for neurotherapy (such as in AD) and so small vesicles (100 nm and less) are often preferred. There are studies, however, that have shown that liposomes from 100 to 140 nm have certain advantages, such as a longer half-life in blood circulation and avoidance of plasma proteins.

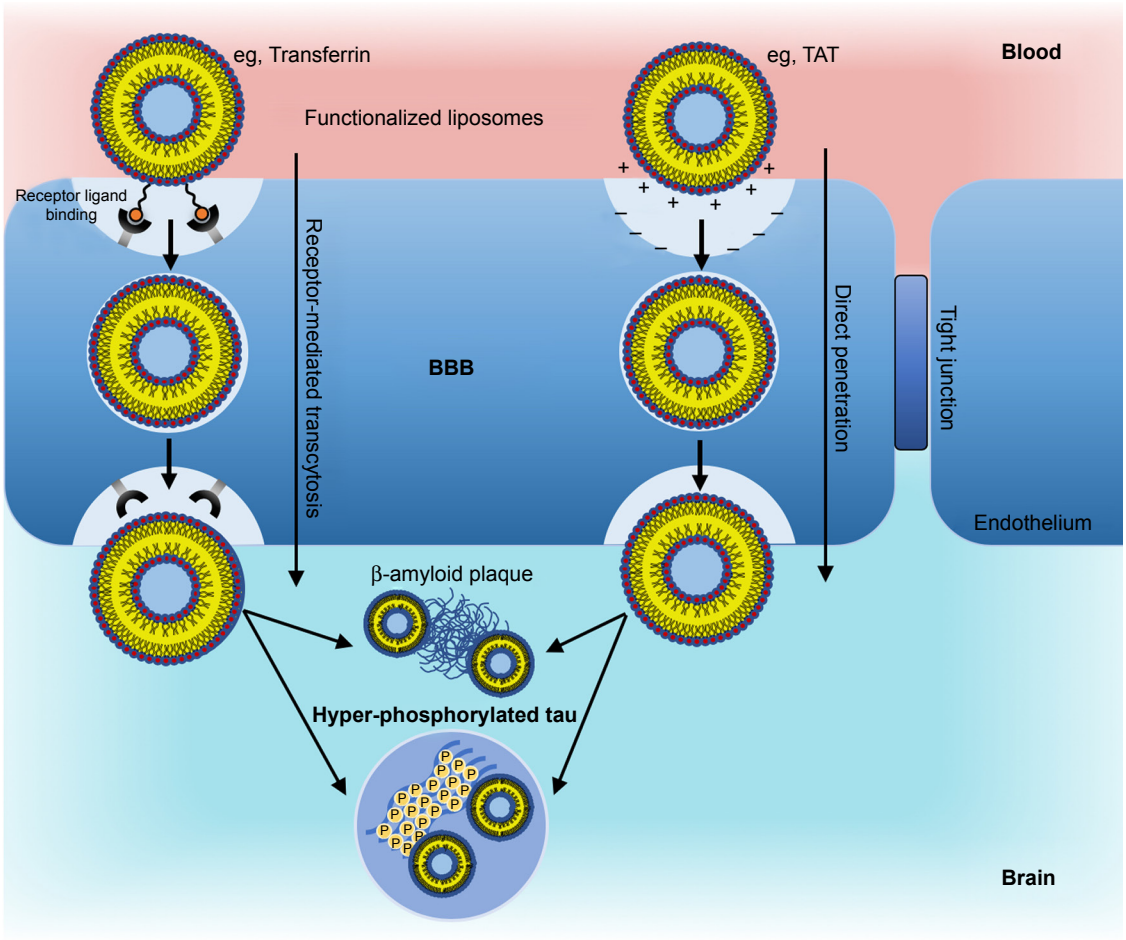

Figure 1 Promising liposomal BBB transport mechanisms.
Notes: Receptor-mediated transcytosis exploits receptors highly expressed at the BBB (eg, transferrin receptor). Receptor ligand binding triggers internalization and brain delivery. A relatively new mechanism, direct penetration, involves internalization primarily exhibited by CPPs (eg, TAT). Positively charged amino acids (+++) permit endocytosis by interacting with the negatively charged endothelial cell membrane (– – –). Once in the brain, multifunctional liposomes can be directed at an appropriate target (eg, at Aβ or tau) for AD therapy.
Abbreviations: BBB, blood–brain barrier; CPPs, cell-penetrating peptides; Aβ, amyloid-β; AD, Alzheimer's disease; TAT, transactivator of transcription of human immunodeficiency virus.

Large nano-liposomes (250 nm in diameter) are cleared twice as fast as 100 nm liposomes.[38] Yet, liposomes 100 nm and smaller have more limited storage capacity, leading to poor encapsulation efficiency.[39] A consideration of size should be made based on factors such as their therapeutic application, encapsulation efficiency, and stability.

Lipid composition

Phospholipids commonly used in liposomes include synthetic lipids such as 1,2-dipalmitoyl-sn-glycero-3-phosphocholine and ethyl-phosphatidylcholine, or natural lipids such as phosphatidylcholine (PC), sphingomyelin (SP), and lecithin (LC). Natural lipids are at risk of contamination from viruses, prions, or toxins, especially if they are isolated from a mammalian source, for example, bovine brain. They are, however, cheaper in large-scale production, use fewer solvents and other chemicals in their extraction, and are more readily accepted by regulatory authorities, especially when derived from a non-animal (eg, plant) source. Cholesterol is often added to liposomes during assembly, which not only maintains the stability of membranes in vivo and in vitro but also reduces permeability and alters the structure and function of the vesicles.[40]

Aβ has been shown to insert preferentially into any anionic phospholipids incorporated into liposomes, which could have a protective effect, by removing toxic Aβ.[41,42] The majority of treatments aimed at AD have used PEGylated 1,2-distearoyl-sn-glycero-3-phosphoethanolamine-PEG 2000 (DSPE) to improve circulation time (see "Stealth liposomes" section), although wheat germ agglutinin, chitosan, silk fibroin, and polyvinyl alcohol have also been used to achieve similar "stealth" properties.

Liposome modifications

Liposomes can be functionalized in various ways in order to realize their potential as a therapeutic carrier (Figure 2). Modification can involve the attachment of molecules to the exterior, or the encapsulation of molecules internally, either in the aqueous core or lipid bilayers.[19] Figure 2 considers possible modifications to liposomes that are particularly relevant for the treatment of AD.

Stealth liposomes

Simple liposomes are covered by plasma proteins (eg, fibrinogen, immunoglobulins, and complement proteins) when in circulation, so that a "protein corona" is formed around them. This leads to the activation of phagocytic systems and removal of these liposomes from the bloodstream.[43] In order to improve their pharmacokinetic profile and allow longer time-periods in circulation, so-called "stealth" liposomes were developed, with polyethylene glycol (PEG), or another polysaccharide, incorporated into one of the lipid components of the liposomal membrane. PEG has high hydration, and this increases hydrodynamic volume and allows the formation of a water cloud around the polymer. Any hydrophilic molecule bound covalently to PEG also exhibits these properties, providing increased solubility and resistance to interaction with plasma proteins. Subsequently, PEGylated liposomes in circulation are less prone to formation of a protein corona, allowing dramatically improved circulation times. However, there is no certainty that these liposomes will be transported across the BBB. To provide this, further modifications are required, often involving the use of PEGylated lipids for attachment of suitable components to the liposome surface.[44]

BBB transport

GSH

The transport of liposomes across the BBB can be facilitated by the attachment of appropriate molecules to the lipid surface. One of these is GSH, an endogenous tripeptide and antioxidant found in almost every cell in the human body. Due to its essential protective role in the brain, GSH is transported actively across the BBB, via a sodium-dependent GSH transporter that is highly expressed on the BBB epithelium. However, the exact mechanism of action of this transporter remains unclear.[45–47] "G-Technology®" is a strategy involving

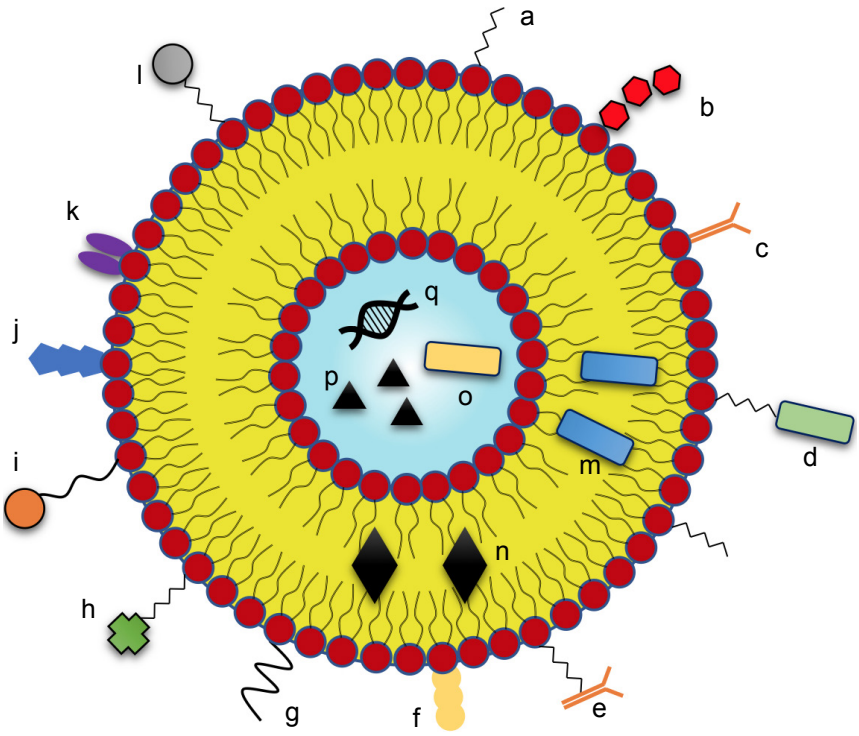

Figure 2 Promising liposomal modifications for AD therapy.
Notes: These modifications improve their stability and bioavailability, aid BBB transportation, and engage therapeutic targets relevant to treatment of AD. Stability – (a) PEGylation. BBB transportation – (b) glutathione, (c) surface antibody, (d) PEG-peptide, (e) PEG-antibody, (f) lactoferrin, (g) glucose, (h) wheat germ agglutinin, (i) PEG-mApoE, (j) transferrin. Targeting systems for AD – (k) phosphatidic acid, (l) PEG-curcumin, (m) lipophilic peptide, (n) lipophilic drug, (o) hydrophilic peptide, (p) hydrophilic drug, (q) nucleic acid.
Abbreviations: AD, Alzheimer's disease; ApoE, apolipoprotein E; BBB, blood–brain barrier; PEG, polyethylene glycol.

PEGylated liposomes with glutathione (GSH-PEG)-mediated delivery across the BBB into the brain, and this has shown some success in double transgenic APPswe/PS1ΔE9 (APP/PS1) mice,[47] but receptor saturation limits this system's effectiveness.[48] Additional research is required to enhance this strategy further.

Glucose

In a similar way to GSH, there are carrier-mediated transport mechanisms in place to facilitate the transport of glucose across the BBB, and the incorporation of glucose onto the liposome surface can enhance BBB delivery.[30] Glucose-modified PEGylated liposomes prepared with various PEG chain lengths have been tested for BBB penetration in mice. Results show that liposomes with shorter PEG chain lengths have little evidence of brain penetration, because the glucose cannot interact effectively with the BBB surface, and therefore cannot utilize the glucose transporter. Longer PEG chain lengths are highly flexible and are able to fold back on themselves in such a way that the ability to cross the BBB is also impaired. Liposomes prepared with medium length PEG chains attached to glucose can cross the BBB more effectively.[49] Thus, liposomal preparations with medium length PEGylation are likely to be the most effective method for utilizing glucose to enhance BBB transport.

Transferrin (Tf)

Tf is the most commonly targeted receptor (TfR), due to its localization on BBB endothelia. This localization is likely to be due to Tf's essential role as an iron-binding blood plasma glycoprotein that controls the level of free iron and oxidative stress in the brain, as well as in other tissues.[50] Fishman et al demonstrated that Tf could cross the BBB via receptor-mediated endocytosis,[51] and more recent studies have shown that liposomes modified with Tf can also penetrate the BBB in vitro.[52,53] However, TfR-mediated endocytosis of liposomes is limited due to endogenous Tf competing for binding to the TfR.[54] This issue can in part be resolved by using antibodies that bind with higher affinity than Tf to TfR, thus avoiding this competition. Still, Tf is likely to be most effective as part of a highly functionalized liposome, where multiple modifications allow an additive increase in BBB transport; a view supported by recent studies.[55,56]

Lactoferrin (Lf)

The lactoferrin receptor (LfR), bound by Lf, is also heavily overexpressed on the BBB, which has led to the development of Lf functionalized liposomes to enhance transport into the brain via receptor-mediated endocytosis.[57] This delivery system has the potential to be particularly efficient, as the expression of the LfR on microvessels and neurons is increased in AD,[58] allowing more effective targeting. Chen et al[57] investigated the ability of Lf procationic liposomes (Lf-PCLs) to cross the BBB of rodents, for potential treatment of AD. Lf-PCLs become positively charged upon binding to the Lf receptor on the BBB epithelium. This allows them to fuse more easily with the BBB and overcome disadvantages such as non-specific binding and poor stability in circulation.[59]

mApoE

The ApoE glycoprotein is responsible for the transport and delivery of cholesterol and other lipids from the plasma to the CNS.[60] It contains a peptide binding domain that permits BBB transport. A peptide sequence containing this binding domain (mApoE) has been used to facilitate BBB transport in vitro.[61,62] However, the success of this peptide alone to facilitate BBB transport is uncertain, as the BBB still limits the transport of ApoE, and therefore mApoE, in and out of the brain.[63] It is likely, therefore, to be used in combination with other liposome modifications.

CPPs

In the last 20 years, CPPs have been identified, which are able to translocate across biological membranes, including the BBB.[64] They cross in a non-toxic manner, independent of membrane receptors and energy, which could reduce the limitations of receptor saturation that have been observed with other methods. Most CPPs rely on positively charged amino acids interacting with the negatively charged membrane. Arginine and to a lesser extent lysine are particularly effective, as they form hydrogen bonds with the negatively charged phosphates, which may lead to internalization. CPPs with different properties vary in their internalization mechanisms (Table 2), but remain similar in their effective direct penetration of cell membranes.

Among all CPPs, the HIV-1 tat (TAT) protein has been best described and has been used successfully for delivery of liposome nanoparticles into the brain.[65] TAT triggers steps for non-specific endocytotic delivery due to ionic interactions between positive charges of the peptide and negative charges of the BBB.[66] Recent studies have utilized a retro-inverted version of TAT, where L-amino acids are replaced with D-amino acids, and the sequence is reversed. This reduces the potential problems with TAT, such as protease degradation and poor bioavailability in vivo, but still maintains the ability for transport across the BBB.[67] Alternative CPPs, such

Table 2 Cell-penetrating peptides (CPPs) and their mechanism of internalization

CPP	Mechanism	Origin	References
TAT	Non-specific endocytosis	HIV-1	66, 67
Penetratin	Endocytosis	Antennapedia *Drosophila melanogaster*	107, 110
Pep-1	Pore formation	Chimeric	111
Pep-7	Pore formation	CHL8 peptide phage clone	112
pVEC	Transporter mediated	Murine endothelial cadherin	113
Transportan	Endocytosis	Galanin-mastoparan	114
Polyarginines	Multiple mechanisms	Chemically synthesized	108, 115
DPV1047	Energy-dependent mechanisms, independent of GAGs (charge interactions, HSPH binding)	Chemically synthesized	116
MPG	Pore formation	HIV glycoprotein 41/SV40 T antigen NLS	117
ARF	Endocytosis	p14 ARF protein	118
p28	Caveolar-mediated/nonclathrin-caveolar-mediated	Azurin	119
BPrPr	Macropinocytosis (fluid-phase endocytosis)	N terminus of unprocessed bovine prion protein	120
VT5	Non-specific endocytosis	Chemically synthesized	121
Bac 7	Likely non-specific endocytosis	Bactenecin family of antimicrobial peptides	122
C105Y	Energy-independent process via caveolin- and clathrin-independent lipid rafts	α1-Antitrypsin	123
PFVYLI	Energy-independent process via caveolin- and clathrin-independent lipid rafts	Derived from synthetic C105Y	123

as polyarginines (eg, octa-arginine) and penetratin have also shown potential for the delivery of therapeutics directly to the brain in SAMP8 mice.[68]

Multifunctionalized liposomes

Many of the modifications discussed above are likely to be more effective as part of a multifunctionalized liposomal system. This will include one or more molecules that enhance BBB transport, but most importantly, it will allow the incorporation of molecules that permit both BBB transport and targeting for AD therapy. The following are multifunctionalized liposomal systems that utilize some of the modifications discussed above and are in development as possible treatments for AD.

Aβ targeting

It is likely that the accumulation and aggregation of Aβ in the brain have an important role, directly or indirectly, in the induction of synaptic damage and memory deficits in AD.[69,70] The accumulation of Aβ oligomers or fibrils may be caused by overproduction, inefficient clearance from the brain, or by a combination of both of these. Effective therapeutic molecules can have an impact on one of these mechanisms to reduce Aβ burden. Many of these molecules on their own have low uptake across the BBB, but their incorporation into a multifunctionalized liposomal system can help to resolve this problem, allowing effective targeting to Aβ.

mApoE-PA liposomes

Balducci et al[71] conducted a key study to look at the ability of multifunctional liposomes to target Aβ. These liposomes were bi-functionalized with mApoE to enhance crossing of the BBB, and with phosphatidic acid (PA), which is a high affinity ligand for Aβ.[61,71] This bifunctional liposome (mApoE-PA-LIP) was able to disaggregate Aβ fibrils in vitro, a property that was not exhibited by liposomes monofunctionalized with either mApoE or PA alone. This synergistic effect could be due to simultaneous interaction of the negatively charged PA phosphate group with positively charged amino acid residues on Aβ and of positively charged amino acids on mApoE with negatively charged regions of Aβ.[72] Results from in vivo studies, showing a reduction in amyloid plaque load only with mApoE-PA-LIP, are supportive of this idea. However, the uptake of mApoE-PA-LIP in the brain was very low, despite the mApoE modification. Mancini et al conducted a follow-up investigation on the

mechanism behind this therapy, and a strategy known as the "sink effect" was proposed, which reduces Aβ burden by peripheral administration of a binding agent that draws excess Aβ out of the brain (Figure 3).[73] The study showed that peripheral administration of mApoE-PA-LIP increased the level of plasma Aβ without significant amounts of mApoE-PA-LIP entering the brain. Aβ oligomers were found to be transported out of the brain, across the BBB, with mApoE-PA-LIP acting in the periphery to mediate a fivefold increase in this efflux.[74]

This provides an insight into future therapies that may only require sequestration of Aβ in the plasma, without the need to cross the BBB. It is evident, however, that this therapy might slow down neurodegeneration, but does not eliminate the cause of Aβ overproduction. Yet, this bifunctional liposome system provides a valuable insight into future research that may effectively prevent amyloid plaque formation.

Curcumin-lipid liposomes

Oxidative damage occurs very early on in course of AD,[75,76] and antioxidants can protect neurons from β-amyloid toxicity,[77] and so clinical trials involving antioxidants for the treatment of AD have been undertaken. So far, these have been unsuccessful,[78] but the use of curcumin, a turmeric derivative, has shown some potential due to its anti-amyloid effects.[79] This phenolic antioxidant binds to amyloid deposits in vitro and in vivo, and it not only disrupts the aggregation of the amyloid peptide but also disaggregates pre-formed fibrils.[80,81] A curcumin analog with a substitution at the C-4 position has been reported to be more effective in this regard than curcumin itself.[82]

Curcumin has relatively poor bioavailability, hence, liposomal delivery systems for curcumin have been developed in an attempt to overcome this.[83,84] In the curcumin-lipid modified liposome developed by Mourtas et al,[84] a PEGylated lipid coating provides stealth characteristics and acts as an anchor allowing the attachment of anti-transferrin monoclonal antibodies, for mediation of transport across the BBB, in addition to a lipid-PEG-curcumin derivative. Results showed that this system has high affinity for amyloid plaques and reduces amyloid plaque formation in APPswe transgenic mice.[79] These liposomes may be useful in the future for the diagnosis and treatment of AD.

Peptide inhibitor nanoparticles (PINPs)

Austen et al[85] showed that a small peptide, named OR2 (RGKLVFFGR-NH_2), inhibits the aggregation of Aβ into oligomers and fibrils, and blocks the toxic effects of Aβ on cultured cells. However, this peptide is sensitive to proteolysis and was not designed to cross the BBB.[85] To improve its stability, a retro-inverso version (RI-OR2) was made,[86] and this was enhanced further by the addition of a retro-inverted version of TAT to RI-OR2, producing RI-OR2-TAT (Ac-rGffvlkGrrrrqrrkkrGy-NH_2).[67] Following its peripheral injection, a fluorescein-labeled version of RI-OR2-TAT was found to cross the BBB and bind to the amyloid plaques present in the cerebral cortex of APPswe/PS1ΔE9 transgenic mice. Daily intraperitoneal (ip) injection

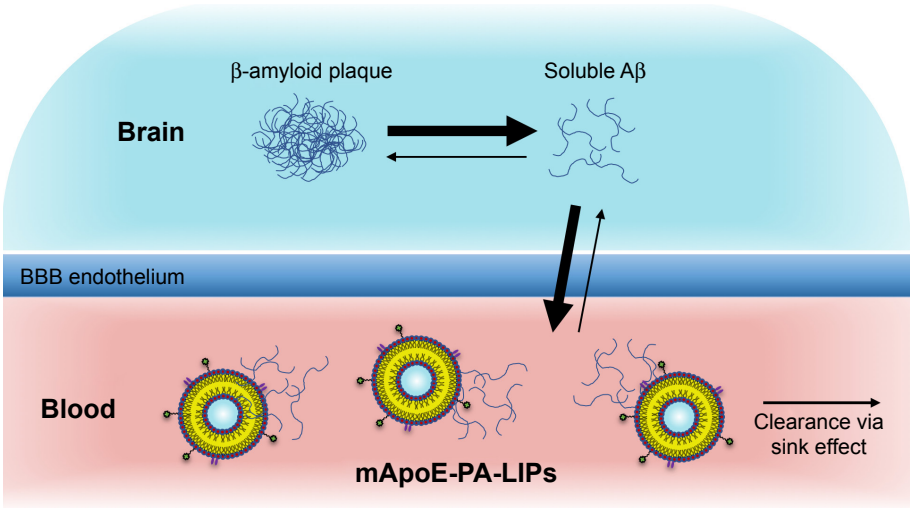

Figure 3 The sink effect strategy.
Notes: Aβ assemblies are in equilibrium between the brain and bloodstream, across the BBB endothelium. It is proposed that mApoE-PA modified liposomes sequester soluble Aβ (monomers or soluble oligomers) in the peripheral bloodstream, which is then cleared. This creates an imbalance of soluble Aβ. Transport of Aβ from the brain to the blood, across the BBB, is then favored, to restore this imbalance. This reduces Aβ burden in the brain and is coined the "sink effect."
Abbreviations: Aβ, amyloid-β; mApoE-PA, apolipoprotein-E-phosphatidic acid; BBB, blood–brain barrier.

of RI-OR2-TAT, for 3 weeks, into these mice resulted in substantial (25%–45%) reductions in brain Aβ oligomer levels, amyloid plaque counts, oxidative damage, and inflammatory processes. However, RI-OR2-TAT inhibits Aβ aggregation only at relatively high concentrations (ie, at a molar ratio of RI-OR2-TAT:Aβ of 1:5 at best) and so its therapeutic potential is likely to be limited.[67]

In order to improve RI-OR2-TAT further, it was attached to the surface of stealth liposomes by covalent linkage to the PEGylated lipid, via an additional cysteine residue on the peptide, to produce PINPs (Figure 4).[65] The presence of the liposome carrier greatly improves the potency of RI-OR2-TAT, so that a molar ratio of 1:2,000 of liposome-linked inhibitory peptide to Aβ now gives ~50% inhibition of Aβ aggregation. This great increase in potency could be due to a multivalent effect. Many copies of the RI-OR2-TAT decorate each liposome, which should allow the simultaneous interaction of multiple inhibitory peptides with any multimeric form of Aβ, thus increasing efficiency as an aggregation inhibitor. EM studies have shown that PINPs can attach themselves to the free ends of amyloid fibrils (Figure 5),[87] apparently terminating fibril growth,

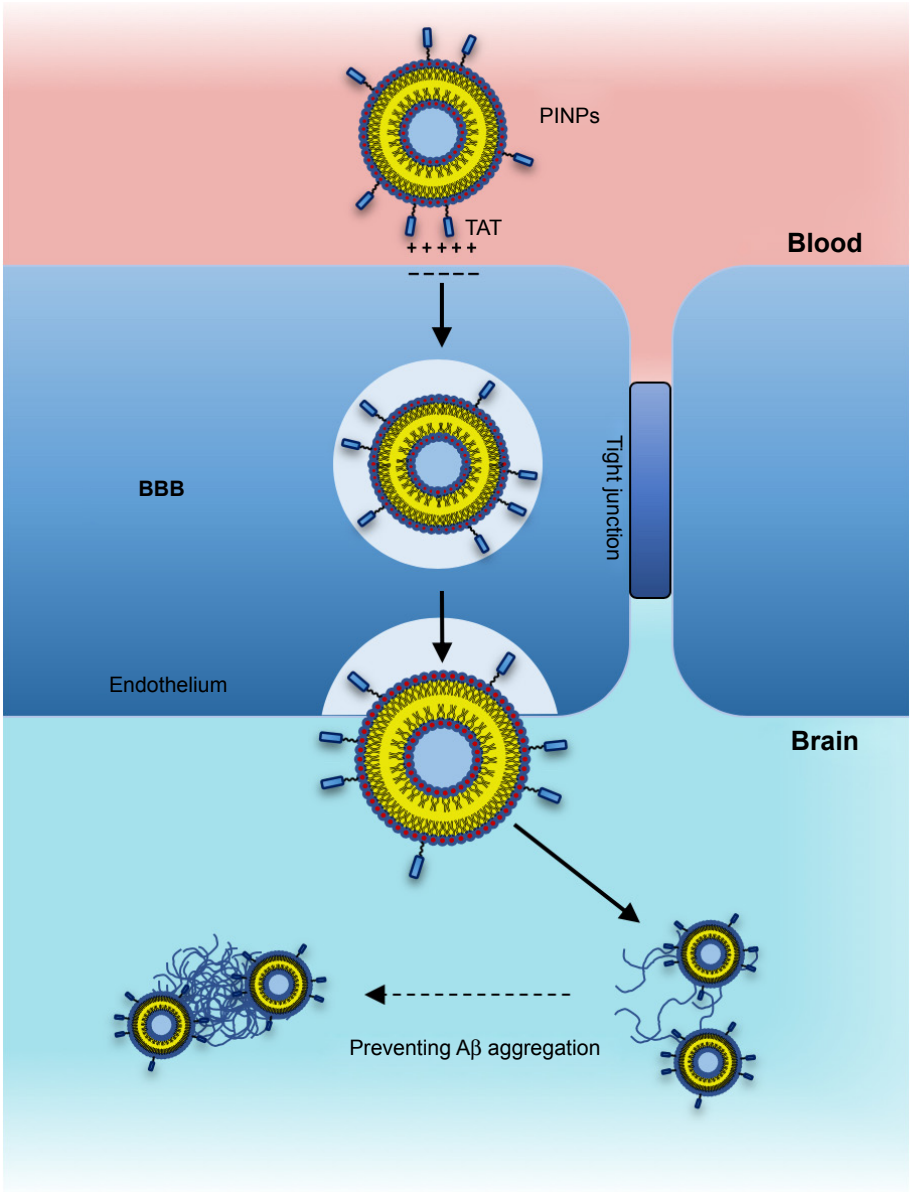

Figure 4 Targeting strategy with PINPs.
Notes: PINPs transport across the BBB by non-specific endocytosis, triggered by positively charged TAT interaction with the negatively charged membrane. RI-OR2-TAT inhibitor acts to prevent the aggregation of Aβ into oligomers and fibrils.
Abbreviations: Aβ, amyloid-β; BBB, blood–brain barrier; PINPs, peptide inhibitor nanoparticles; TAT, transactivator of transcription of human immunodeficiency virus.

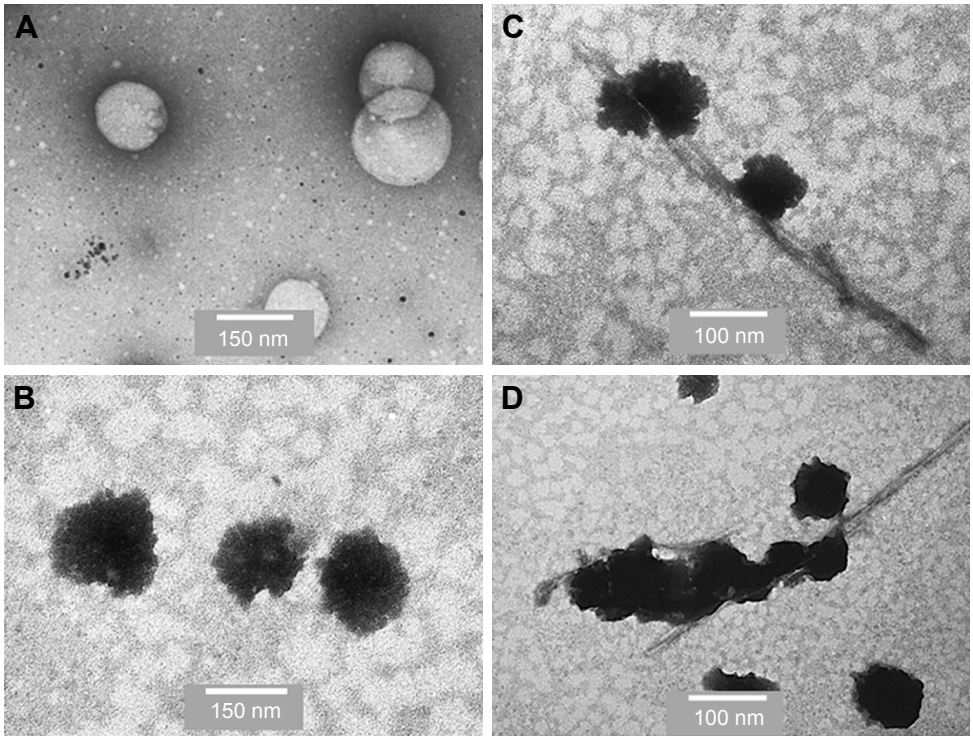

Figure 5 Incubation of PINPs with Aβ.
Notes: Figure shows TEM images of negatively stained PINPs. (**A**) Individual PINPs before incubation with Aβ. (**B**) Individual PINPs after incubation with Aβ. (**C**) and (**D**) PINPs after extended incubation with Aβ bound to amyloid fibrils. Scale bars: **A** and **B** 150 nm, **C** and **D** 100 nm.
Abbreviations: Aβ, amyloid-β; PINPs, peptide inhibitor nanoparticles; TEM, transmission electron microscope.

and possibly preventing the formation of Aβ oligomers (the free ends of fibrils act as "factories" for generation of oligomeric Aβ).[88] Studies in transgenic mice have shown that peripheral injection of PINPs protects against memory loss in TG2576 mice.[65] The TAT region of the inhibitory peptide facilitates brain penetration, with a brain:blood ratio of around 50% being achieved shortly after intravenous (iv) injection. However, most of the dose accumulates in peripheral tissues, such as lungs, liver, and spleen, most likely due to clearance of liposomes via the reticuloendothelial system, and so it is possible that the "sink" effect (see above) could explain some of the in vivo properties of PINPs. The effectiveness of these PINPS could be improved in future by incorporation of alternative or additional brain delivery systems.

Neurotransmission targeting

Synaptic loss and degeneration in AD include the loss of brain cholinergic neurons, which results in decreased acetylcholine (ACh) levels, reduced ACh receptor (AChR) density, and an overall decrease in cholinergic neurotransmission. Many limitations and side effects are associated with the existing AChEIs that attempt to rebalance cholinergic neurotransmission in AD. They have poor stability in circulation, unpredictable uptake and bioavailability, and can cause gastrointestinal complications and, occasionally, even esophageal tears.[89] They also provide only temporarily improved cognition. Yet, it may be worthwhile to improve these existing therapies, especially since viable alternatives have failed to emerge. Subsequently, studies have investigated the potential use of multifunctionalized liposomes, incorporating existing drugs, to treat AD.

Rivastigmine-loaded liposomes

Rivastigmine is a reversible, noncompetitive inhibitor of brain acetylcholinesterase (AChE).[90] As stated previously, oral rivastigmine administration has many limitations, such as poor stability and low ability to pass through the BBB. An alternative intranasal delivery route has shown some potential as an alternative for rivastigmine administration.[91] A study from Yang et al[92] has considered whether intranasal delivery of liposomes loaded with rivastigmine can enhance brain delivery and improve therapeutic effect. These liposomes were modified with a PEGylated derivative of a polyarginine CPP (DSPE-PEG-CPP) to increase stability and enhance BBB delivery, respectively, in an attempt to improve the limitations exhibited by the administration of rivastigmine alone. It was found that liposomes improved the therapeutic

effect of rivastigmine, due to enhanced transcytosis across both the BBB and cellular membranes.[92]

El-Helaly et al[94] have reported an alternative modification strategy for the intranasal administration of rivastigmine-loaded liposomes. In order to maintain their stability, a positively charged inducer called didecyldimethyl ammonium bromide was added to these liposomes, leading to electrostatic repulsion and reduced interactions between them. This, coupled with the use of a PEGylated lipid, resulted in a highly stabile "electrosteric stealth liposome."[93] Results showed a fourfold increase in both plasma and brain drug levels, compared to rivastigmine itself. This effect was increased further with liposomes bound to Tween 80, a nonionic surfactant that has been found to enhance BBB transport.[94] Tween 80 is likely to act as an anchor for apolipoproteins (APO-E and APO-B), enhancing BBB transport via receptor-mediated endocytosis.[95] Further preclinical studies on rivastigmine-loaded liposomes are required, such as toxicity and dose–response studies, before they can be considered as suitable for therapeutic use.

Liposomes with multiple therapeutic targets

Liposomes have great potential for modification, including the development of multifunctional liposomes directed against more than one therapeutic target. In the case of AD, one of the legitimate goals would be to target the formation of both Aβ plaques and tau tangles. Theoretically, it is possible to conceive of a multifunctional liposome that also incorporates other therapeutics, such as those directed at the ACh system, neuroprotectants, autophagy, anti-inflammatory agents, or antioxidants.

Wheat germ agglutinin-conjugated liposomes

The multifunctional liposomes produced by Kuo et al aim to improve the overall neuronal survival in AD by inhibiting the phosphorylation of p38 and c-Jun N-terminal kinase (JNK), two key members of the mitogen-activated protein kinase (MAPK) family, in neurons damaged by the accumulation of Aβ (Figure 6).[42] Study of this kinase cascade is essential

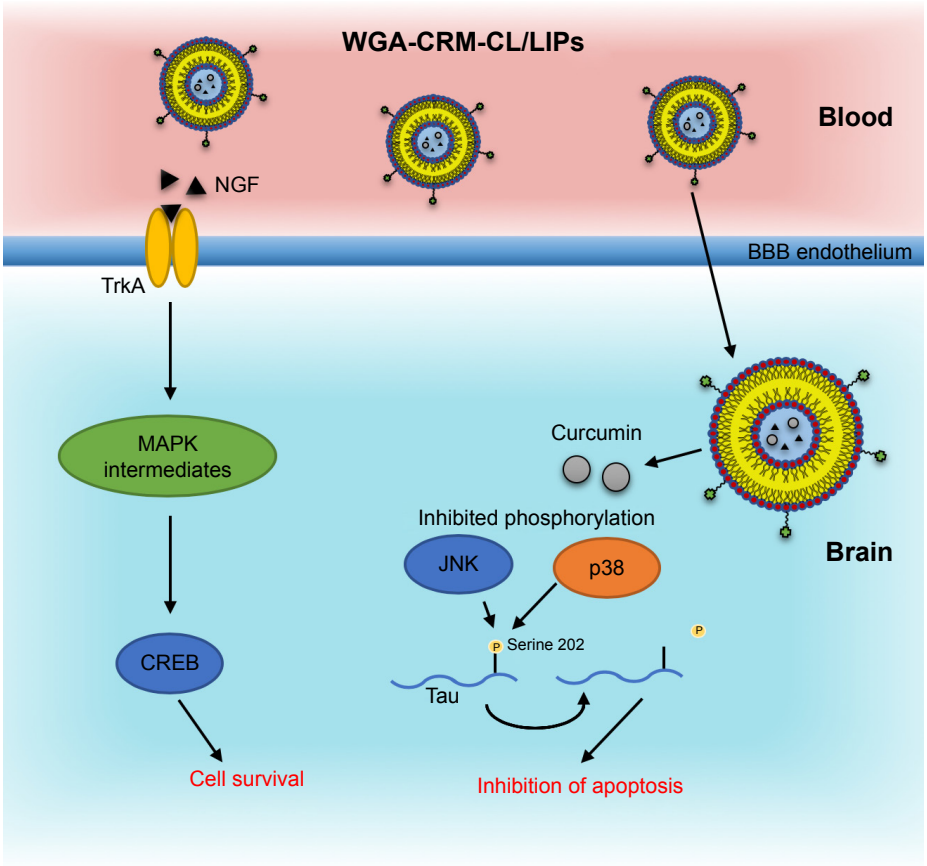

Figure 6 Cell survival and apoptotic pathway in AD therapy.
Notes: Action of WGA-CRM-CL/LIPs: Curcumin inhibits phosphorylation of JNK and p38, preventing downstream phosphorylation of tau serine 202, leading to prevention of apoptotic neurodegeneration. NGF binds TrkA and mediates MAPK phosphorylation cascade and recruitment of CREB, enhancing overall cell survival.
Abbreviations: CL, cardiolipin; CREB, cAMP response element binding protein; CRM, curcumin; JNK, c-Jun N-terminal kinase; LIPs, liposomes; MAPK, mitogen-activated protein kinase; NGF, neuronal growth factor; TrkA, tyrosine kinase receptor type-1; WGA, wheat germ agglutinin; AD, Alzheimer's disease.

for the understanding of AD progression, since MAPK-catalyzed phosphorylation events in the brain have a key role in the downstream activity of cellular components (eg, phosphatases, kinases) that impact on apoptosis and overall neuronal survival. It would also provide valuable insight into possible future therapies.

The key constituents of this multifunctional liposome (coined WGA-CRM-CL/LIP) are curcumin (CRM), nerve growth factor (NGF), cardiolipin (CL), and wheat germ agglutinin (WGA). In addition to acting as an Aβ aggregation inhibitor, curcumin alters the expression of phosphorylated p38 (p-p38) and phosphorylated c-Jun N-terminal kinase (p-JNK), key players in the apoptotic pathway. NGF promotes the activity of tyrosine kinase receptor type 1 (TrkA), which is involved in slowing down neuronal apoptosis. In order to enhance the targeting of apoptotic neurons surrounding Aβ, CL was included, as it has a strong affinity for Aβ. In this case, both PEGylation and WGA provided an additional novel dual functionalization, with the aim of improving delivery across the BBB.[42]

WGA-CRM-CL/LIPs reduced Aβ "plaque" deposition in AD model SK-N-MC cells and increased the percentage of healthy neurons with cholinergic activity in a Wistar rat AD model (established by injection of Aβ into CA1 neurons). Additionally, curcumin mediates downstream inhibition of tau phosphorylation at serine 202, which is a key site for axonogenesis (Figure 6).[96] While the therapeutic potential of this inhibition is unclear, this is an illustrative method of targeting and altering tau phosphorylation, while also targeting and reducing Aβ burden. The authors suggest that WGA-CRM-CL/LIP should have little effect on a healthy brain, since it is not in an inflammatory state and that this type of AD therapy would most likely be given to patients in the later stages of AD.[42]

Aβ targeting nanosweepers

Luo et al[97] have developed "nanosweepers" (M_3) that not only capture extracellular Aβ and direct it into cells but also upregulate autophagy and digestion of Aβ. The nanosweepers are composed of a cationic chitosan core with PEGylated GKLVFF (that can co-assemble with Aβ) and Becln-1 (that induces autophagy to degrade Aβ). They work by capturing and co-assembling with extracellular Aβ, inhibiting toxic Aβ formation, then specifically directing Aβ into cells and activating autophagy. This strategy has been shown to degrade insoluble Aβ from a level of 1,539 down to 914 ng/mg, and soluble Aβ from 585 to 190 ng/mg, in APPswe/PS1dE9 transgenic mice, and also increase neuronal cell viability. M_3 is a multifunctional peptide-polymer that could provide a novel therapeutic approach for the treatment of AD, by clearance of Aβ.[97] By design, it is not a good aggregation inhibitor and could be useful in combination with additional therapies.

Future prospects

The majority of studies employing liposomal carrier systems to target the CNS are still restricted to early experimental work on cell and animal models, or follow on preclinical development, with none so far entering human clinical trials. Further investment and research is required to develop and optimize these carrier systems for AD therapy, since many of the studies considered in this article report promising findings, with a drive toward early clinical testing. A reoccurring problem is that some of the modifications on their own do not allow sufficient penetration through the BBB, or adequate targeting for AD therapy. Since liposomes have great potential for heavy functionalization, future steps should incorporate several different modifications into the same liposomes that can work together in synergy.

Furthermore, current systems in development have tended to target only Aβ, due to its fundamental role in AD, yet liposomes have the potential to be adapted to incorporate a therapeutic cocktail of molecules that aid BBB transport and are able to treat multiple areas of AD pathology. Further studies could prevent the formation of tau tangles, by using an anti-tau antibody, or tau-directed peptides, or small molecule inhibitors, in addition to preventing formation or dissolution of amyloid plaques, and targeting of phosphorylation cascades. A therapeutic system that can target Aβ, tau, neuronal survival, and apoptosis, and cholinergic neurotransmission, for example, could become the gold standard treatment for AD; liposomes are certainly a good candidate for the development of such a therapy. CPPs have great potential for AD therapy, yet their non-specific uptake by peripheral tissue limits their use. TAT peptide, which is derived from HIV, is an example of utilizing aspects of pathogens for therapeutic purposes. The future of CPPs for brain delivery could involve using trans-membrane peptide domains derived from trypanosomes,[98] or the Zika virus,[99] both of which contain peptides that target enhanced uptake into the brain.

Drawbacks and barriers

There remain some issues for liposomes as a drug delivery system. There is an increased cost when they are used, but this is ameliorated by the fact that they may allow a drug

to reach its target with a liposome, but not without, or the overall dose may be decreased as a greater proportion of the drug reaches its target. They are not suitable for oral delivery because they will rupture due to osmotic shock when entering the hypotonic environment of the stomach (depending on the osmolarity of the internal aqueous filling of the liposome) and the lipids will be digested in the small intestine. Once in the bloodstream, the majority of liposomes are taken up non-specifically by the mononuclear phagocyte system, and this includes those with a stealth coating. This reduces the number available to be delivered to the brain, although this can be overcome by administering a larger dose in a single bolus, rather than multiple smaller doses.[100] There are two main strategies for crossing the BBB (see "BBB transport" section) by either targeting a transporter system or by use of a CPP. The former approach may lead to saturation of the transporter system, whereas this is less of a limiting factor in the latter as it is non-specific. Finally, as this is a relatively new technology, there are still some technical issues regarding the supply of liposome products to the consumer in terms of sterility and product shelf life. Liposomes are not suitable for heat sterilization, but bacterial contamination can be avoided by filtration due to the small size of the liposomes.[101] In terms of stability, liposomes in suspension will eventually start to fuse together, changing the size to the point at which they become ineffective as a delivery system. To avoid this, the liposomes can be lyophilized or spray dried in the presence of trehalose or sucrose and will retain their size on rehydration.[102,103]

Conclusion

Despite these challenges, the use of liposomal carriers is proving to be a potentially good strategy for future therapy of AD. They have a unique ability for modification to cross the BBB, while also showing some evidence of effectiveness without brain delivery, via the peripheral sink effect. Multiple molecules are able to enhance BBB transport, and many others allow targeting toward key molecular systems involved in AD pathogenesis. It is likely that future development will focus mainly on early intervention to slow down the progression of this disease, rather than attempting to reverse it in more advanced cases. Current study is moving toward targeting more than just one aspect of brain pathology, using multifunctional liposomes, and this holds great promise for the future, but is currently in the very early stages of development. Further study and substantial funding will be required to achieve success, so that this type of strategy can be driven into human clinical trials and beyond.

Acknowledgments

Research in our own laboratory on peptide-liposome-based therapy has received funding from the European Community's Seventh Framework Program (FP7/2007–2013) under grant agreement no 212043, Alzheimer's Research UK, The Alzheimer's Society UK, The Sir John Fisher Foundation, and Lancaster University's "Defying Dementia" charity.

Disclosure

Lancaster University has a granted patent on intellectual property related to this area of research based on the inventions of DA and MT. The other authors (CR and NF) report no conflicts of interest in this work.

References

1. World Health Organization. *Neurological Disorders: Public Health Challenges*. Geneva: WHO; 2006.
2. Prince M, Ali G-C, Guerchet M, Prina AM, Albanese E, Wu Y-T. Recent global trends in the prevalence and incidence of dementia, and survival with dementia. *Alzheimers Res Ther*. 2016;8(1):13.
3. Krstic D, Knuesel I. Deciphering the mechanism underlying late-onset Alzheimer disease. *Nat Rev Neurol*. 2013;9(1):25–34.
4. Karran E, de Strooper B. The amyloid cascade hypothesis: are we poised for success or failure? *J Neurochem*. 2016;139 (Suppl 2): 237–252.
5. Murphy MP, Levine H. Alzheimer's disease and the amyloid-β peptide. *J Alzheimers Dis*. 2010;19(1):311–323.
6. Haass C, Selkoe DJ. Soluble protein oligomers in neurodegeneration: lessons from the Alzheimer's amyloid β-peptide. *Nat Rev Mol Cell Biol*. 2007;8(2):101–112.
7. Lipton SA, Gu Z, Nakamura T. Inflammatory mediators leading to protein misfolding and uncompetitive/fast off-rate drug therapy for neurodegenerative disorders. *Int Rev Neurobiol*. 2007;82:1–27.
8. Moreira PI, Siedlak SL, Aliev G, et al. Oxidative stress mechanisms and potential therapeutics in Alzheimer disease. *J Neural Transm*. 2005;112(7):921–932.
9. Oddo S, Laferla FM. The role of nicotinic acetylcholine receptors in Alzheimer's disease. *J Physiol Paris*. 2006;99(2–3):172–179.
10. Hansen RA, Gartlehner G, Webb AP, Morgan LC, Moore CG, Jonas DE. Efficacy and safety of donepezil, galantamine, and rivastigmine for the treatment of Alzheimer's disease: a systematic review and meta-analysis. *Clin Interv Aging*. 2008;3(2):211–225.
11. Yiannopoulou KG, Papageorgiou SG. Current and future treatments for Alzheimer's disease. *Ther Adv Neurol Disord*. 2013;6(1):19–33.
12. Brown D, Superti-Furga G. Rediscovering the sweet spot in drug discovery. *Drug Discov Today*. 2003;8(23):1067–1077.
13. Szuromi P, Vinson V, Marshall E. Rethinking drug discovery – Introduction. *Science*. 2004;303(5665):1795.
14. Overington JP, Al-Lazikani B, Hopkins AL. How many drug targets are there? *Nat Rev Drug Discov*. 2006;5(12):993–996.
15. Gregori M, Masserini M, Mancini S. Nanomedicine for the treatment of Alzheimer's disease. *Nanomedicine*. 2015;10(7):1203–1218.
16. Wolburg H, Noell S, Mack A, Wolburg-Buchholz K, Fallier-Becker P. Brain endothelial cells and the glio-vascular complex. *Cell Tissue Res*. 2009;335(1):75–96.
17. Lai F, Fadda AM, Sinico C. Liposomes for brain delivery. *Expert Opin Drug Deliv*. 2013;10(7):1003–1022.
18. Vieira DB, Gamarra LF. Getting into the brain: liposome-based strategies for effective drug delivery across the blood-brain barrier. *Int J Nanomedicine*. 2016;11:5381–5414.

19. Noble GT, Stefanick JF, Ashley JD, Kiziltepe T, Bilgicer B. Ligand-targeted liposome design: challenges and fundamental considerations. *Trends Biotechnol*. 2014;32(1):32–45.
20. Bhowmik A, Khan R, Ghosh MK. Blood brain barrier: a challenge for effectual therapy of brain tumors. *Biomed Res Int*. 2015;2015:1–20.
21. Sánchez-Navarro M, Giralt E, Teixidó M. Blood-brain barrier peptide shuttles. *Curr Opin Chem Biol*. 2017;38:134–140.
22. Abbott NJ, Patabendige AA, Dolman DE, Yusof SR, Begley DJ. Structure and function of the blood-brain barrier. *Neurobiol Dis*. 2010; 37(1):13–25.
23. Chen Y, Liu L. Modern methods for delivery of drugs across the blood-brain barrier. *Adv Drug Deliv Rev*. 2012;64(7):640–665.
24. Hersh DS, Wadajkar AS, Roberts N, et al. Evolving drug delivery strategies to overcome the blood brain barrier. *Curr Pharm Des*. 2016;22(9): 1177–1193.
25. Agrawal M, Ajazuddin, Tripathi DK, et al. Recent advancements in liposomes targeting strategies to cross blood-brain barrier (BBB) for the treatment of Alzheimer's disease. *J Control Release*. 2017;260: 61–77.
26. Li W, Zhou Y, Zhao N, Hao B, Wang X, Kong P. Pharmacokinetic behavior and efficiency of acetylcholinesterase inhibition in rat brain after intranasal administration of galanthamine hydrobromide loaded flexible liposomes. *Environ Toxicol Pharmacol*. 2012;34(2):272–279.
27. Zheng X, Shao X, Zhang C, et al. Intranasal H102 peptide-loaded liposomes for brain delivery to treat Alzheimer's disease. *Pharm Res*. 2015;32(12):3837–3849.
28. Illum L. Nasal drug delivery – recent developments and future prospects. *J Control Release*. 2012;161(2):254–263.
29. Gao H. Progress and perspectives on targeting nanoparticles for brain drug delivery. *Acta Pharm Sin B*. 2016;6(4):268–286.
30. Patching SG. Glucose transporters at the blood-brain barrier: Function, regulation and gateways for drug delivery. *Mol Neurobiol*. 2017; 54(2):1046–1077.
31. Arumugam K, Subramanian GS, Mallayasamy SR, Averineni RK, Reddy MS, Udupa N. A study of rivastigmine liposomes for delivery into the brain through intranasal route. *Acta Pharm*. 2008;58(3):287–297.
32. Mutlu NB, Değim Z, Yilmaz Ş, Eşsiz D, Nacar A. New perspective for the treatment of Alzheimer diseases: liposomal rivastigmine formulations. *Drug Dev Ind Pharm*. 2011;37(7):775–789.
33. Confaloni A, Tosto G, Tata AM. Promising therapies for Alzheimer's disease. *Curr Pharm Des*. 2016;22(14):2050–2056.
34. Spuch C, Navarro C. Liposomes for targeted delivery of active agents against neurodegenerative diseases (Alzheimer's disease and Parkinson's disease). *J Drug Deliv*. 2011;469679.
35. Joshi S, Singh-Moon RP, Ellis JA, et al. Cerebral hypoperfusion-assisted intra-arterial deposition of liposomes in normal and glioma-bearing rats. *Neurosurgery*. 2015;76(1):92–100.
36. Abra RM, Hunt CA. Liposome disposition in vivo. III. Dose and vesicle-size effects. *Biochim Biophys Acta*. 1981;666(3):493–503.
37. Harashima H, Kiwada H. Liposomal targeting and drug delivery: kinetic consideration. *Adv Drug Deliv Rev*. 1996;19(3):425–444.
38. Fanciullino R, Ciccolini J. Liposome-encapsulated anticancer drugs: still waiting for the magic bullet? *Curr Med Chem*. 2009;16(33): 4361–4373.
39. Allen TM. Liposomes. Opportunities in drug delivery. *Drugs*. 1997; 54(Suppl 4):8–14.
40. Briuglia ML, Rotella C, McFarlane A, Lamprou DA. Influence of cholesterol on liposome stability and on in vitro drug release. *Drug Deliv Transl Res*. 2015;5(3):231–242.
41. Alarcón JM, Brito JA, Hermosilla T, Atwater I, Mears D, Rojas E. Ion channel formation by Alzheimer's disease amyloid β-peptide (Aβ40) in unilamellar liposomes is determined by anionic phospholipids. *Peptides*. 2006;27(1):95–104.
42. Kuo YC, Lin CY, Li JS, Lou YI. Wheat germ agglutinin-conjugated liposomes incorporated with cardiolipin to improve neuronal survival in Alzheimer's disease treatment. *Int J Nanomedicine*. 2017;12: 1757–1774.
43. Palchetti S, Colapicchioni V, Digiacomo L, et al. The protein corona of circulating PEGylated liposomes. *Biochim Biophys Acta*. 2016;1858(2): 189–196.
44. Veronese FM, Mero A. The impact of PEGylation on biological therapies. *BioDrugs*. 2008;22(5):315–329.
45. Ballatori N, Krance SM, Marchan R, Hammond CL. Plasma membrane glutathione transporters and their roles in cell physiology and pathophysiology. *Mol Aspects Med*. 2009;30(1–2):13–28.
46. Gaillard PJ, Appeldoorn CC, Dorland R, et al. Pharmacokinetics, brain delivery, and efficacy in brain tumor-bearing mice of glutathione pegylated liposomal doxorubicin (2B3-101). *PLoS One*. 2014;9(1):10.
47. Rotman M, Welling MM, Bunschoten A, et al. Enhanced glutathione PEGylated liposomal brain delivery of an anti-amyloid single domain antibody fragment in a mouse model for Alzheimer's disease. *J Control Release*. 2015;203:40–50.
48. Zhang CX, Zhao WY, Liu L, et al. A nanostructure of functional targeting epirubicin liposomes dually modified with aminophenyl glucose and cyclic pentapeptide used for brain glioblastoma treatment. *Oncotarget*. 2015;6(32):32681–32700.
49. Xie F, Yao N, Qin Y, et al. Investigation of glucose-modified liposomes using polyethylene glycols with different chain lengths as the linkers for brain targeting. *Int J Nanomedicine*. 2012;7:163–175.
50. Li H, Qian ZM. Transferrin/transferrin receptor-mediated drug delivery. *Med Res Rev*. 2002;22(3):225–250.
51. Fishman JB, Rubin JB, Handrahan JV, Connor JR, Fine RE. Receptor-mediated transcytosis of transferrin across the blood-brain barrier. *J Neurosci Res*. 1987;18(2):299–304.
52. Gao JQ, Lv Q, Li LM, et al. Glioma targeting and blood-brain barrier penetration by dual-targeting doxorubincin liposomes. *Biomaterials*. 2013;34(22):5628–5639.
53. Chen ZL, Huang M, Wang XR, et al. Transferrin-modified liposome promotes α-mangostin to penetrate the blood-brain barrier. *Nanomedicine*. 2016;12(2):421–430.
54. Chen YC, Chiang CF, Chen LF, Liang PC, Hsieh WY, Lin WL. Polymersomes conjugated with des-octanoyl ghrelin and folate as a BBB-penetrating cancer cell-targeting delivery system. *Biomaterials*. 2014; 35(13):4066–4081.
55. Papadia K, Markoutsa E, Mourtas S, et al. Multifunctional LUV liposomes decorated for BBB and amyloid targeting. A. In vitro proof-of-concept. *Eur J Pharm Sci*. 2017;101:140–148.
56. Song XL, Liu S, Jiang Y, et al. Targeting vincristine plus tetrandrine liposomes modified with DSPE-PEG_{2000}-transferrin in treatment of brain glioma. *Eur J Pharm Sci*. 2017;96:129–140.
57. Chen H, Tang L, Qin Y, et al. Lactoferrin-modified procationic liposomes as a novel drug carrier for brain delivery. *Eur J Pharm Sci*. 2010;40(2): 94–102.
58. Kawamata T, Tooyama I, Yamada T, Walker DG, McGeer PL. Lactotransferrin immunocytochemistry in Alzheimer and normal human brain. *Am J Pathol*. 1993;142(5):1574–1585.
59. Zhong Z-R, Liu J, Deng Y, et al. Preparation and characterization of a novel nonviral gene transfer system: procationic-liposome-protamine-DNA complexes. *Drug Deliv*. 2007;14(3):177–183.
60. Mahley RW. Apolipoprotein E: cholesterol transport protein with expanding role in cell biology. *Science*. 1988;240(4852):622–630.
61. Gobbi M, Re F, Canovi M, et al. Lipid-based nanoparticles with high binding affinity for amyloid-β1-42 peptide. *Biomaterials*. 2010; 31(25):6519–6529.
62. Re F, Cambianica I, Sesana S, et al. Functionalization with ApoE-derived peptides enhances the interaction with brain capillary endothelial cells of nanoliposomes binding amyloid-β peptide. *J Biotechnol*. 2011;156(4):341–346.
63. Lane-Donovan C, Wong WM, Durakoglugil MS, et al. Genetic restoration of plasma ApoE improves cognition and partially restores synaptic defects in ApoE-deficient mice. *J Neurosci*. 2016;36(39): 10141–10150.
64. Lindgren M, Hällbrink M, Prochiantz A, Langel U. Cell-penetrating peptides. *Trends Pharmacol Sci*. 2000;21(3):99–103.

65. Gregori M, Taylor M, Salvati E, et al. Retro-inverso peptide inhibitor nanoparticles as potent inhibitors of aggregation of the Alzheimer's Aβ peptide. *Nanomedicine*. 2017;13(2):723–732.
66. Vivès E, Richard JP, Rispal C, Lebleu B. TAT peptide internalization: seeking the mechanism of entry. *Curr Protein Pept Sci*. 2003;4(2):125–132.
67. Parthsarathy V, McClean PL, Hölscher C, et al. A novel retro-inverso peptide inhibitor reduces amyloid deposition, oxidation and inflammation and stimulates neurogenesis in the APPswe/PS1ΔE9 mouse model of Alzheimer's disease. *PLoS One*. 2013;8(9):11.
68. Kamei N, Tanaka M, Choi H, et al. Effect of an enhanced nose-to-brain delivery of insulin on mild and progressive memory loss in the senescence-accelerated mouse. *Mol Pharm*. 2017;14(3):916–927.
69. Hardy J, Allsop D. Amyloid deposition as the central event in the aetiology of Alzheimer's disease. *Trends Pharmacol Sci*. 1991;12(10):383–388.
70. Hardy J, Selkoe DJ. The amyloid hypothesis of Alzheimer's disease: progress and problems on the road to therapeutics. *Science*. 2002;297(5580):353–356.
71. Balducci C, Mancini S, Minniti S, et al. Multifunctional liposomes reduce brain β-amyloid burden and ameliorate memory impairment in Alzheimer's disease mouse models. *J Neurosci*. 2014;34(42):14022–14031.
72. Bana L, Minniti S, Salvati E, et al. Liposomes bi-functionalized with phosphatidic acid and an ApoE-derived peptide affect Aβ aggregation features and cross the blood-brain-barrier: implications for therapy of Alzheimer disease. *Nanomedicine*. 2014;10(7):1583–1590.
73. Matsuoka Y, Saito M, Lafrancois J, et al. Novel therapeutic approach for the treatment of Alzheimer's disease by peripheral administration of agents with an affinity to β-amyloid. *J Neurosci*. 2003;23(1):29–33.
74. Mancini S, Minniti S, Gregori M, et al. The hunt for brain Aβ oligomers by peripherally circulating multi-functional nanoparticles: Potential therapeutic approach for Alzheimer disease. *Nanomedicine*. 2016;12(1):43–52.
75. Friedlich AL, Butcher LL. Involvement of free oxygen radicals in β-amyloidosis: an hypothesis. *Neurobiol Aging*. 1994;15(4):443–455.
76. Tabner BJ, El-Agnaf OM, Turnbull S, et al. Hydrogen peroxide is generated during the very early stages of aggregation of the amyloid peptides implicated in Alzheimer disease and familial British dementia. *J Biol Chem*. 2005;280(43):35789–35792.
77. Behl C, Davis JB, Lesley R, Schubert D. Hydrogen peroxide mediates amyloid β protein toxicity. *Cell*. 1994;77(6):817–827.
78. Sano M, Ernesto C, Thomas RG, et al. A controlled trial of selegiline, α-tocopherol, or both as treatment for Alzheimer's disease. *N Engl J Med Overseas Ed*. 1997;336(17):1216–1222.
79. Lim GP, Chu T, Yang F, Beech W, Frautschy SA, Cole GM. The curry spice curcumin reduces oxidative damage and amyloid pathology in an Alzheimer transgenic mouse. *J Neurosci*. 2001;21(21):8370–8377.
80. Yanagisawa D, Amatsubo T, Morikawa S, et al. In vivo detection of amyloid β deposition using ^{19}F magnetic resonance imaging with a ^{19}F-containing curcumin derivative in a mouse model of Alzheimer's disease. *Neuroscience*. 2011;184:120–127.
81. Lee I, Yang J, Lee JH, Choe YS. Synthesis and evaluation of 1-(4-[^{18}F]fluoroethyl)-7-(4′-methyl)curcumin with improved brain permeability for β-amyloid plaque imaging. *Bioorg Med Chem Lett*. 2011;21(19):5765–5769.
82. Yanagisawa D, Ibrahim NF, Taguchi H, et al. Curcumin derivative with the substitution at C-4 position, but not curcumin, is effective against amyloid pathology in APP/PS1 mice. *Neurobiol Aging*. 2015;36(1):201–210.
83. Taylor M, Moore S, Mourtas S, et al. Effect of curcumin-associated and lipid ligand-functionalized nanoliposomes on aggregation of the Alzheimer's Aβ peptide. *Nanomedicine*. 2011;7(5):541–550.
84. Mourtas S, Lazar AN, Markoutsa E, Duyckaerts C, Antimisiaris SG. Multifunctional nanoliposomes with curcumin-lipid derivative and brain targeting functionality with potential applications for Alzheimer disease. *Eur J Med Chem*. 2014;80:175–183.
85. Austen BM, Paleologou KE, Ali SA, Qureshi MM, Allsop D, El-Agnaf OM. Designing peptide inhibitors for oligomerization and toxicity of Alzheimer's β-amyloid peptide. *Biochemistry*. 2008;47(7):1984–1992.
86. Taylor M, Moore S, Mayes J, et al. Development of a proteolytically stable retro-inverso peptide inhibitor of β-amyloid oligomerization as a potential novel treatment for Alzheimer's disease. *Biochemistry*. 2010;49(15):3261–3272.
87. Sherer M, Fullwood NJ, Taylor M, Allsop D. A preliminary electron microscopic investigation into the interaction between $A\beta_{1-42}$ peptide and a novel nanoliposome-coupled retro-inverso peptide inhibitor, developed as a potential treatment for Alzheimer's disease. *J Phys Conference Series*. 2015;644:012040.
88. Eisenberg D, Jucker M. The amyloid state of proteins in human diseases. *Cell*. 2012;148(6):1188–1203.
89. Tenovuo O. Central acetylcholinesterase inhibitors in the treatment of chronic traumatic brain injury-clinical experience in 111 patients. *Prog Neuropsychopharmacol Biol Psychiatry*. 2005;29(1):61–67.
90. Spencer CM, Noble S. Rivastigmine. A review of its use in Alzheimer's disease. *Drugs Aging*. 1998;13(5):391–411.
91. Illum L. Nasal drug delivery – possibilities, problems and solutions. *J Control Release*. 2003;87(1–3):187–198.
92. Yang ZZ, Zhang YQ, Wang ZZ, Wu K, Lou JN, Qi XR. Enhanced brain distribution and pharmacodynamics of rivastigmine by liposomes following intranasal administration. *Int J Pharm*. 2013;452(1–2):344–354.
93. Yadav AV, Murthy MS, Shete AS, Sakhare S. Stability aspects of liposomes. *Indian J Pharm Educ Res*. 2011;45(4):402–413.
94. Nageeb El-Helaly S, Abd Elbary A, Kassem MA, El-Nabarawi MA. Electrosteric stealth Rivastigmine loaded liposomes for brain targeting: preparation, characterization, *ex vivo*, bio-distribution and *in vivo* pharmacokinetic studies. *Drug Deliv*. 2017;24(1):692–700.
95. Kreuter J, Alyautdin RN, Kharkevich DA, Ivanov AA. Passage of peptides through the blood-brain barrier with colloidal polymer particles (nanoparticles). *Brain Res*. 1995;674(1):171–174.
96. Mandell JW, Banker GA. A spatial gradient of tau protein phosphorylation in nascent axons. *J Neurosci*. 1996;16(18):5727–5740.
97. Luo Q, Lin Y-X, Yang P-P, et al. A self-destructive nanosweeper that captures and clears amyloid β-peptides. *Nat Commun*. 2018;9(1):12.
98. Goto Y, Duthie MS, Kawazu S, Inoue N, Carter D. Biased cellular locations of tandem repeat antigens in African trypanosomes. *Biochem Biophys Res Commun*. 2011;405(3):434–438.
99. Jun S-R, Wassenaar TM, Wanchai V, Patumcharoenpol P, Nookaew I, Ussery DW. Suggested mechanisms for Zika virus causing microcephaly: what do the genomes tell us? *BMC Bioinformatics*. 2017;18(S14):12.
100. van Etten EW, Ten Kate MT, Snijders SV, Bakker-Woudenberg IA. Administration of liposomal agents and blood clearance capacity of the mononuclear phagocyte system. *Antimicrob Agents Chemother*. 1998;42(7):1677–1681.
101. Toh M-R, Chiu GNC. Liposomes as sterile preparations and limitations of sterilisation techniques in liposomal manufacturing. *Asian J Pharm Sci*. 2013;8(2):88–95.
102. Payton NM, Wempe MF, Xu Y, Anchordoquy TJ. Long-term storage of lyophilized liposomal formulations. *J Pharm Sci*. 2014;103(12):3869–3878.
103. Chen C, Han D, Cai C, Tang X. An overview of liposome lyophilization and its future potential. *J Control Release*. 2010;142(3):299–311.
104. Qian ZM, Li H, Sun H, Ho K. Targeted drug delivery via the transferrin receptor-mediated endocytosis pathway. *Pharmacol Rev*. 2002;54(4):561–587.
105. Guo L, Ren J, Jiang X. Perspectives on brain-targeting drug delivery systems. *Curr Pharm Biotechnol*. 2012;13(12):2310–2318.
106. Fillebeen C, Descamps L, Dehouck MP, et al. Receptor-mediated transcytosis of lactoferrin through the blood-brain barrier. *J Biol Chem*. 1999;274(11):7011–7017.

107. Derossi D, Joliot AH, Chassaing G, Prochiantz A. The third helix of the Antennapedia homeodomain translocates through biological membranes. *J Biol Chem*. 1994;269(14):10444–10450.
108. Futaki S, Ohashi W, Suzuki T, et al. Stearylated arginine-rich peptides: a new class of transfection systems. *Bioconjug Chem*. 2001;12(6):1005–1011.
109. Lu W, Zhang Y, Tan YZ, Hu KL, Jiang XG, Fu SK. Cationic albumin-conjugated pegylated nanoparticles as novel drug carrier for brain delivery. *J Control Release*. 2005;107(3):428–448.
110. Tseng YL, Liu JJ, Hong RL. Translocation of liposomes into cancer cells by cell-penetrating peptides penetratin and tat: a kinetic and efficacy study. *Mol Pharmacol*. 2002;62(4):864–872.
111. Henriques ST, Castanho MA. Translocation or membrane disintegration? Implication of peptide-membrane interactions in pep-1 activity. *J Pept Sci*. 2008;14(4):482–487.
112. Gao C, Mao S, Ditzel HJ, et al. A cell-penetrating peptide from a novel pVII-pIX phage-displayed random peptide library. *Bioorg Med Chem*. 2002;10(12):4057–4065.
113. Koren E, Torchilin VP. Cell-penetrating peptides: breaking through to the other side. *Trends Mol Med*. 2012;18(7):385–393.
114. Pooga M, Hällbrink M, Zorko M, Langel U. Cell penetration by transportan. *FASEB J*. 1998;12(1):67–77.
115. Wender PA, Mitchell DJ, Pattabiraman K, Pelkey ET, Steinman L, Rothbard JB. The design, synthesis, and evaluation of molecules that enable or enhance cellular uptake: peptoid molecular transporters. *Proc Natl Acad Sci U S A*. 2000;97(24):13003–13008.
116. de Coupade C, Fittipaldi A, Chagnas V, et al. Novel human-derived cell-penetrating peptides for specific subcellular delivery of therapeutic biomolecules. *Biochem J*. 2005;390(Pt 2):407–418.
117. Morris MC, Deshayes S, Heitz F, Divita G. Cell-penetrating peptides: from molecular mechanisms to therapeutics. *Biol Cell*. 2008;100(4):201–217.
118. Johansson HJ, El-Andaloussi S, Holm T, et al. Characterization of a novel cytotoxic cell-penetrating peptide derived from p14ARF protein. *Molecular Therapy*. 2008;16(1):115–123.
119. Taylor BN, Mehta RR, Yamada T, et al. Noncationic peptides obtained from azurin preferentially enter cancer cells. *Cancer Res*. 2009;69(2):537–546.
120. Magzoub M, Sandgren S, Lundberg P, et al. N-terminal peptides from unprocessed prion proteins enter cells by macropinocytosis. *Biochem Biophys Res Commun*. 2006;348(2):379–385.
121. Oehlke J, Krause E, Wiesner B, Beyermann M, Bienert M. Extensive cellular uptake into endothelial cells of an amphipathic β-sheet forming peptide. *FEBS Lett*. 1997;415(2):196–199.
122. Sadler K, Eom KD, Yang JL, Dimitrova Y, Tam JP. Translocating proline-rich peptides from the antimicrobial peptide bactenecin 7. *Biochemistry*. 2002;41(48):14150–14157.
123. Rhee M, Davis P. Mechanism of uptake of C105Y, a novel cell-penetrating peptide. *J Biol Chem*. 2006;281(2):1233–1240.